The geochemistry and petrology of tertiary basalt lavas from east Greenland

Panjasawatwong, Yuenyong

THE GEOCHEMISTRY AND PETROLOGY OF TERTIARY BASALT LAVAS FROM EAST GREENLAND

By

Yuenyong Panjasawatwong

(B.S., Chiang Mai University, Thailand)

University College, Durham.

Thesis submitted for the degree of Master of Science in the University of Durham

1978

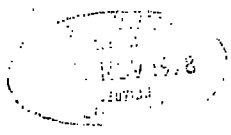

ABSTRACT

The 2,660m-thick basalt pile described in this thesis represents one of the upper parts, which were extruded predominantly under subaerial conditions, of the Tertiary basalt sequence in East Greenland. The pile rests on Lower Cretaceous sediments and is overlain by the sediments of Kap Dalton Formation.

Chemically (XRF analysis), the basalts can be classified as ocean-island tholeiites and are broadly comparable to the Tertiary tholeiites from mid-west Iceland and the tholeiites of the Neovolcanic zone of Iceland. Although they have rather limited compositional ranges, they show evidence of two episodes of fractionation. The magma compositions were controlled largely by olivine fractionation in the initial stage and subsequently by plagioclase fractionation. Comparisons between bivariate and multivariate analyses have been made and it is found that in the case of rather narrow compositional ranges, the multivariate analysis (R-mode factor analysis) is the best method for illustrating geochemical patterns.

Petrographically, the basalt suite consists chiefly of plagioclase (average labradorite), augite and Fe-Ti oxides with small amounts of olivine, pigeonite and interstitial glass, except for pillow lavas where the groundmass is entirely glass. The textures are variable from glassy

to coarse-grained types. Thus they can be divided, in terms of textures and field observations, into four main groups and then subdivided into a number of rock types. The majority appear to be aphyric types. The principal microphenocryst and/or phenocryst assemblages are plagioclase, plagioclase + olivine, plagioclase + olivine + augite, Fe-Ti oxides, or Fe-Ti oxides + plagioclase.

The plagioclase compositions (electron probe analysis) vary from $An_{83.4}Ab_{16.3}Or_{0.3}$ to $An_{27.3}Ab_{68.7}Or_{4.0}$. The great majority of analysed clinopyroxenes are augite and they follow the equilibrium fractionation trend typified in the Skaergaard tholeiitic intrusion. Olivine microphenocrysts and groundmass olivines were analysed and have chrysolitic and hyalosideritic compositions, respectively. Temperatures and oxygen fugacities, which have been estimated from the coexisting phases of titaniferous magnetite and ilmenite, are comparable to those of the Icelandic Thingmuli tholeiitic suite.

The origin of these East Greenland tholeiites is attributed to low-degree partial melting of undepleted mantle beneath the region on the present seaward side of the Blosseville coast and, subsequently, low-pressure crystal fractionation.

ACKNOWLEDGEMENTS

Financial support from the British Council under the Colombo Plan, through a grant to the Department of Geological Sciences, Chiang Mai University, Thailand is gratefully acknowledged. Thanks are also expressed to the British Council officers for the various arrangements made during my study period in England.

Thanks are expressed to Professor M.H.P. Bott (Chairman) for the Departmental research facilities provided and also to several members of the Department of Geological Sciences, Durham University for help and cooperation throughout this work.

I am grateful to my supervisors, Professor G.M. Brown and Dr. J.G. Holland, for their guidance and support, and am particularly indebted to Professor G.M. Brown for critically reading the thesis manuscript.

I thank the Geological Survey of Greenland and Dr. C. H. Emeleus (Durham) for providing the rock samples used in this study, and also record my gratitude to Dr. Emeleus for giving useful field information and advice, and critically reading parts of the thesis manuscript.

Dr. J.G. Holland and Mr. R.G. Hardy are thanked for instruction and assistance on X-ray fluorescence analysis,

and Dr. A. Peckett and Dr. B. Beddoe-Stephens for instruction and assistance on electron microprobe analysis.

Thanks are expressed to Mr. G. MacGregor and Mr. G. Randall for cutting and polishing the thin sections and to fellow research students, Mr. I.T. Williamson, Mr. R. M. Forster, Mr. A.P. Jones and Mr. M. Ozcelik, for their kind help and discussions.

Finally, I thank Mrs. C.L. Mines for typing the thesis.

LIST OF CONTENTS

LIST OF FIGURES

LIST OF TABLES

CHAPTER 1

INTRODUCTION

1.1. Scope of study

The lavas described in this thesis are a part of the Tertiary basalt plateau occurring along the East Greenland coast. They lie between Kap Brewster (70° 10'N 22°W) and about 70°N 23°W and cover an area of about 10 x 20 kilometres (Figs. 1-1 and 1-2).

The field investigation in the research area was carried out by Dr. C.H. Emeleus during the summer of 1971. Several vertical sections were measured at different localities and were grouped into a number of self-contained areas, based on geographical and geological boundaries. The successions in each self-contained area were linked together by correlating the recognizable horizons, i.e. pillow lavas, big-feldspar basalts and coarse-grained basalts, and large-scale features such as thickness of flows or groups of flows, colour of individual flows or groups of flows, and similar large-scale features. However, these recognizable horizons cannot be regarded as good marker horizons because they appear to occur at more than one level in the successions. One of the main problems of the investigation was the correlation between the successions mapped in different

fault blocks and in the areas separated by glaciers and superficial deposits; however, a tentative stratigraphical succession has been constructed.

The present study was carried out on the successions of five self-contained areas of Dr. Emeleus' collection. The details of each succession in the five self-contained areas will be delineated in the following discussion. The main aim of this study was to establish geochemical features of the Tertiary lavas and to compare with certain Tertiary lavas of the west of Scotland (Skye), Iceland and the Atlantic ocean floor; petrographical and mineralogical studies were also conducted. According to the previously mentioned problem, it was also important to correlate the successions of the region by comparing the geochemistry of the lava successions. It was also hoped that the study would reveal information on the origin of the lavas.

In addition to bivariant geochemical plots, a comparison between bivariate analysis and multivariate analysis was performed. It was anticipated that this would be significant in interpreting the geochemical features inherent in such a small-scale study.

1.2. General geology and thicknesses of successions (according to Emeleus, 1971)

The lavas in this region have been divided, as mentioned above, into eleven self-contained areas (Fig.1-2):

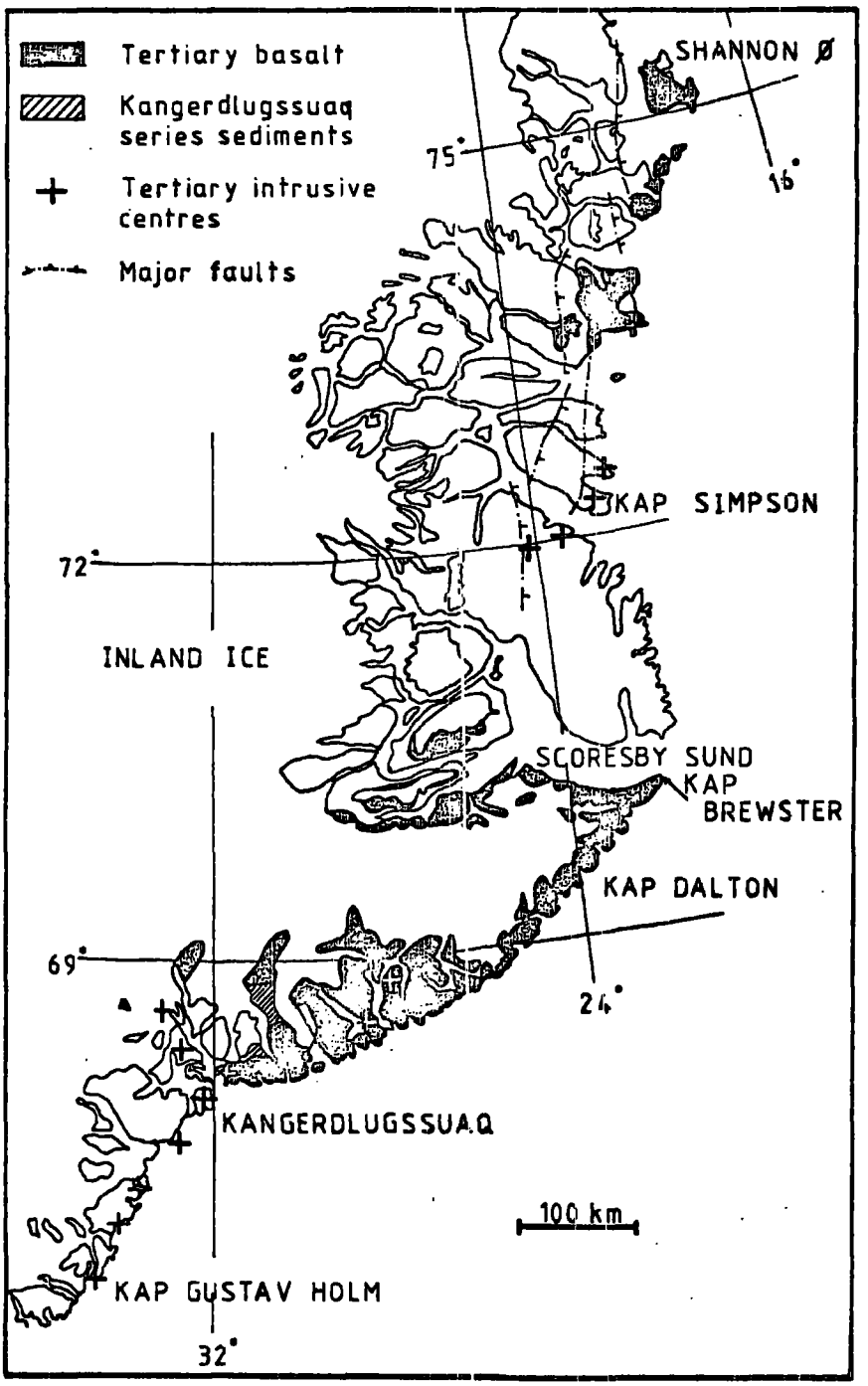
Tertiary basalt
Kangerdlugssuaq series sediments
Tertiary intrusive centres
Major faults
SHANNON Ø
75°
16°
KAP SIMPSON
72°
INLAND ICE
SCORESBY SUND
KAP BREWSTER
KAP DALTON
69°
24°
KANGERDLUGSSUAQ
100 km
KAP GUSTAV HOLM
32°

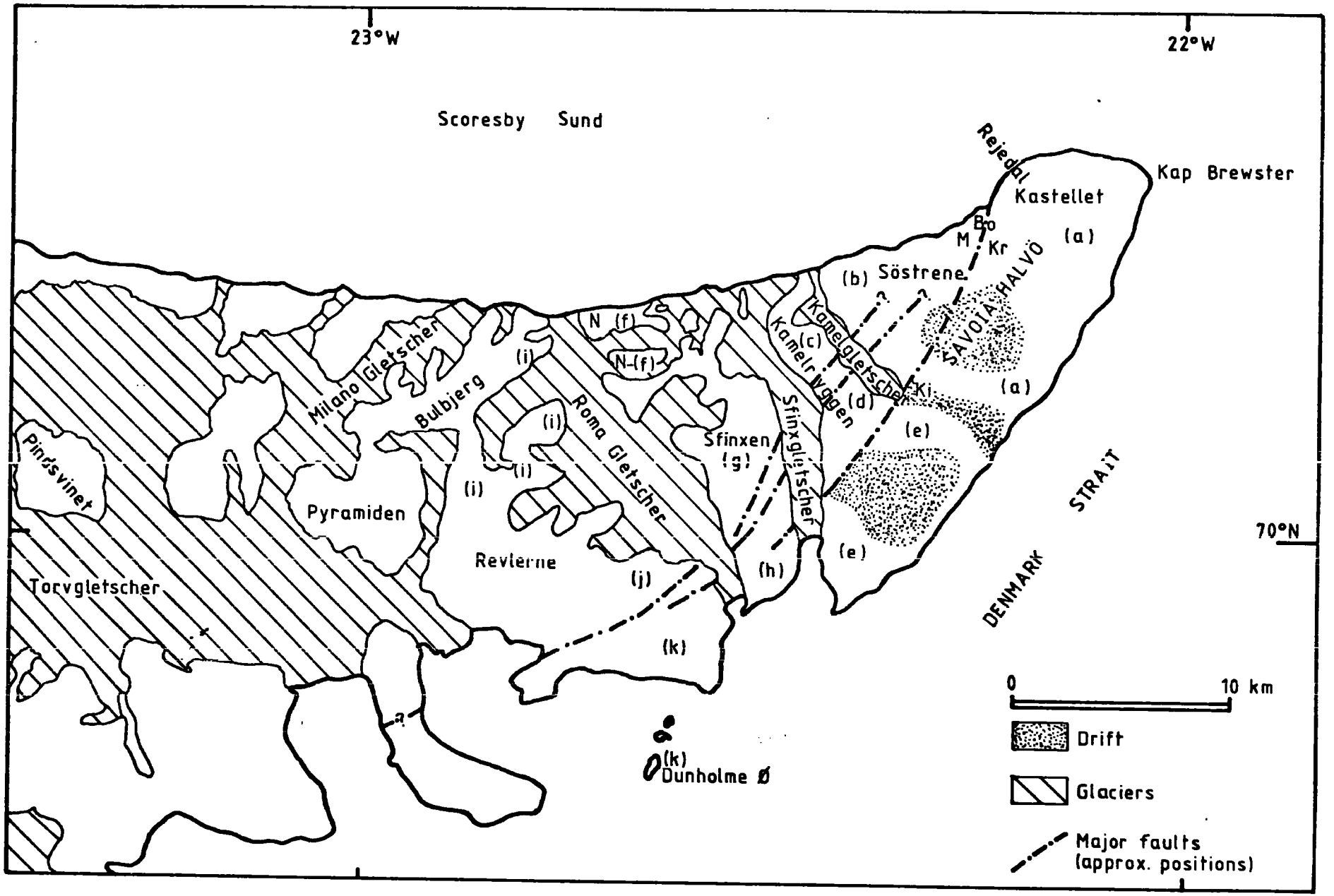
23°W
22°W
Scoresby Sund
Rejedal
Kap Brewster
Kastellet
Bo
M
Kr
(a)
(b) Söstrene
SAVOIA HALVÖ
Kamelgletscher
(c)
N (f)
N-(f)
Kamelryggen
(d)
Ki
(a)
(e)
Milano Gletscher
Bulbjerg
(i)
Roma Gletscher
Sfinxen (g)
Sfinxgletscher
Pingsvinet
Pyramiden
Revlerne
(j)
(h)
(e)
70°N
STRAIT
DENMARK
Torvgletscher
(k)
(k)
Dunholme Ø
0
10 km
Drift
Glaciers
Major faults (approx. positions)

(a) Kap Brewster, Rejedal, Krabbedalen, and the southern part of Savoia Halvø to Kikiakajik;

(b) the west of Bopladsdalen, Muslingehjørnet and the summit area of Søstrene east of Kamelgletscher;

(c) the area of Kamelryggen north of the 850 m summit;

(d) the area of Kamelryggen's 850 m top and ground south for about 2-3 kilometres;

(e) the southern part of Kamelryggen peninsula from area (d) to the sea;

(f) the area of nunataks northeast of the Roma Gletscher and north and northwest of Sfinxen,

(g) the Sfinxen summit area as far south as the major fault striking SW-NE across the south side of the mountain;

(h) the peninsula south of the major fault on Sfinxen;

(i) the high, dessected ground north of Revlerne and west of the northern part of Roma Gletscher to Pyramiden;

(j) the Revlerne summit area;

(k) the southern slopes of Revlerne with Dunholme Ø.

The successions studied here are from (a), (b), (d), (f) and (g); self-contained areas which entirely cover the main (composite) profile.

The majority of the rocks exposed in this region are basaltic lavas with occasionally intercalated sediments. Sediments of the Kap Dalton Formation and of Lower Cretaceous age have also been recorded. The lavas appear to have been erupted under subaerial conditions in view of red partings and they frequently show the typical three-fold vertical division of vesicular base, massive with columnar centre and vesicular top, which are classified as the blocky or aa type of flow. Subaqueous eruptions have also been detected on the evidence of pillow lavas and associated palagonitic material.

Structurally, the northwest of the research area consists of flat-lying flows whereas towards the south and southeast, the flows are disturbed by a system of normal faults striking approximately WSW-ENE and down-throwing to the south. The flows in the faulted area dip southerly or southeasterly at angles of up to 20^{o}. No dykes or other intrusions have been recorded.

Petrographically, the lavas have been classified by Emeleus into five main groups: pillow lavas; big-feldspar basalts; coarse-grained, non-porphyritic basalts; medium- to fine-grained porphyritic basalts; and medium- to fine-grained, sparsely-porphyritic and non-porphyritic basalts. The correlation between successions has been made by linking the first three petrographic groups of rocks and

the large-scale features (Fig. 1-3). The total thickness of the main (composite) profile is of the order of 2,660 metres. The field details of the five self-contained areas will be briefly described.

(a) The Kap Brewster, Rejedal, Krabbedalen, and the southern part of Savoia Halvø to Kikiakajik area (Fig. 1-3) The lavas are overlain by the sediments of the Kap Dalton Formation without a major structural break and the lavas have a total thickness of about 900 metres. The lowest 200 metres consist of sparsely porphyritic or non-porphyritic, medium- to fine-grained basalts. In the middle part of the succession, thin flows of coarse-grained, non-porphyritic basalts, big-feldspar basalt flows with plagioclase phenocysts ranging up to 1 centimetre and more in length, a horizon of pillow lavas, and several thin shale and coal horizons appear. In higher parts, coarse-grained, non-porphyritic basalts; medium- to fine-grained, sparsely-porphyritic, and non-porphyritic basalts; and medium- to fine-grained, porphyritic basalts are common.

(b) The west of Bopladsdalen, Muslingehjørnet area and the summit area of Søstrene east of Kamelgletscher (Fig. 1-3). The basalt succession in this area rests on micaceous, shaly sediments of Lower Cretaceous age (Prof. K. Birkenmajor, personal communication). As the sediments are now proved to be Mesozoic, the lavas lying immediately

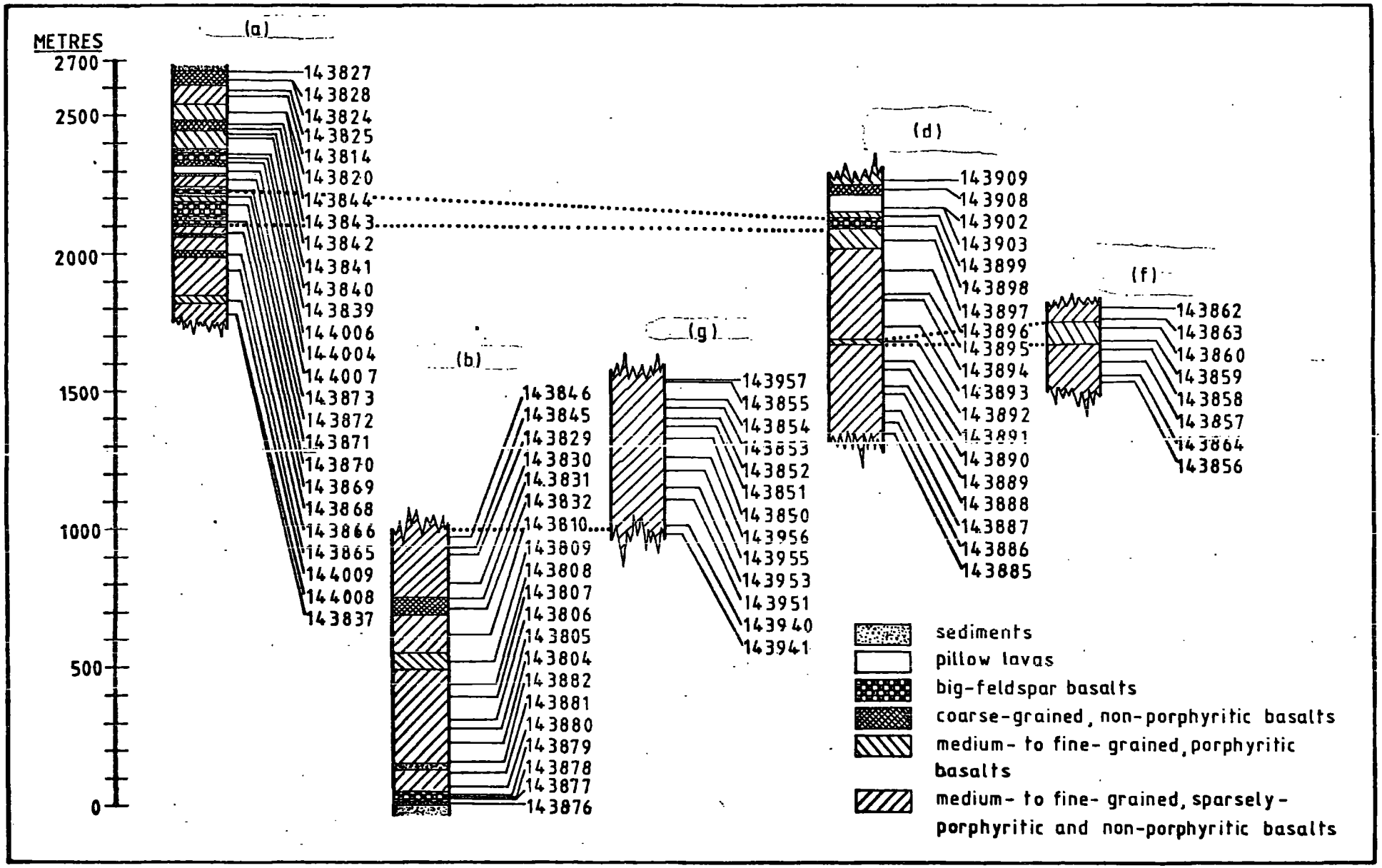
METRES
2700
2500
2000
1500
1000
500
0
(a)
143827
143828
143824
143825
143814
143820
143844
143843
143842
143841
143840
143839
144006
144004
144007
143873
143872
143871
143870
143869
143868
143866
143865
144009
144008
143837
(b)
143846
143845
143829
143830
143831
143832
143810
143809
143808
143807
143806
143805
143804
143882
143881
143880
143879
143878
143877
143876
(g)
143957
143855
143854
143853
143852
143851
143850
143956
143955
143953
143951
143940
143941
(d)
143909
143908
143902
143903
143899
143898
143897
143896
143895
143894
143893
143892
143891
143890
143889
143888
143887
143886
143885
(f)
143862
143863
143860
143859
143858
143857
143864
143856
sediments
pillow lavas
big-feldspar basalts
coarse-grained, non-porphyritic basalts
medium- to fine- grained, porphyritic basalts
medium- to fine- grained, sparsely-porphyritic and non-porphyritic basalts

on the sediments represent the local base of the lava succession.

The basalts in this succession are about 1000 metres in thickness and are composed chiefly of non-porphyritic or sparsely porphyritic type. The lowest 50 metres of flows are coarse-grained, non-porphyritic basalts and several thin horizons of big-feldspar basalts with abundant plagioclase phenocrysts ranging up to 1 centimetre or more in length. Pillow lavas have also been reported from this part of the succession (Fawcett et al., 1973). Above the 50 metre level, the greater part of this section is made up of medium- to fine-grained, sparsely porphyritic or non-porphyritic basalts. Two thin horizons of medium- to fine-grained, porphyritic basalts together with coarse-grained, non-porphyritic basalts exist at about the 700 metre and 500 metre levels. There is also evidence that the pre-lava surface was available for erosion, provided by the presence of sandstone with some garnet at around the 150 metre level.

The geographic proximity of this and succession (a) might be used to correlate across the fault at Muslingeh-jørnet. Nevertheless, the correlation does not appear reasonable due to differences in the thicknesses of the horizons and the absence of sandstone from succession (a).

(d) The area of Kamelrygg en's 850 m summit and ground south for 2-3 kilometres (Fig. 1-3). The basaltic lavas in this succession are about 950 metres thick. The lowest 750 metres consist of fine- to medium-grained, sparsely-porphyritic or non-porphyritic basalts with occasional flows of medium- to fine-grained, porphyritic basalts. Higher in the succession, there are big-feldspar basalts which are overlain by pillow lavas of approximately 40 metres in thickness and then a series of thin, coarse-grained, non-porphyritic basalts with thin intercalated flows of medium- to fine-grained, porphyritic basalt.

The similarities between the upper part of this succession and the middle part of succession (a) indicate them to be at the same general level in the lavas, although they are not matched in every detail.

(f) The area of nunataks NE of the Roma Gletscher and north and northwest of Sfinxen (Fig. 1-3). The 300 m-thick flows in this succession are chiefly composed of fine- to medium-grained, non-porphyritic or sparsely porphyritic basalts. Flows of medium- to fine-grained, porphyritic basalts exist in the middle part. The succession can be correlated with the lower part of succession (d) by linking the medium- to fine-grained, porphyritic basalt flows.

(g) The Sfinxen summit area as far south as the major fault striking SW-NE across the south side of the mountain (Fig. 1-3). This 550 m-thick succession consists solely of fine- to medium-grained, sparsely porphyritic or non-porphyritic basalts.

1.3. Other previous investigations

The existence of flood basalts around the Scoresby Sund area has been reported since William Scoresby Jun. discovered the fjord, named after him in 1822. They have been considered as related in time to the opening of the northeast Atlantic ocean basin (Heirtzler, 1968; Scrutton, 1973; Brooks, 1973a,b; Fawcett et al., 1973; Hallam, 1975; Soper et al., 1976; Brown and Whitley, 1976).

From 1883 to 1965, the Holm Expedition (1883-1885), Nordenskjöld Expedition (1883), British Arctic Air Route Expedition (1930-1931), and the Scoresby Sund Committee's 2nd East Greenland Expedition (1932) visited various localities along the East Greenland coast between Angmagssalik and Scoresby Sund. Brief descriptions of the petrography, petrology, structure, and field relationships have been published by Holmes (1918), Wager (1934, 1935, 1947) and Anwar (1955). Work on geological mapping along the coast started in 1900. Most of the lavas in the region were extruded subaerially and are tholeiitic basalts in composition. They cover an area of about

41,500 square kilometres and reach a maximum of about 7 kilometres in thickness near Kangerdlugssuaq . The lower basalts were extruded under water and are associated with well-bedded tuffs and agglomerates. The upper basalts, WSW of Scoresby Sund, grade upwards from pillow lavas into subaerial lavas. From the evidence of the sediments in the Kangerdlugssuaq and Kap Dalton regions, the extrusion of the lavas began in the late Palaeocene and ended no later than Eocene times. The basalt structures around the Kangerdlugssuaq area are complicated by the coastal flexure and dyke swarm.

Particularly detailed work was first carried out in 1965 in the Sovoia Halvø area by the Oxford University Expedition to East Greenland, which has been described by Fawcett, Rucklidge and Brooks (1966). The palaeomagnetic measurements have been published by Tarling (1967). Beckinsale, Brooks and Rex (1970) made K-Ar age determinations and found that the oldest basalt ages are 55-60 m.y., which are in agreement with the relative age given by the earlier workers, and are similar to those found for basalt plateaux elsewhere in the North Atlantic Tertiary Province. Glaciological observations have also been reported by Rucklidge (1966). In 1968, W.S. Watt started mapping the area due west of Scoresby Sund and divided the basalts into two main groups (corresponding to the amygdale minerals present), namely quartz tholeiites and olivine tholeiites.

Fawcett et al. (1973) have published data on the chemical petrology of 114 basalt samples from eight localities which lie between Kap Brewster and Kong Christian IX's Land (Fig. 1-4). Microscopically, the basalts are typical tholeiites consisting of plagioclase (labradorite), clinopyroxene, Fe-Ti oxides and glass, with sporadic olivine and pigeonite. They show no significant variations, excluding grainsize. Chemically, they are of quartz-normative tholeiitic type and have a relatively homogeneous composition. Fawcett et al. suggested that the original magma was olivine-normative tholeiite and that secondary alteration might be responsible for the appearance of normative quartz. The outstanding chemical characteristics are high Fe-Ti oxide and low K_2O contents. Comparisons have been drawn with ocean-floor tholeiites and tholeiites from regions of the North Atlantic Tertiary Province. The results of the comparisons support the suggestion of Brooks (1973a) that the lavas were generated during a prolonged period of ocean-floor spreading in a region of abnormal heatflow. Mineralogically, the great majority of pyroxene compositions (about 550 analyses) fall in the augite and subcalcic augite fields with a small number in the pigeonite and ferroaugite fields. They show extensive variation both of an equilibrium fractionation type and of various metastable "quench" trends towards

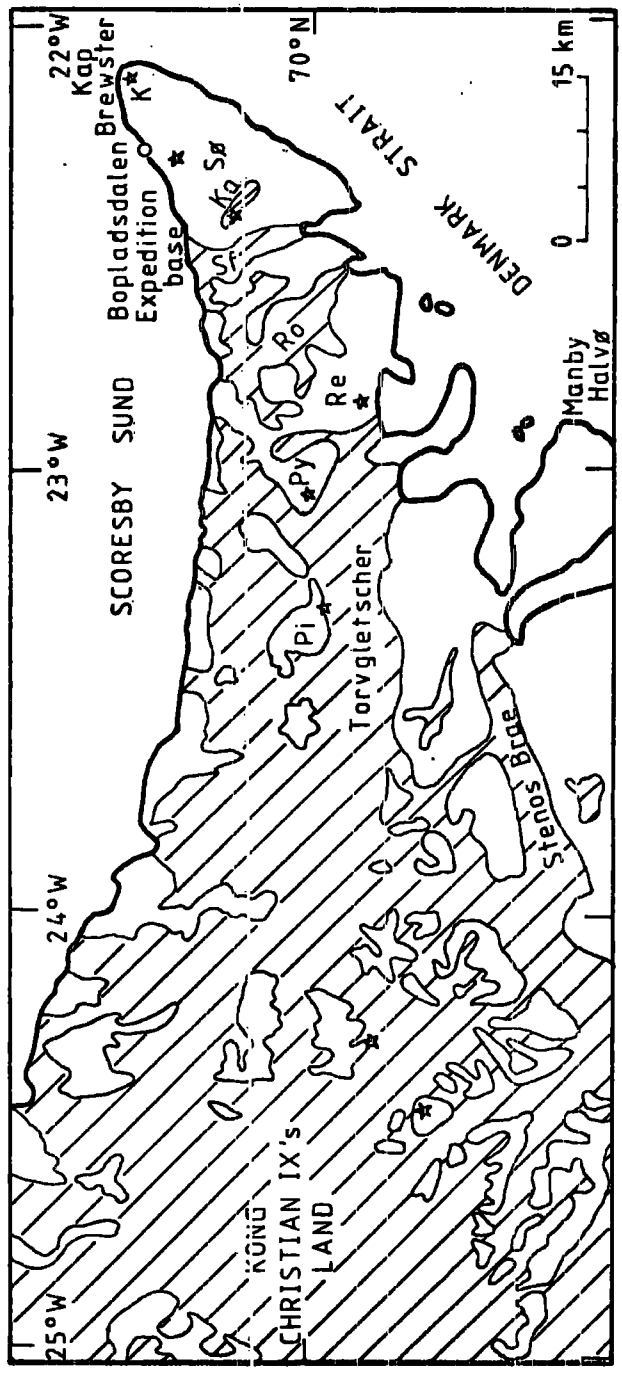
22°W
Kap Brewster
70°N
15 km
0
DENMARK STRAIT
Bopladsdalen Expedition base
SCORESBY SUND
23°W
Manby Halvø
Torvgletscher
Stenos Brae
24°W
CHRISTIAN IX's LAND
25°W

subcalcic augites. The plagioclase compositions (about 500 analyses) range (molecular proportions) from $An_{87.0}Ab_{12.5}Or_{0.5}$ to $An_{27.3}Ab_{69.3}Or_{3.4}$ and do not vary much from groundmass to phenocrysts in a single flow but show a little variation from one flow to another. Coexisting oxide phases (magnetite and ilmenite) are present in all analysed samples. The temperature and oxygen fugacity of crystallisation have been determined. Three specimens give the values of temperature and oxygen fugacity at about 1050°C and 10^{-11} bars, respectively. Another four samples have lower values of temperature and oxygen fugacity. Interstitial glass has undergone hydration and does not appear to have a late-differentiated composition.

Brooks (1973b) has depicted that the effusion of considerable volumes of flood basalt in East Greenland and on the Faeroe Islands records the initial North Atlantic rifting episode immediately before plate separation. The postulated eruptive cause is plume activity centred about the triple junction of which Kangerdlugssuaq is the failed arm. The volcanic activity took place in the latest Palaeocene, over a very restricted time interval around 3 million years. The postulated short period of volcanicity has been supported by the evidence of biostratigraphic and palaeomagnetic data (Soper et al., 1976).

Schilling and Noe-Nygaard (1974) studied the light

REE-enriched patterns of the basaltic lavas from East Greenland and the Faeroes and found that the lava pile on the Faeroes is comparable to the lava pile in East Greenland. A "mantle blob" model can, he postulates, account for the change in REE patterns of the lava profile on the Faeroe Islands.

Soper et al. (1976) studied the Late Cretaceous - Early Tertiary stratigraphy from Mikis Fjord to Jensens Fjord and they have found that there was a shallow marine basin to the northeast of Kangerdlugssuaq in Late Cretaceous - Early Palaeocene time. Before vulcanicity took place, there was an uplift which was followed by rapid subsidence of about 1.5 km to accommodate the submarine effusive and clastic rocks. Subsequently, the rate of effusion exceeded the rate of subsidence and the upper 8 km of basaltic pile, which was extruded subaerially, was formed. The main source of the lavas was an extensive fissure system on the seaward side of the Blosseville Coast.

Brooks et al. (1976) have presented major and trace element analyses for 23 basalt samples from the area between Kangerdlugssuaq and Scoresby Sund. These basalts are similar to tholeiites on many oceanic islands and have a very uniform composition. They suggested that the bulk of the observed variation might be due to olivine fractionation control. The volcanism is thought to have

begun with updoming by a mantle diapir rising from great depth, probably in the Kangerdlugssuaq region, which was initially enriched in heat, giving rise to a high degree of partial melting. The products of this episode are picritic lavas around the Mikis Fjord. Subsequently, the diapir assumed a more mushroom-like form with melting spreading over a large area, and with a lower percentage of source-rock partial melting. Prior to eruption, although there is no significant differentiation, the magmas had time to collect into large bodies, giving rise to voluminous tholeiitic basalts. The area was then removed from the region of mantle upwelling. In the final stage of volcanism, small amounts of alkali basalts and more evolved rocks were produced. The alkali basalts may have been produced either by fractionation of residual pockets of magma at depth or by a zone-refining process.

Brown and Whitley (1976) have reviewed the origin of the East Greenland flood basalts in the light of petrological characteristics and spatial distribution. They concluded that the lavas do not easily conform to the model of a narrow plume beneath continental crust. Alternatively, they propose the linking of several lithothermal systems into a major convective system. However, the problem between the dual magma-source model and the model of disequilibrium partial melting with phlogopite stability still exists.

CHAPTER 2

GEOCHEMISTRY

2.1. Methods

Eighty-six samples from the five self-contained areas, described in Chapter 1, were analysed for 11 major and minor elements (Si, Al, Fe, Mg, Ca, Na, K, Ti, P, Mn and S), and a selected number of 10 trace elements (Ba, Nb, Zr, Y, Sr, Rb, Zn, Cu, Ni and Cr). All analyses were carried out by the X-ray fluorescence technique. The details of sample preparation and analytical methods are given below.

The samples were split into conveniently sized fragments using a hydraulic cutter, and cleared of the weathered surfaces and amygdale minerals. The fresh fragments were then coarsely crushed with a jaw crusher, followed by grinding for a few minutes to a fine powder in a Tema swing mill. The powder of each sample was mixed thoroughly with a few drops of Mowiol solution, which was used as a binder, and pressed into bricquettes using a confining pressure of about 5-6 tons per square inch in a hydraulic ram.

The bricquettes were analysed on a Philips PW 1212, automatic X-ray fluorescence spectrometer using a TE 108 automatic loader. Routine operating conditions for this machine are given by Reeves (1971).

The major and minor elements (Si, Al, Fe, Ca, Mg,

Na, K, Ti, P and S) were determined using a Cr target. Mn was determined separately using W target. The method of 'fixed counts' was used in analysing these elements in order to minimise systematic and random errors due to any instrument instabilities. In this method, three unknown samples are run along side a monitor which gives an accumulation of pre-determined "N" counts during a period of time (T). The time (T) is automatically recorded, and the three unknown samples are counted over the same time interval, for the same element. Thus allowance can be made for irregularities in the count rates as detected by the monitor.

The standards used in major and minor element analysis were the international standards: G-1, G-2, W-1, GR, GH, GA, BR, AGV-1, BCR-1, GSP-1, DTS-1 and PCC-1. The compositions of these standards have been reviewed by Flanagan (1973).

Mass absorption corrections between the standards and the unknowns were made by the iterative computer procedure of Holland and Brindle (1966) and of Reeves (1971). The FeO content was determined by using a fixed FeO/Fe_2O_3 ratio of 0.7, which is approximately equal to the standard ratio proposed by Brooks (1976).

The trace elements (Ba, Nb, Zr, Y, Sr, Rb, Zn, Cu, Ni and Cr) were determined using W radiation and an absolute

method. The analytical data were converted to concentrations (ppm) by the computer programme "TRATIO" developed by Gill (1972). The programme uses the count-rate function (peak intensity/background intensity -1) which enables scattered background radiation to be used as the internal standard to compensate for matrix and mass absorption effects.

The standards used in trace element analysis were synthetic, spiked glass prepared by the Pilkington Research Laboratory for use in lunar-sample analysis (Brown et al., 1970).

All XRF data and normative minerals are tabulated in Table A-1 and Table A-2 (Appendix).

2.2. Major and minor element analyses

Manson (1967) has published data on major and minor elements of various typical basalts. In this study, the average major and minor oxide values for quartz tholeiites and olivine tholeiites, taken from Manson (1967), were recalculated to 100% to disregard H_2O^+ and H_2O^-. The recalculated values for these basalts and the average values for the eighty-six, studied samples are given in Table 2-1 for comparison. It is obvious that in the broadest sense, the East Greenland tholeiites have high TiO_2, FeO and Fe_2O_3, and low K_2O contents relative to those of Manson (1967).

Table 2-1. Average values for major and minor oxides (weight percent) of the analysed basalts from East Greenland compared with average quartz tholeiites and olivine tholeiites. All analyses are recalculated to 100%

	1	2	3
SiO_2	48.16±0.68	51.47	49.04
TiO_2	2.70±0.37	1.61	1.71
Al_2O_3	15.28±0.15	16.32	15.64
Fe_2O_3	3.24±0.00	3.12	2.62
FeO	10.14±0.49	7.65	8.78
MnO	0.21±0.00	0.17	0.17
MgO	6.27±0.88	6.24	8.48
CaO	11.15±0.52	9.97	10.39
Na_2O	2.46±0.30	2.52	2.32
K_2O	0.22±0.09	0.71	0.60
P_2O_5	0.25±0.00	0.22	0.23

Key: 1. Average of 86 East Greenland lavas

2. Average of 715 quartz tholeiites (Manson, 1967)

3. Average of 182 olivine tholeiites (Manson, 1967)

Fig. 2-1 shows the major and minor oxide variations in relation to the differentiation index of Thornton and Tuttle (1960). The index is defined as the sum of the weight percentage of normative quartz + orthoclase + albite + nepheline + leucite + kalsilite. Al_2O_3, total iron oxide in terms of $FeO+Fe_2O_3$, and TiO_2 seem to be fairly constant throughout the differentiation index range of 16 to 30. MnO and P_2O_5 form linear trends, and appear to increase slightly with the differentiation index. In contrast, the CaO trend diminishes slightly relative to the differentiation index, and MgO shows a noteworthy negative trend.

Because of the rather uniform nature of the East Greenland lavas and the narrow range of the differentiation index compared to those of many other areas, the aphyric, basaltic lavas from mid-west Iceland (Johannesson, 1975), which are believed to have the same origin (primary hot mantle plume) as those of East Greenland (Brooks, 1973b; Schilling and Noe-Nygaard, 1974) have also been plotted in Fig. 2-1. Thus the limited range of the studied lavas is emphasised.

When both of the data sets are taken into account, the slopes of the trends seem to change at a differentiation index value of about 21. The trends for Al_2O_3, $FeO + Fe_2O_3$, TiO_2, P_2O_5, and MnO are nearly constant in differentiation-

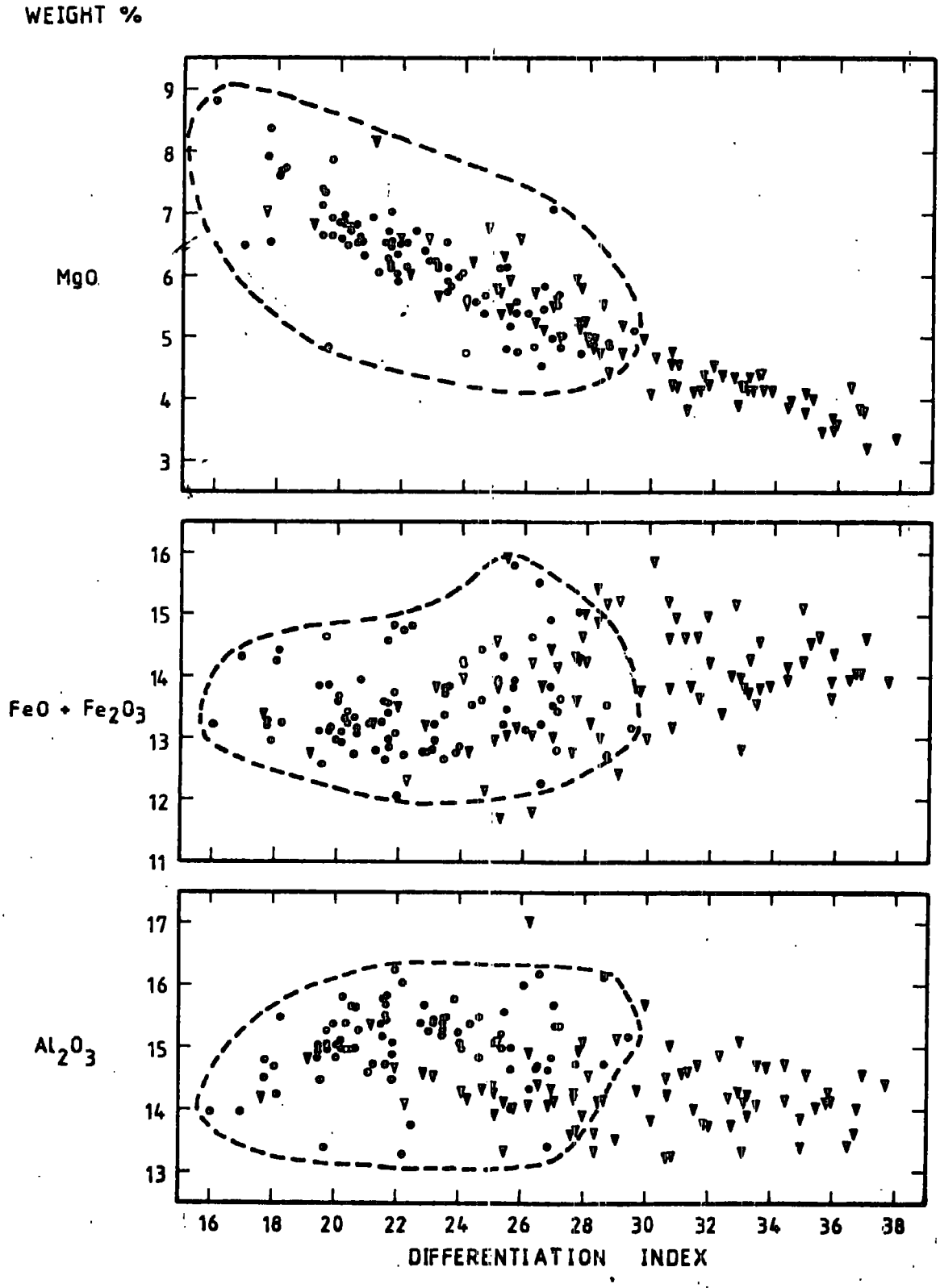
WEIGHT %
MgO
FeO + Fe2O3
Al2O3
DIFFERENTIATION INDEX

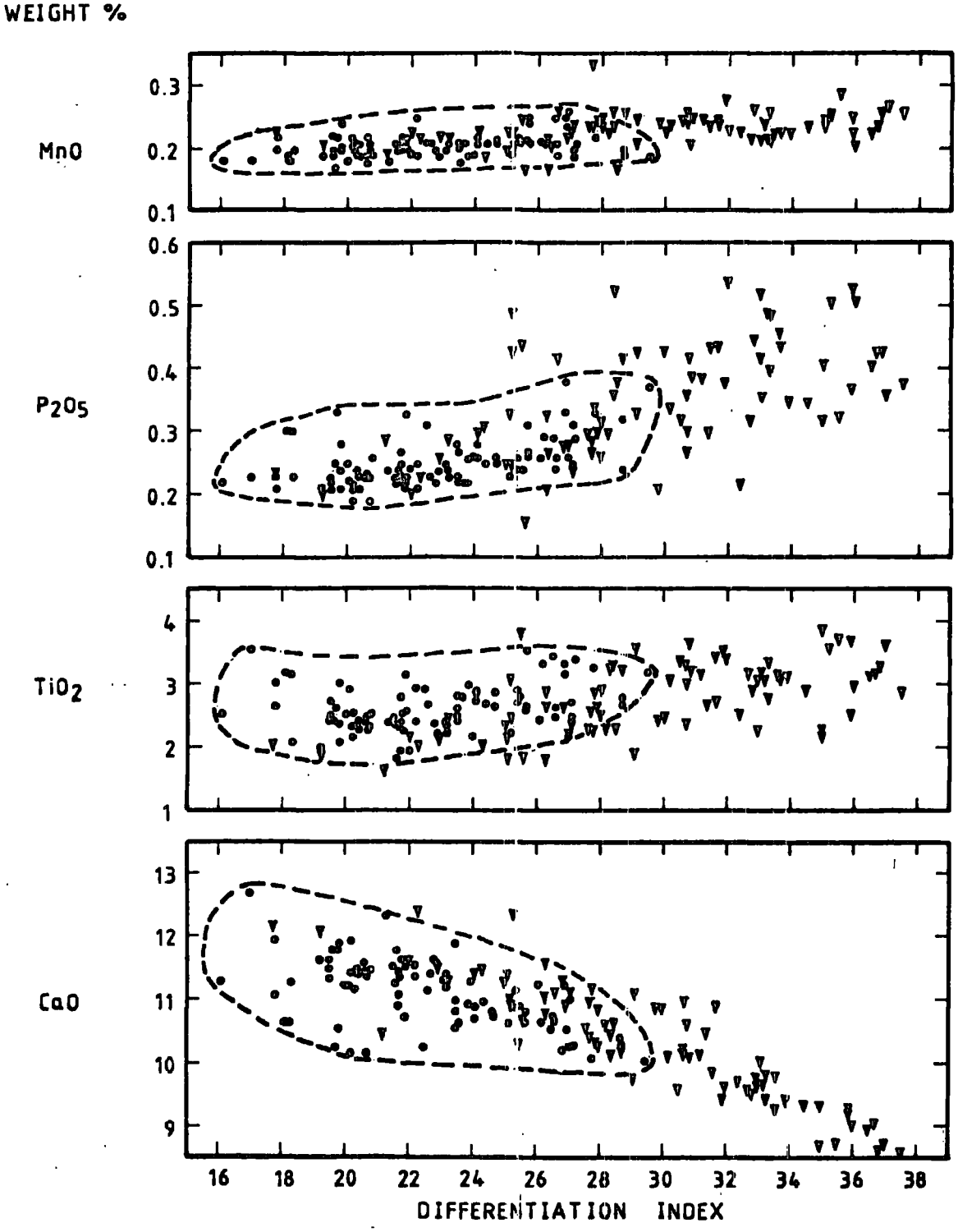
WEIGHT %
MnO
0.3
0.2
0.1
P2O5
0.6
0.5
0.4
0.3
0.2
0.1
TiO2
4
3
2
1
CaO
13
12
11
10
9
16
18
20
22
24
26
28
30
32
34
36
38
DIFFERENTIATION INDEX

index, ranging from 16 to 21. However, in the more evolved magmas, the trend for Al_2O_3 shows a slight decrease, but the trends for Fe_2O_3 + FeO, TiO_2, P_2O_5 and MnO appear to increase. The MgO and CaO trends descend in almost linear fashion, relative to differentiation index.

The pattern of the trends is probably attributable to the different proportions of minerals separating from successive liquids. In the earlier stage, the decreases in MgO and CaO, while Al_2O_3 is still constant, imply that the lavas might be controlled by removal of olivine and pyroxene. The slight depletion of Al_2O_3 in the later stage seems to be an indication of plagioclase involvement in controlling the composition of the more differentiated magma. Suppression of crystallisation of the Fe-Ti oxide phases might also be included in the earlier differentiation process, according to the constancy in the total iron and TiO_2 trends.

In spite of little variation in SiO_2 contents, the eighty-six analyses, including their total alkalis and Fe/Mg ratios, have been divided into five groups based on 1% intervals in the SiO_2 percentage. Where there is too great a sample population relative to other groups, SiO_2 intervals of 0.5% have been used. The total iron oxides used here were calculated as Fe_2O_3, and all oxide analyses were adjusted to total 100% The results of averaging major

and minor oxides within each group are given in Table 2-2. It is discerned that MgO contents decrease steadily; on the contrary, Na_2O (including total alkalis) and Fe/Mg ratios increase systematically. This supports the inference from Fig. 2-1 that separation of olivine + clinopyroxene, and subsequently of clinopyroxene + plagioclase, probably took place during the cooling history.

The relative proportions of iron ($FeO+Fe_2O_3$), total alkalis and MgO (as weight percent) in the rocks from East Greenland are plotted on the AFM diagram in Fig. 2-2. The same plots for the basaltic lavas from mid-west Iceland (Johannesson, 1975), the low-alkali tholeiites of Skye (I.T. Williamson, personal communication), the Atlantic ocean-floor tholeiites (Engel et al., 1965), and the picritic lava from East Greenland (Brooks et al., 1976) are also illustrated. It is clearly seen that these lavas fall on nearly the same trend, except for the ocean-floor tholeiites, all lying close to the Hawaiian tholeiitic trend (Macdonald and Katsura, 1964). If the ocean-floor tholeiites are not taken into consideration, the course of the plotted trend seems to show a strong decrease in MgO in the initial stage and a slight decrease in both MgO and $FeO+Fe_2O_3$. The divergence of the trend (at approximately 65% $FeO+Fe_2O_3$, 15% Na_2O+K_2O and 20% MgO) can be ascribed to differing proportions of the control minerals in the

Table 2-2. Average compositions (major and minor oxides, weight percent) of the analysed lavas, grouped according to silica content. Total iron oxides are expressed as Fe_2O_3.

Group No.	1	2	3	4	5	6
SiO_2 % grouping	45.0-46.0	46.0-47.0	47.0-47.5	47.5-48.0	48.0-49.0	>49.0
Abundance of specimens	2	11	23	30	18	2
SiO_2	45.56	46.55	47.28	47.66	48.37	49.31
Al_2O_3	14.47	14.47	14.92	15.07	15.01	14.63
Fe_2O_3	14.63	15.23	14.77	14.52	14.29	14.66
MgO	6.89	6.90	6.34	6.16	5.64	5.12
CaO	11.59	11.06	11.15	11.05	10.77	10.36
Na_2O	2.18	2.20	2.35	2.45	2.62	2.74
K_2O	0.28	0.26	0.16	0.20	0.28	0.35
TiO_2	2.68	2.89	0.62	2.49	2.59	2.40
MnO	0.20	0.21	0.21	0.20	0.20	0.23
P_2O_5	0.21	0.26	0.24	0.27	0.27	0.25
Na_2O+K_2O	2.46	2.46	2.52	2.65	2.89	3.09
FeO/FeO+MgO	0.60	0.61	0.62	0.62	0.64	0.67

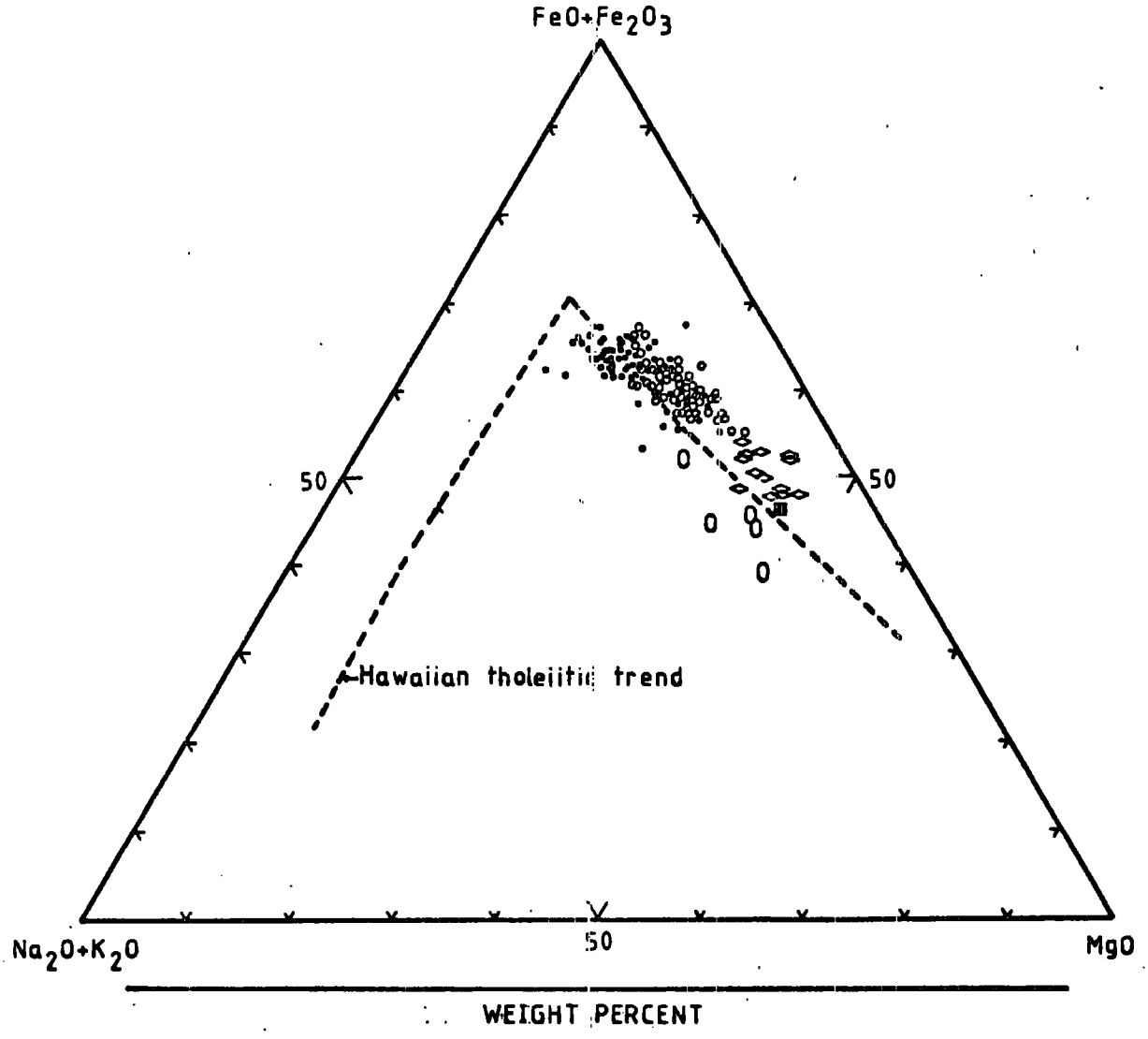
FeO+Fe2O3
50
50
Hawaiian tholeiitic trend
Na2O+K2O
50
MgO
WEIGHT PERCENT

fractionation process. Olivine and/or clinopyroxene fractionation can account for the depletion in MgO and the enrichment of $FeO+Fe_2O_3$ in the earlier stage. The subsequent slight impoverishment in both MgO and $FeO+Fe_2O_3$ could be explained by substraction of either Fe-Ti oxide minerals + olivine $\pm$ clinopyroxene or calcic plagioclase + olivine $\pm$ clinopyroxene from the successive liquid.

Holland and Brown (1972) studied the geochemistry of the Ardnamurchan cone sheets, which are part of the North Atlantic Tertiary Igneous Province, and proposed Hebridean tholeiitic trends based on total alkalis against SiO_2, and on total alkalis versus Fe/Mg ratio diagrams. In this study, the tholeiitic lavas from East Greenland, mid-west Iceland and Skye were plotted on such diagrams (Figs. 2-3, a,b). These lavas form a distinct linear trend, extending the Hebridean tholeiitic trend towards the lower range of SiO_2 values, on the total alkalis - silica plot (Fig. 2-3, a). However, on the total alkalis versus Fe/Mg ratio plot (Fig. 2-3, b), the plotted trend is not conformable to the Hebridean tholeiitic trend between Fe/Mg ratios of 0.65 to 0.80, and is slightly lower in $Na_2O + K_2O$ than the proposed Hebridean tholeiitic trend (Tilley et al., 1967) when the Fe/Mg ratio is lower than 0.60, and then gradually increases in Na_2O+K_2O compared to that of the Hawaiian tholeiite series. At an Fe-Mg ratio of about 0.75, the newly established trend

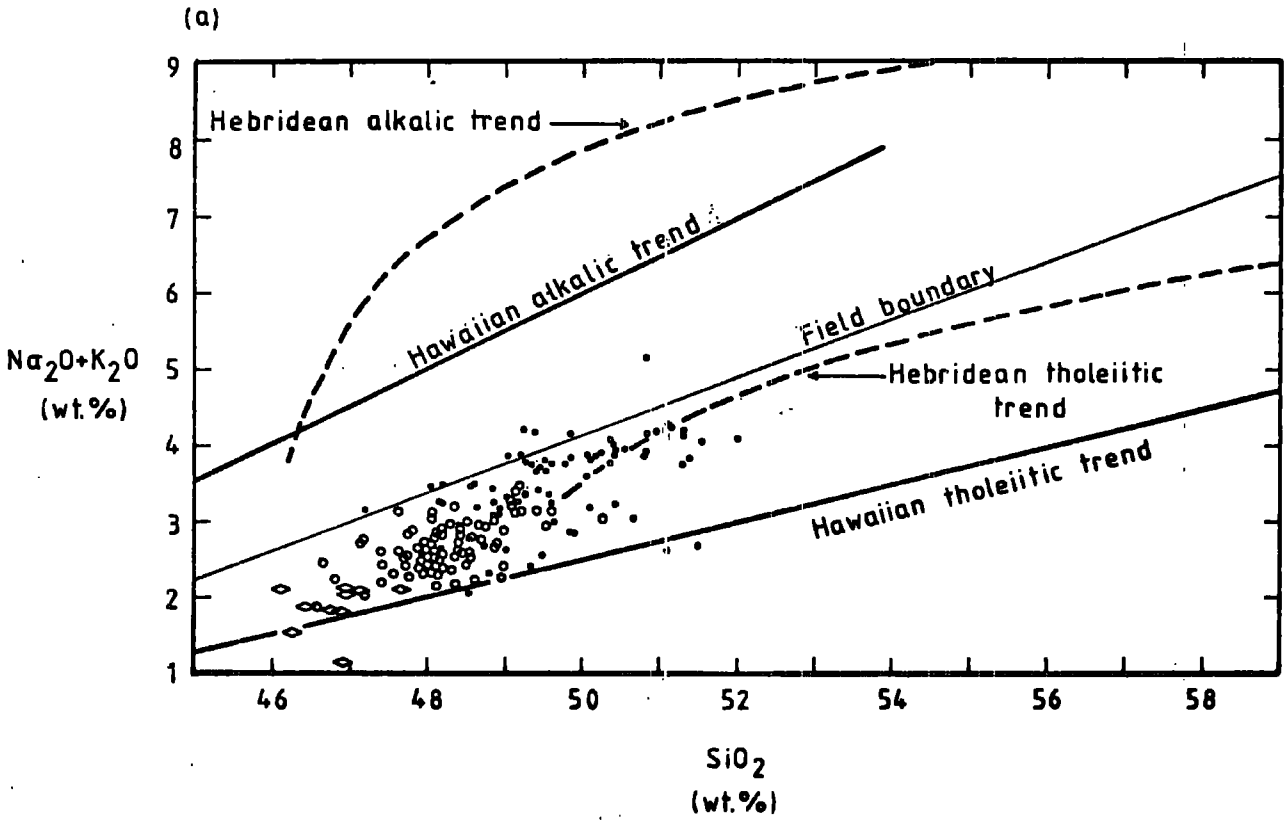
(a)
Hebridean alkalic trend
Hawaiian alkalic trend
Field boundary
Hebridean tholeiitic trend
Hawaiian tholeiitic trend
Na2O+K2O (wt.%)
SiO2 (wt.%)
9
8
7
6
5
4
3
2
1
46
48
50
52
54
56
58

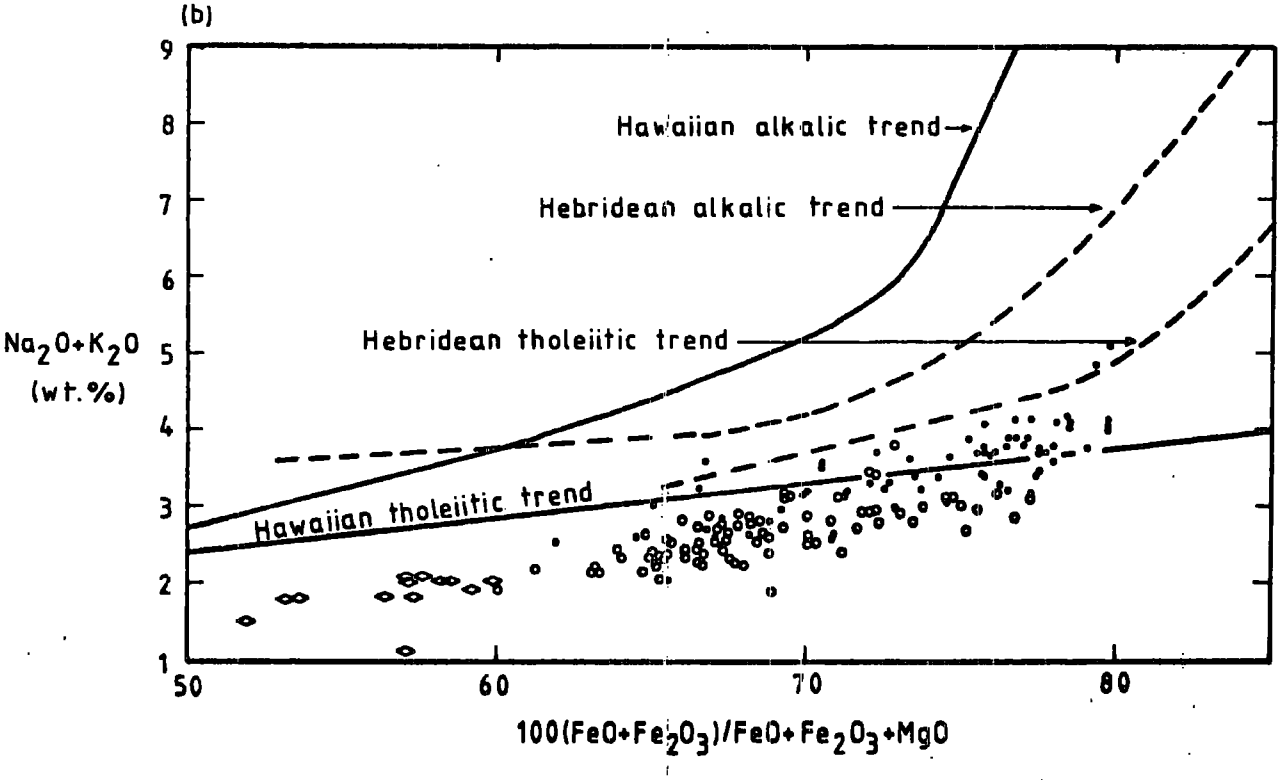
(b)
Hawaiian alkalic trend
Hebridean alkalic trend
Hebridean tholeiitic trend
Hawaiian tholeiitic trend
Na2O+K2O (wt.%)
100(FeO+Fe2O3)/FeO+Fe2O3+MgO
9
8
7
6
5
4
3
2
1
50
60
70
80

ascends rapidly, and is in harmony with the Hebridean tholeiitic trend.

In Fig.2-3, b, the East Greenland trend, which is a segment of the newly established trend, lying between an Fe/Mg ratio of 0.60 and 0.70, appears to change direction at an Fe/Mg ratio of about 0.67. This pattern, again, can be ascribed to the result of differing proportions of minerals separating from the successive liquids. Ferromagnesian mineral fractionation can account for the earlier trend, and plagioclase, together with ferromagnesian fractionation for the more evolved trend.

Fig. 2-4 shows the plot of FeO+MgO against FeO/MgO (Macdonald and Katsura, 1964) for the studied lavas and the mid-west Icelandic lavas (Johannesson, 1975). It appears that the majority of the East Greenland lavas fall close to the point where the change in the Hawaiian tholeiitic trend occurs, and have a similar pattern to the Hawaiian tholeiitic trend. In other words, the lavas were mainly controlled by olivine in the first stage, and subsequently by plagioclase and pyroxene. The tholeiitic lavas of mid-west Iceland form a trend, slightly lower in FeO+MgO than the East Greenland tholeiites, and subparallel to the Hawaiian feldspar-pyroxene control line. The higher FeO+MgO in the East Greenland tholeiites might be due to the uncertainty of oxidation ratio.

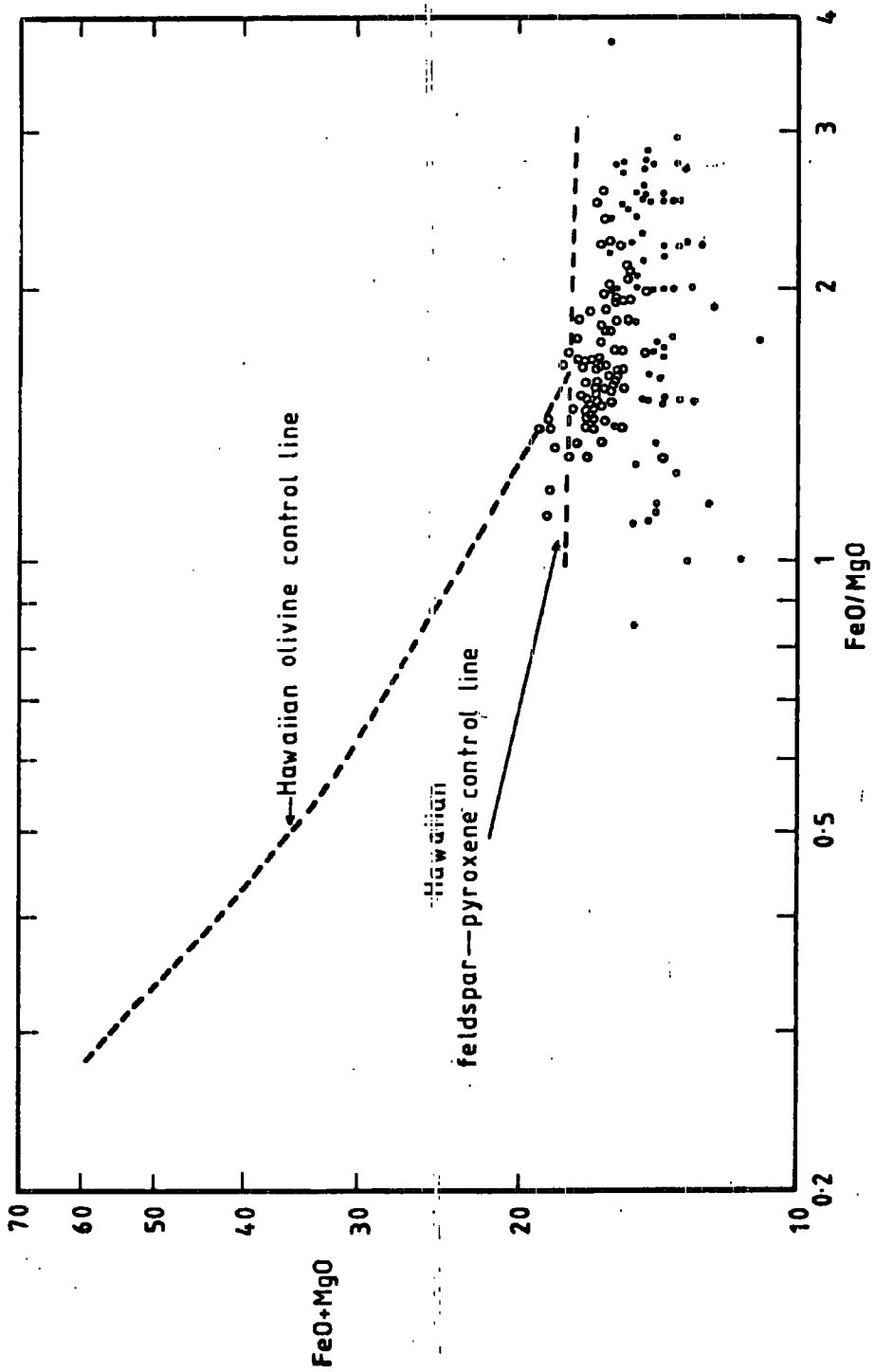
Hawaiian olivine control line
Hawaiian
feldspar—pyroxene control line
FeO+MgO
FeO/MgO
70
60
50
40
30
20
10
0·2
0·5
1
2
3
4

2.3. Trace element analyses

The chemical data tabulated in Table 2-3 are the average trace-element values for the lavas described in this thesis, and for certain quartz tholeiites and olivine tholeiites (Prinz, 1967). It is clearly seen that the average values for the East Greenland tholeiites are higher in Zr and Cu, and lower in Ba, Sr and Rb than those taken from Prinz's data.

The variation diagrams for the studied trace elements in relation to the differentiation index (Thornton and Tuttle, 1960) are shown in Fig. 2-5. In addition to the data from East Greenland, the data for aphyric, tholeiitic lavas from mid-west Iceland (Johannesson, 1975) have also been displayed for comparative purposes.

From Fig. 2-5, if only the East Greenland data are taken into consideration then they do not define clear trends except for Nb, Y, Rb and Zn. However, the trend for Cu seems to increase whereas that for Cr seems to decrease with the differentiation index. The Nb, Y, Rb and Zn trends are approximately parallel to the axis representing the differentiation index.

The trends are much more pronounced when both of the data, i.e. East Greenland and mid-west Iceland, are considered. These trends seem to change their slopes at a differentiation index of about 21 as do those for major

Table 2-3. Average values (ppm) for trace elements of the analysed basalts from East Greenland, compared with average quartz tholeiites and olivine tholeiites

	1	2	3
Ba	89 ± 21	250 (146 samples)	215 (32 samples)
Nb	17 ± 4	*	*
Zr	167 ± 32	111 (146 samples)	91 (31 samples)
Y	32 ± 5	32 (123 samples)	32 (23 samples)
Sr	237 ± 38	471 (145 samples)	350 (31 samples)
Rb	9 ± 4	33 (51 samples)	18 (11 samples)
Zn	90 ± 12	*	*
Cu	241 ± 36	141 (83 samples)	75 (22 samples)
Ni	90 ± 34	77 (156 samples)	130 (29 samples)
Cr	139 ± 53	153 (151 samples)	218 (25 samples)

Key: 1. Average of 86 analysed samples

2. Average of quartz tholeiites (Prinz, 1967)

3. Average of olivine tholeiites (Prinz, 1967)

* No data available.

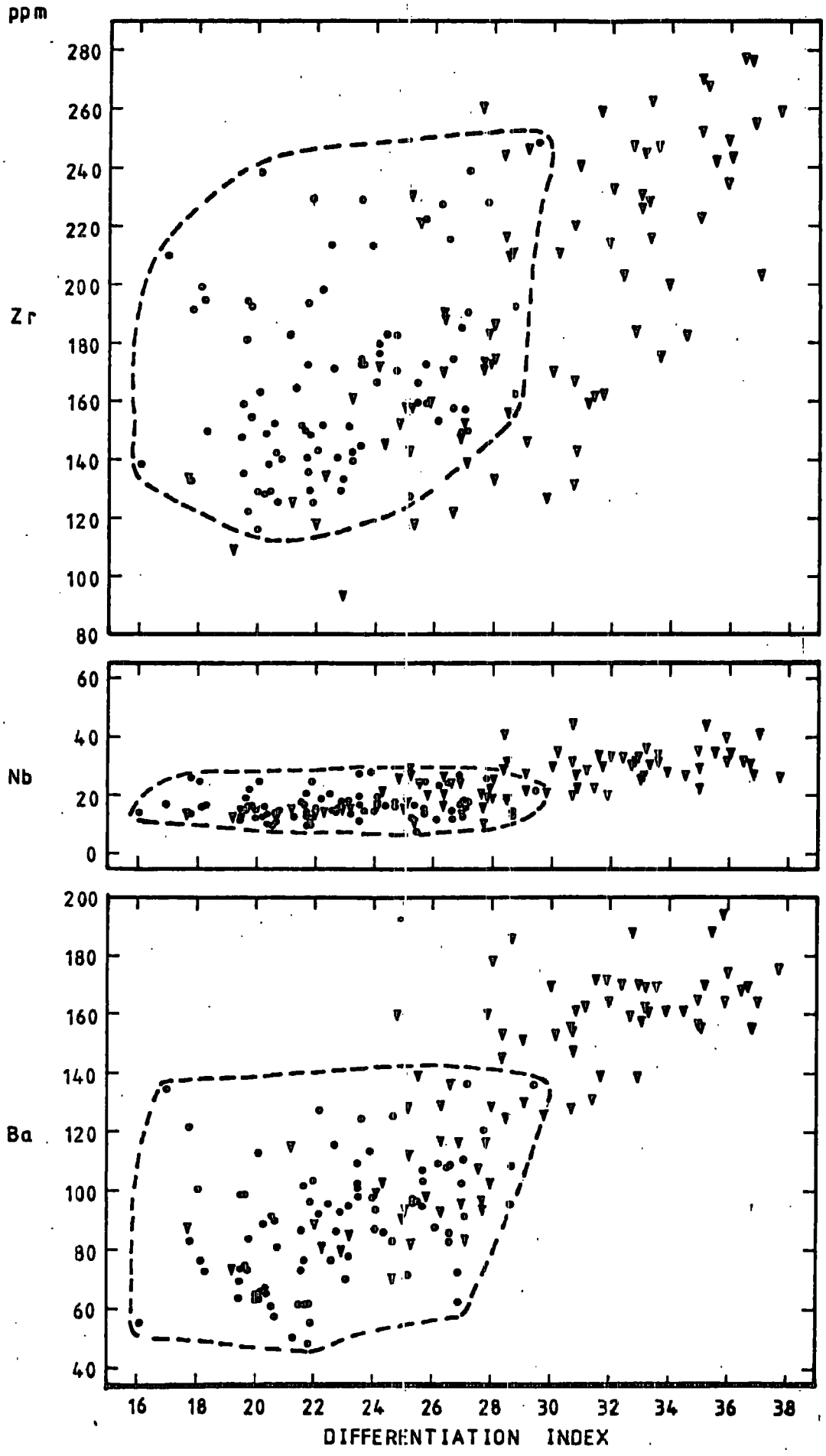
ppm
Zr
280
260
240
220
200
180
160
140
120
100
80
Nb
60
40
20
0
Ba
200
180
160
140
120
100
80
60
40
16
18
20
22
24
26
28
30
32
34
36
38
DIFFERENTIATION INDEX

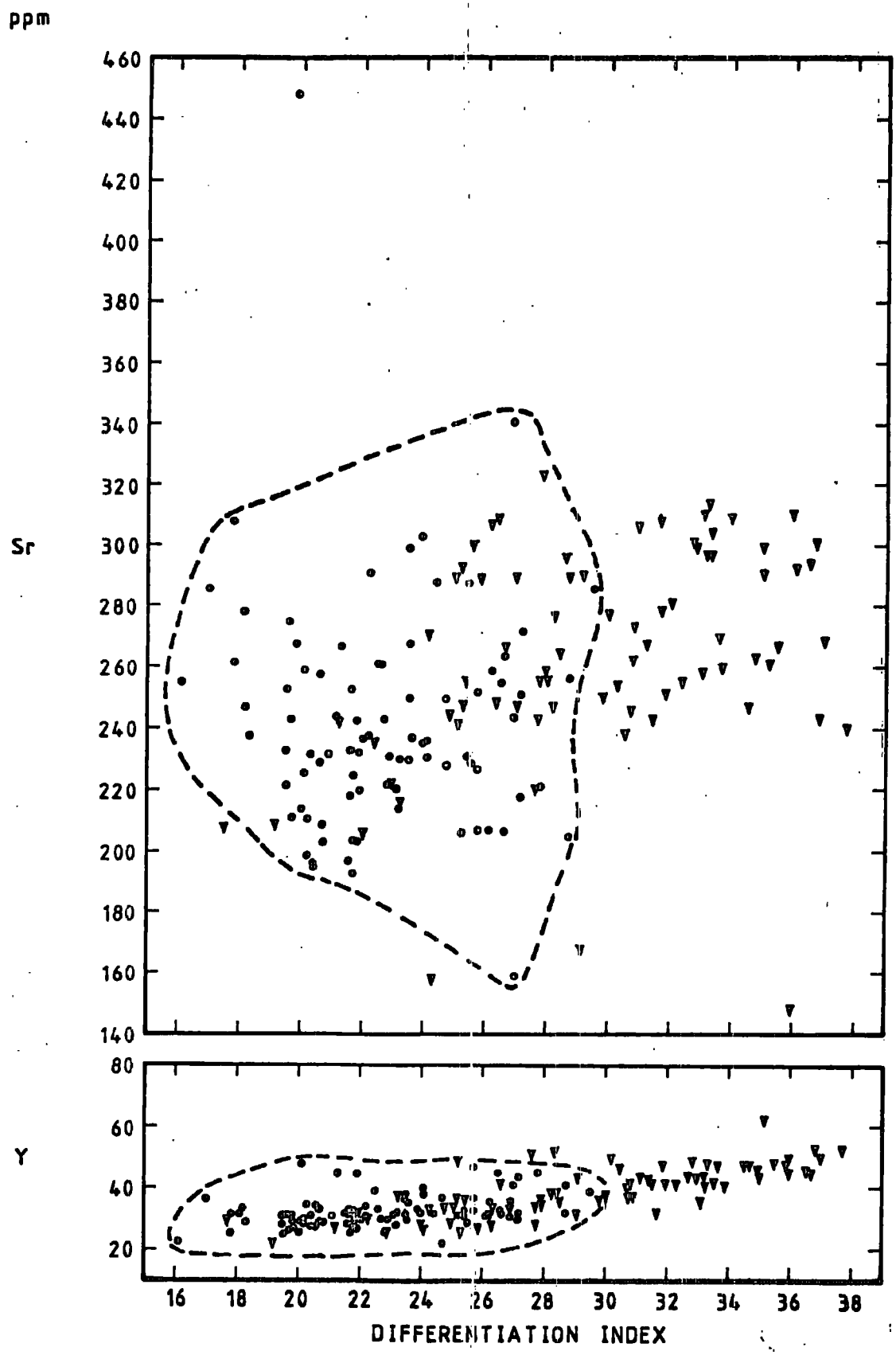
ppm
Sr
Y
460
440
420
400
380
360
340
320
300
280
260
240
220
200
180
160
140
80
60
40
20
16
18
20
22
24
26
28
30
32
34
36
38
DIFFERENTIATION INDEX

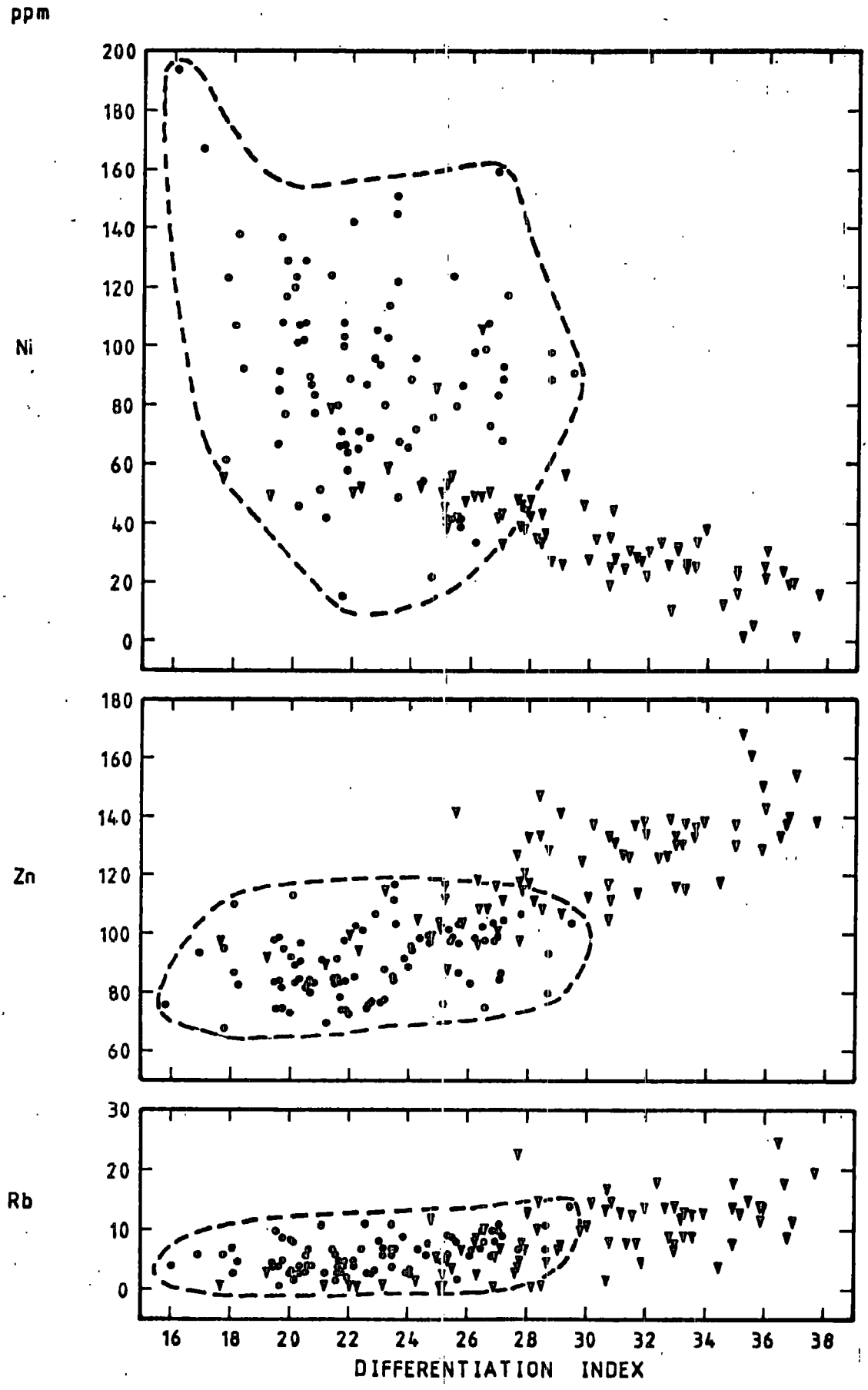
ppm
Ni
Zn
Rb
200
180
160
140
120
100
80
60
40
20
0
180
160
140
120
100
80
60
30
20
10
0
16
18
20
22
24
26
28
30
32
34
36
38
DIFFERENTIATION INDEX

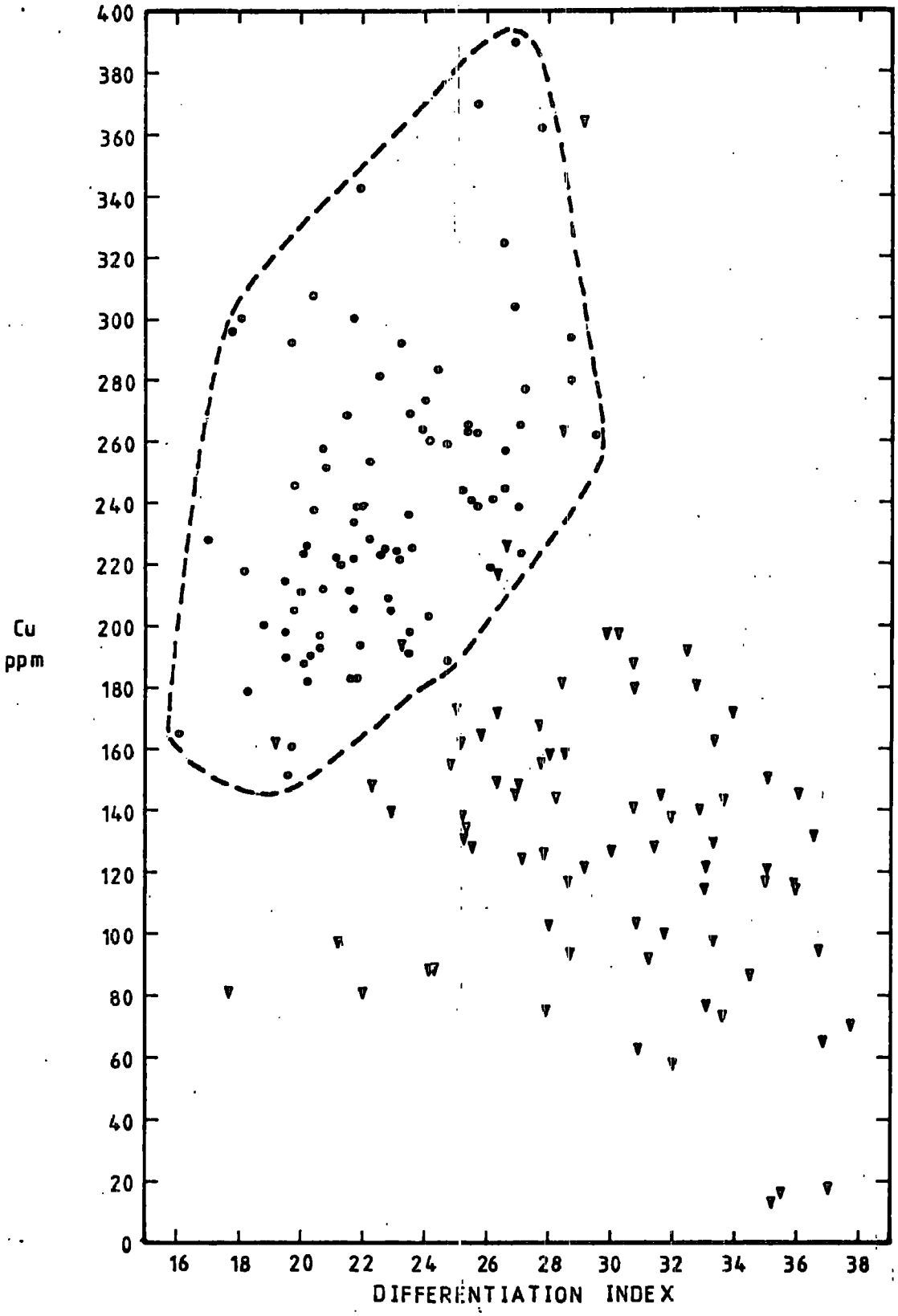
Cu
ppm
400
380
360
340
320
300
280
260
240
220
200
180
160
140
120
100
80
60
40
20
0
16
18
20
22
24
26
28
30
32
34
36
38
DIFFERENTIATION INDEX

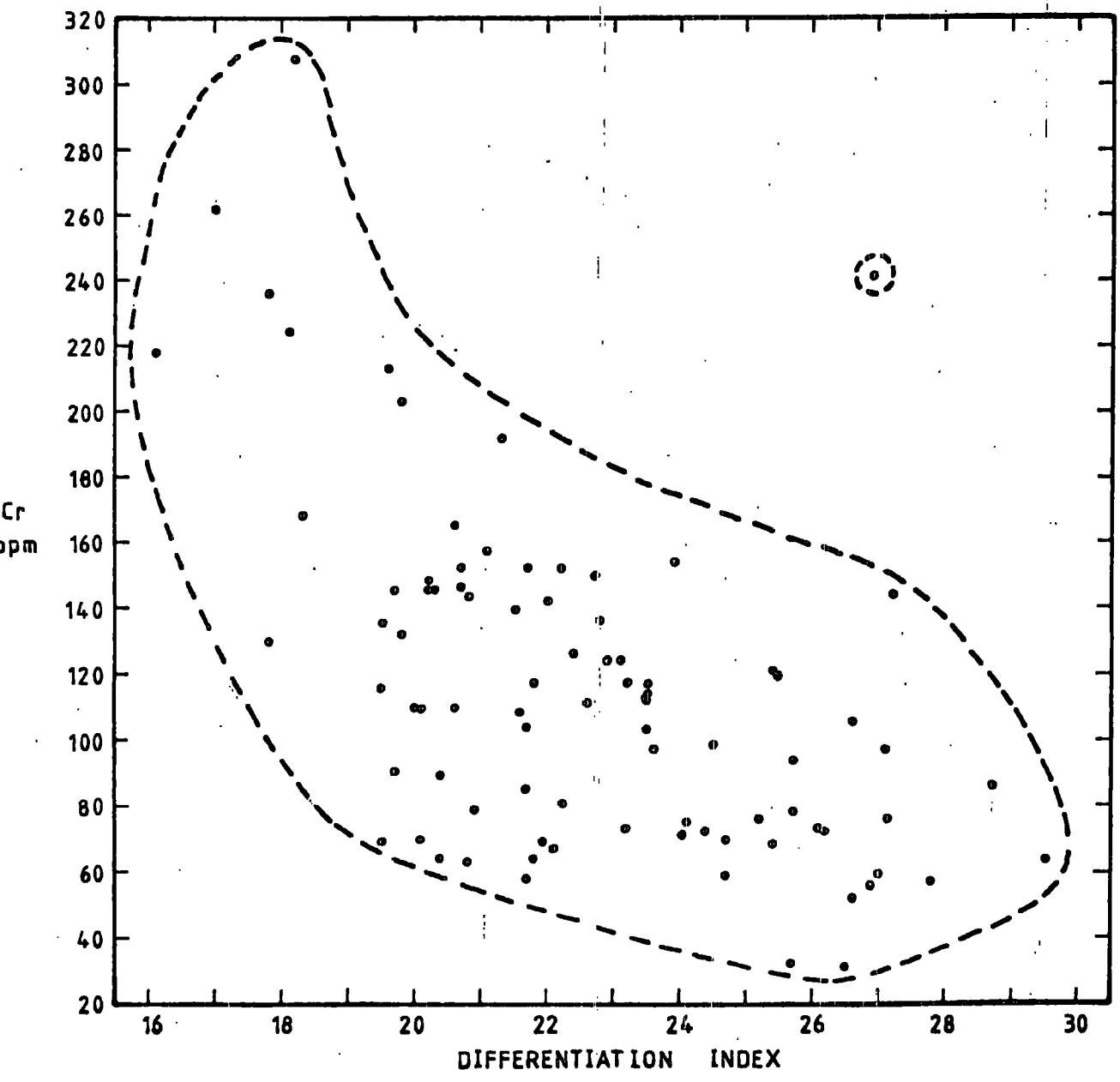
320
300
280
260
240
220
200
180
160
140
120
100
80
60
40
20
Cr
ppm
16
18
20
22
24
26
28
30
DIFFERENTIATION INDEX

and minor oxides/elements. Nb, Y, Rb and Zn form markedly linear trends, with constant values in the earlier stage, and with positive slopes in the more advanced stage represented by the differentiation index. Ba, Zr and Sr appear to increase but Cu seems to diminish relative to the differentiation index. The trend for Ni shows a strong negative slope in the first stage, and is fairly constant in the more advanced magma. Although there are no data on Cr for the mid-west Icelandic lavas, the Cr trend appears to consist of two different slopes, with similar pattern to the Ni trend. From such evidence, as well as petrographic evidence, it can be inferred that the lavas were controlled by olivine, spinel (picotite) and clinopyroxene fractionation in the initial stage of cooling history. Furthermore, the criteria for discriminating between the oceanic tholeiites initially governed by separation of olivine, and those firstly controlled by plagioclase fractionation were summarised by G. Thompson et al. (1972). The tholeiites characterised by olivine as the first mineral to crystallise, show a decrease in Cr and Ni concentrations in the early stage of fractionation. In contrast, those characterised by plagioclase as the first mineral to crystallise do not show a systematic Ni and Cr trend in the initial stage of fractionation. That summary supports the deduction in this study that olivine crystallised earlier than plagioclase.

Pearce and Flower (1977) have shown the role of fractional crystallisation for lavas at accreting plate margins by using diagrams based on Ce/Sm, Sm/Yb and the other ratios of Al_2O_3/TiO_2 and Cr/Ti. Two of these diagrams, i.e. Al_2O_3/TiO_2 versus Ti, and Cr/Ti versus Ti diagrams, have been displayed. In view of the Al_2O_3/TiO_2 - Ti plot (Fig. 2-6), it is obvious that the East Greenland tholeiites form a linear pattern approximately parallel to the trend for garnet fractionation. However, in terms of mantle-source control, garnet could be involved but it is more likely that the fractionation of the basalts occurred at lower pressures, where plagioclase was the dominant aluminous phase; hence, the lavas might be largely controlled by plagioclase with small amounts of olivine and clinopyroxene. In contrast, when the Cr/Ti - Ti diagram (Fig. 2-7) is considered, the East Greenland trend seems to conform with the models of olivine + 1.2% spinel, and clinopyroxene fractionation. The difference between the East Greenland patterns in Fig. 2-6 and Fig. 2-7 might be explained by two episodes of different mineral fractionation.

The tholeiitic lavas from East Greenland and those of mid-west Iceland (Johannesson, 1975) are plotted on the CaO-Y diagram of Lambert and Holland (1974) in Fig. 2-8. These lavas appear to form the L-type trend indicating plagioclase-augite control in their fractionation processes.

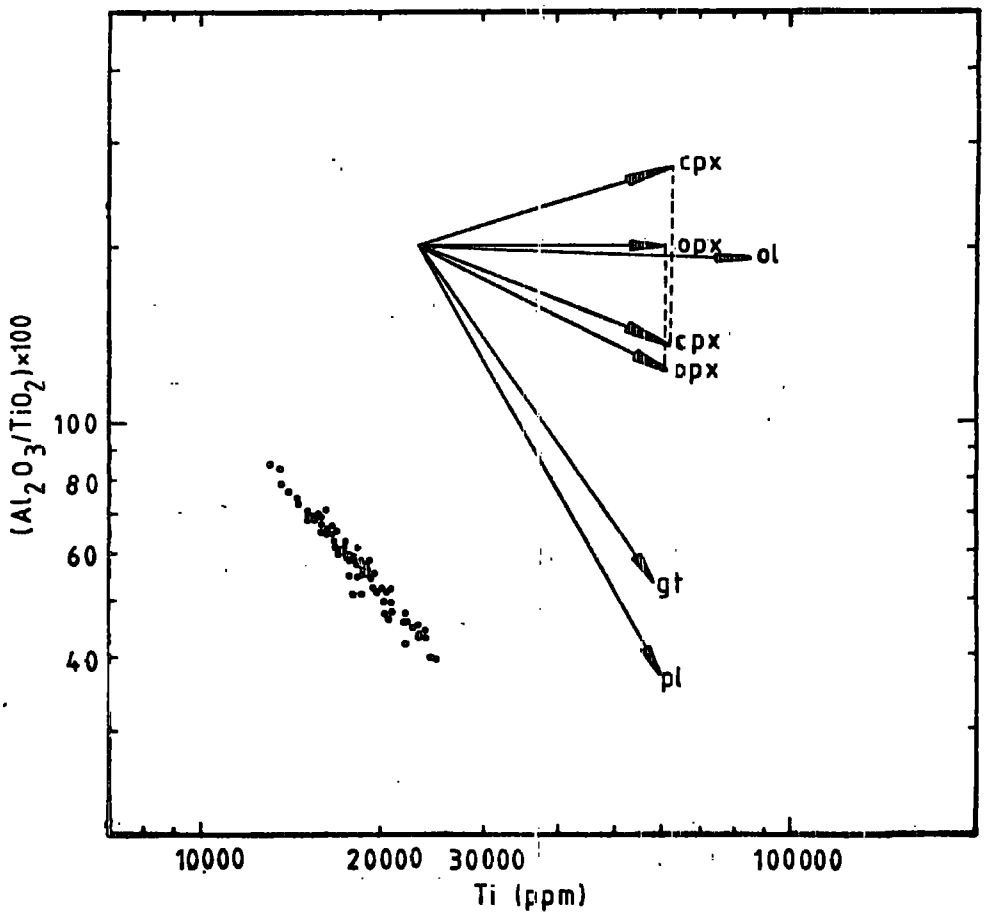
cpx
opx
ol
cpx
opx
gt
pl
100
80
60
40
10000
20000
30000
100000
Ti (ppm)
$(Al_2O_3/TiO_2)\times100$

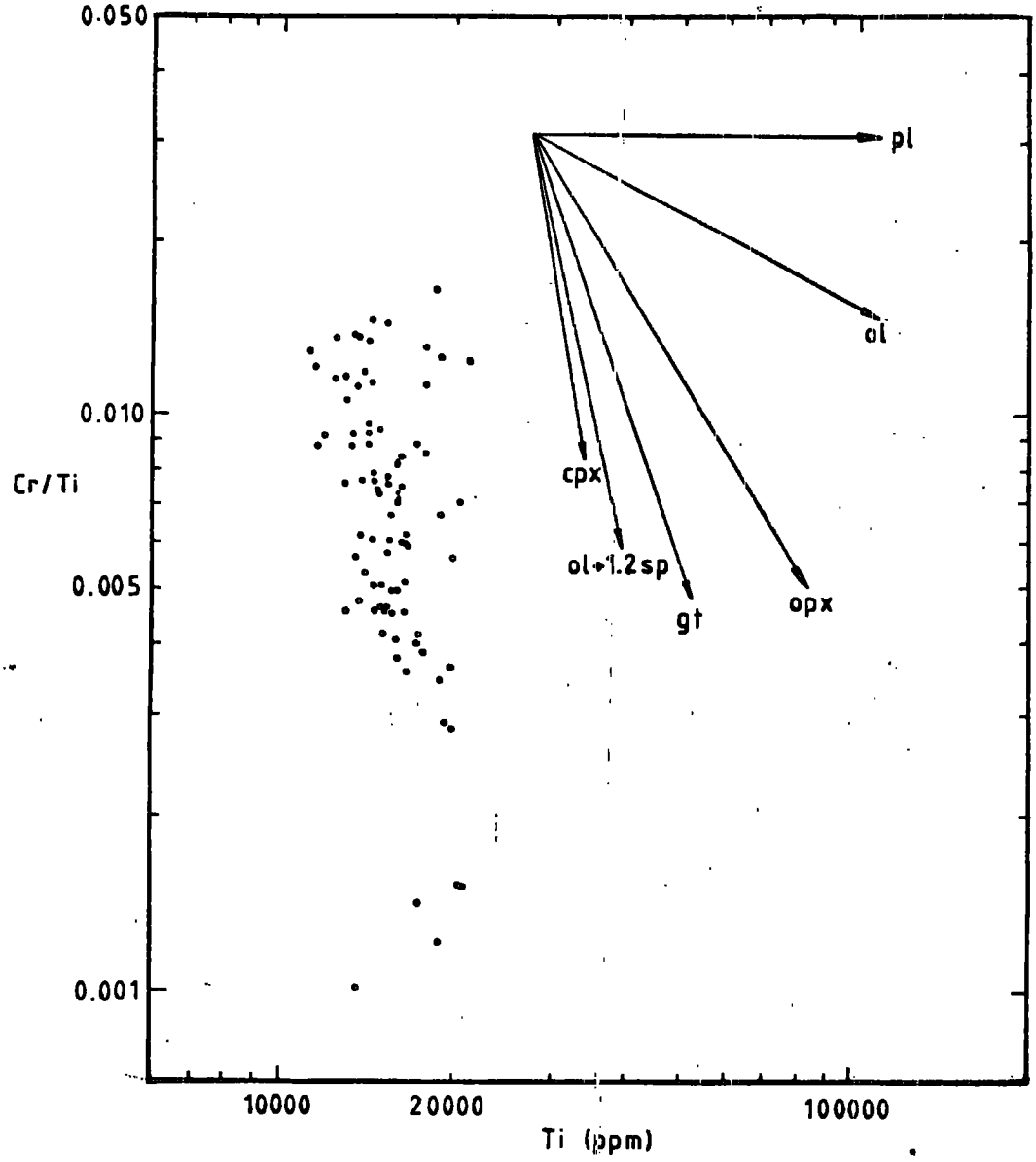
0.050
0.010
0.005
0.001
Cr/Ti
pl
ol
cpx
ol+1.2sp
gt
opx
10000
20000
100000
Ti (ppm)

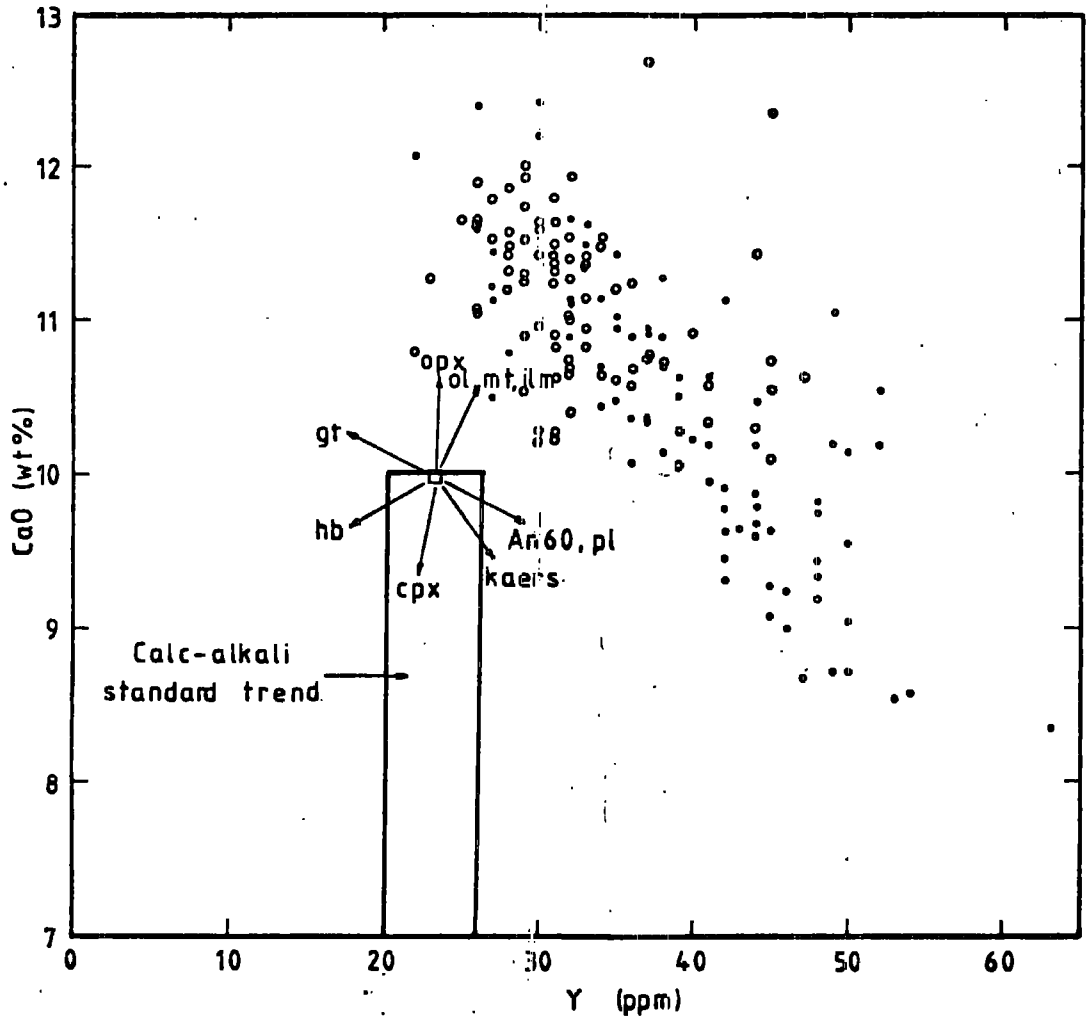
13
12
11
10
9
8
7
CaO (wt%)
0
10
20
30
40
50
60
Y (ppm)
opx
ol, mt, ilm
gt
hb
cpx
An60, pl
kaers.
Calc-alkali
standard trend

The appearance of the slight kink at CaO and Y contents of about 10% and about 30 ppm, respectively, might be the singificant evidence in interpreting their petrogenesis. These lavas are likely to be dominantly controlled by olivine + ilmenite + magnetite initially, and subsequently by plagioclase + clinopyroxene.

2.4. Other chemical relationships

Fig. 2-9 shows the variations of the major oxides and trace elements for the tholeiites belonging to each self-contained area, with the relative heights as described in Chapter 1. The coefficient of variation is comparatively low for all major and minor oxides, and some trace elements (Rb, Y, Nb and Zn), but is relatively high for the other trace elements (Ba, Zr, Sr, Cu, Ni and Cr). The high peaks for Sr in sample number 143908 (2,225 m in height), Cu in sample number 143889 (1,520 m in height), and Ni and Cr in sample number 143902 (2,160 m in height) were of interest to ascertain some special minerals in these rocks in addition to their common constituents. From the results of investigations, the high peak for Sr can be ascribed to the presence of zeolites and apophyllite as amygdale minerals. For the specimens with high Cu peak, copper minerals were carefully searched for, petrographically, but have not been detected. Nevertheless, partial analyses for Cu in feldspar, pyroxene and Fe-Ti oxides were performed by electron microprobe;

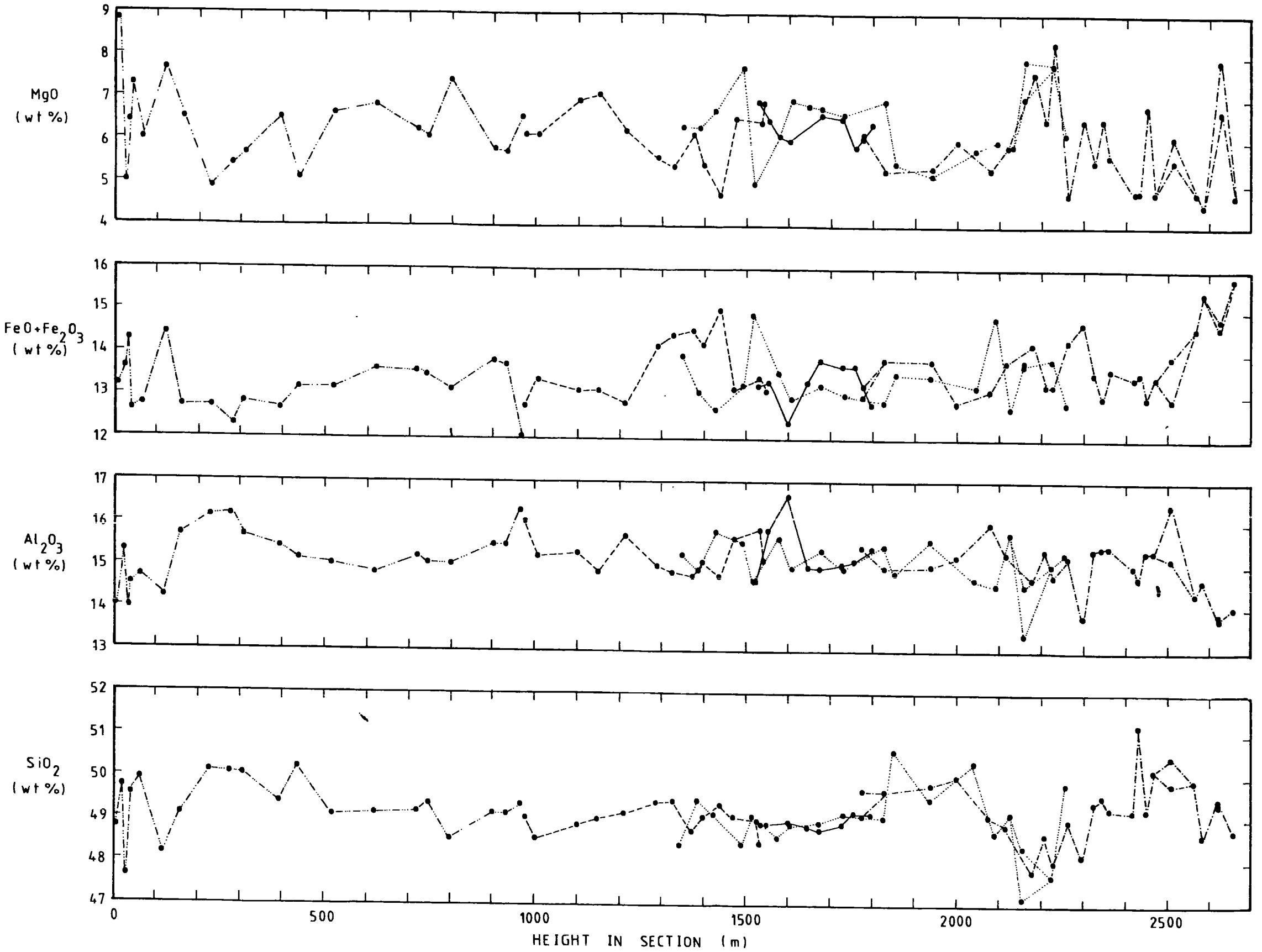
MgO
(wt %)
9
8
7
6
5
4
FeO+Fe2O3
(wt %)
16
15
14
13
12
Al2O3
(wt %)
17
16
15
14
13
SiO2
(wt %)
52
51
50
49
48
47
0
500
1000
1500
2000
2500
HEIGHT IN SECTION (m)

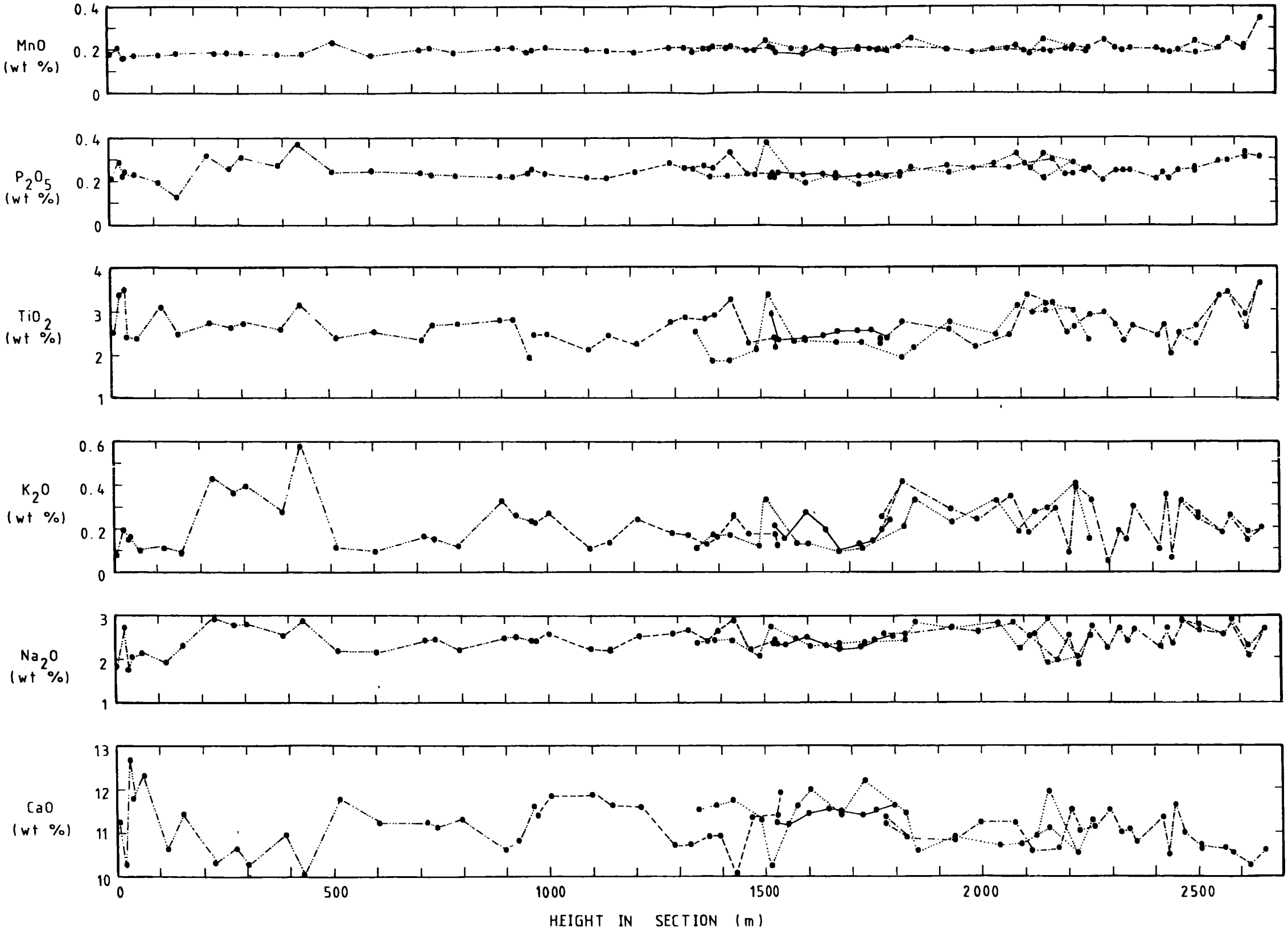
MnO (wt %)
0.4
0.2
0
P_2O_5 (wt %)
0.4
0.2
0
TiO_2 (wt %)
4
3
2
1
K_2O (wt %)
0.6
0.4
0.2
0
Na_2O (wt %)
3
2
1
CaO (wt %)
13
12
11
10
0
500
1000
1500
2000
2500
HEIGHT IN SECTION (m)

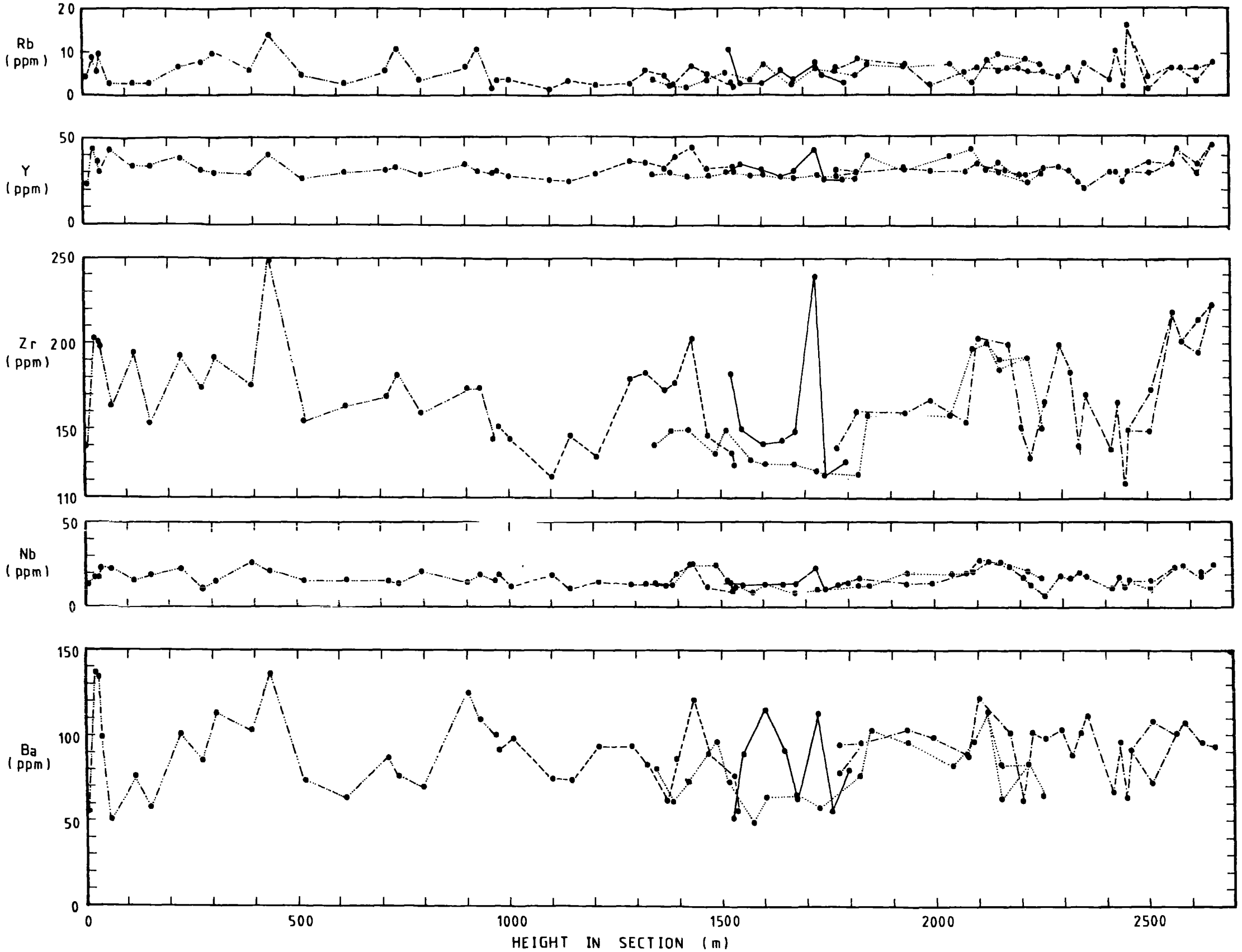
Rb
(ppm)
20
10
0
Y
(ppm)
50
0
Zr
(ppm)
250
200
150
110
Nb
(ppm)
50
0
Ba
(ppm)
150
100
50
0
0
500
1000
1500
2000
2500
HEIGHT IN SECTION (m)

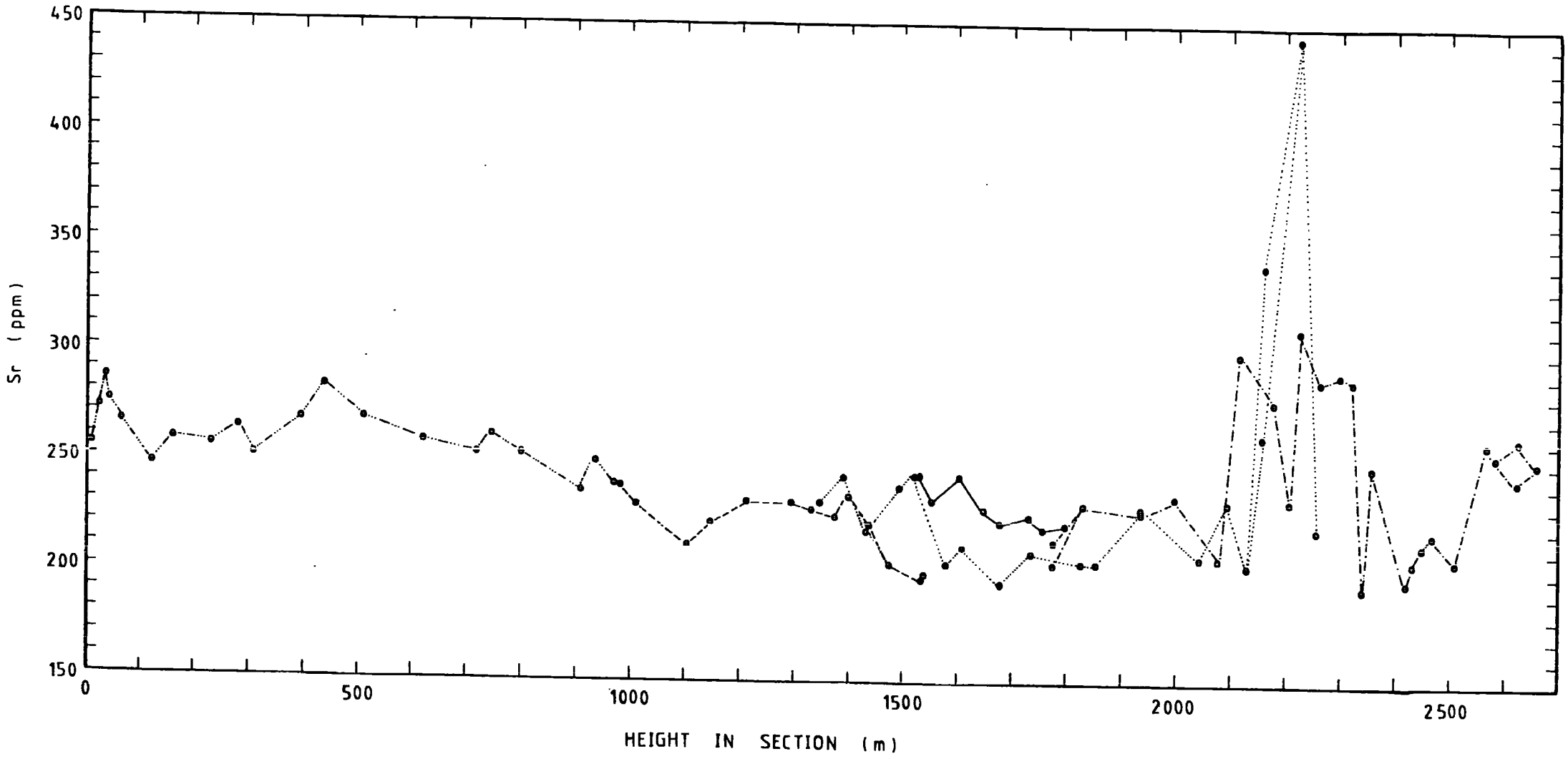
450
400
350
300
250
200
150
Sr (ppm)
0
500
1000
1500
2000
2500
HEIGHT IN SECTION (m)

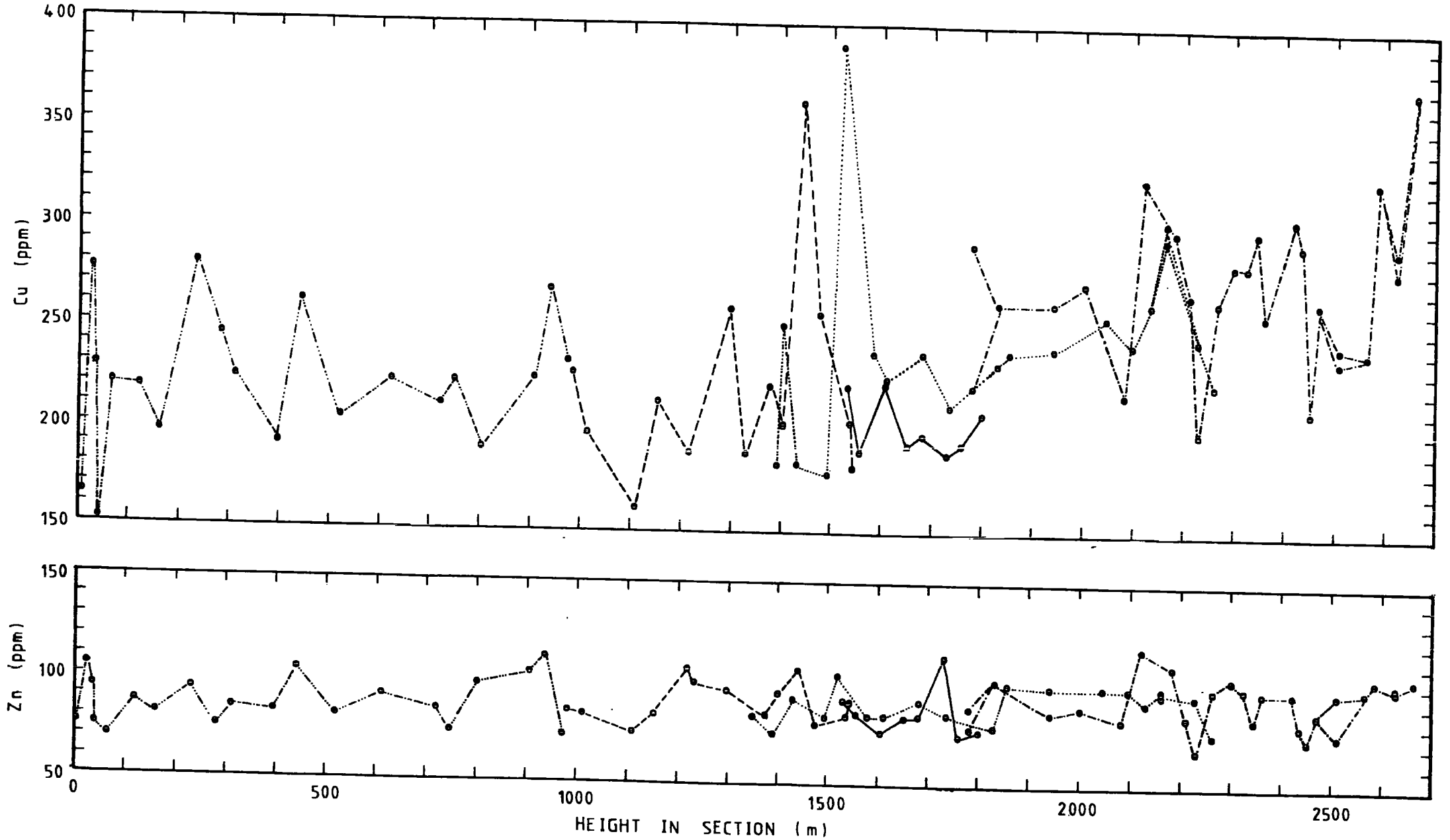
Cu (ppm)
400
350
300
250
200
150
Zn (ppm)
150
100
50
0
500
1000
1500
2000
2500
HEIGHT IN SECTION (m)

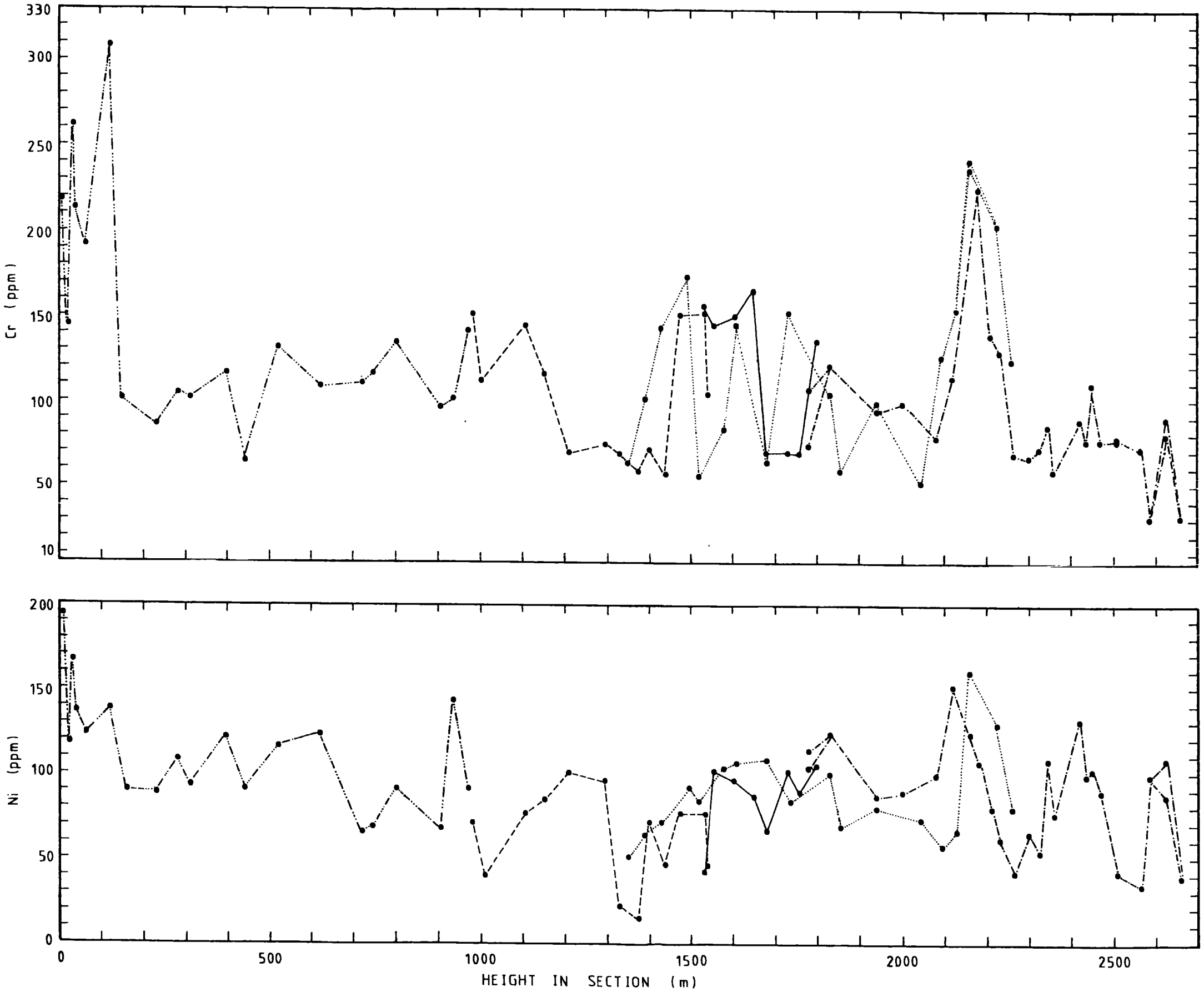
Cr (ppm)
330
300
250
200
150
100
50
10
Ni (ppm)
200
150
100
50
0
0
500
1000
1500
2000
2500
HEIGHT IN SECTION (m)

although the detection limits are low, the Cu contents in the minerals of the high Cu rock are high in relation to those of the lower Cu samples. The existence of olivines and brownish chrome-spinel inclusions in some olivines, could account for the high Ni and Cr peaks.

The variation in the oxides and the elements can be explained by the following reasons. In the first place, they might be due to parental magma variation as suggested by Pearce and Flower (1977). Secondly, variation could develop during the initial cooling of magma pulses as shown by Watkins et al. (1970), where lavas from different parts of a single flow have variable values for major and minor oxides, and trace elements. Thirdly, different degrees of weathering, and the proportions of secondary minerals, can also induce variations. Fourthly, the amounts of phenocryst and/or microphenocryst assemblages can cause variable values in some oxides and elements corresponding to the assemblages. Finally, errors in analyses might be integrated into the plausible reasons.

Fig. 2-9 also shows the correlations between the lavas in each self-contained area in terms of geochemical data. These correlations and those made by Emeleus (1971) are generally in unison. The displacement of some peaks between these stratigraphic positions might be due to variable thicknesses of corresponding flows in different self-contained areas, as well as the reasons given above.

In addition to simple geochemical relationships, R-mode factor analysis was performed to show the overall geochemical pattern. The principal factor matrix was first calculated to minimise constraint by using a logarithmic transform (Chayes, 1960) and it was found that 95% of the total variance of the data could be resolved into seven factors with eigen values greater than 0.5 (Spencer, 1966). Spencer (1967) has argued that the principal factor matrix is usually inadequate for many geochemical purposes, and suggested that a clearer resolution can be achieved by translation into a promax oblique primary pattern matrix (Hendrickson and White, 1964).

The raw data used to calculate the factors were the percentages of major and minor oxides (Total Fe as Fe_2O_3), trace elements (ppm), and height (m). The computer programme of Reeves (1971) was used in this calculation. The significant values of the promax oblique primary pattern matrix, including eigen values and the percentages of the variance of Factor 1 to Factor 7, are given in Table 2-4. Factor scores are also listed in Table A-3 (Appendix).

Fig. 2-10 is the plot of the factor scores of each sample for Factor 6 which represents NaO and Al_2O_3 (negative pole) and MgO (positive pole), against differentiation index. The strong negative correlation leads Factor 6 to be a differentiation factor. On the same diagram, the average values of the factor scores on the basis of

Table 2-4. Promax oblique primary pattern matrix, Kmin = 6. Only the significant values are listed

Variable	Factor						
	1	2	3	4	5	6	7
SiO_2	-0.86						
Al_2O_3						-0.53	
Fe_2O_3 (total Fe)		0.45					
Fe_2O_3		0.45					
MgO						0.85	
CaO			-0.62				
Na_2O						-0.73	
K_2O			0.60		-0.74		
TiO_2			0.65				0.40
MnO				0.64			
S					0.51		
P_2O_5			0.49				0.48
Ba					-0.87		0.58
Nb			-0.50				1.21
Zr							1.30
Y			-0.52				1.25
Sr			0.67				
Rb			0.91				-0.50
Zn			-0.51				1.10
Cu		-0.51		0.49			0.41
Ni		-0.93					
Cr		-0.47					
Height				1.01			
Eigen value	0.60	0.62	0.71	1.15	2.31	3.56	7.36
Eigen value %	3.50	3.62	4.13	6.70	13.42	20.72	42.85

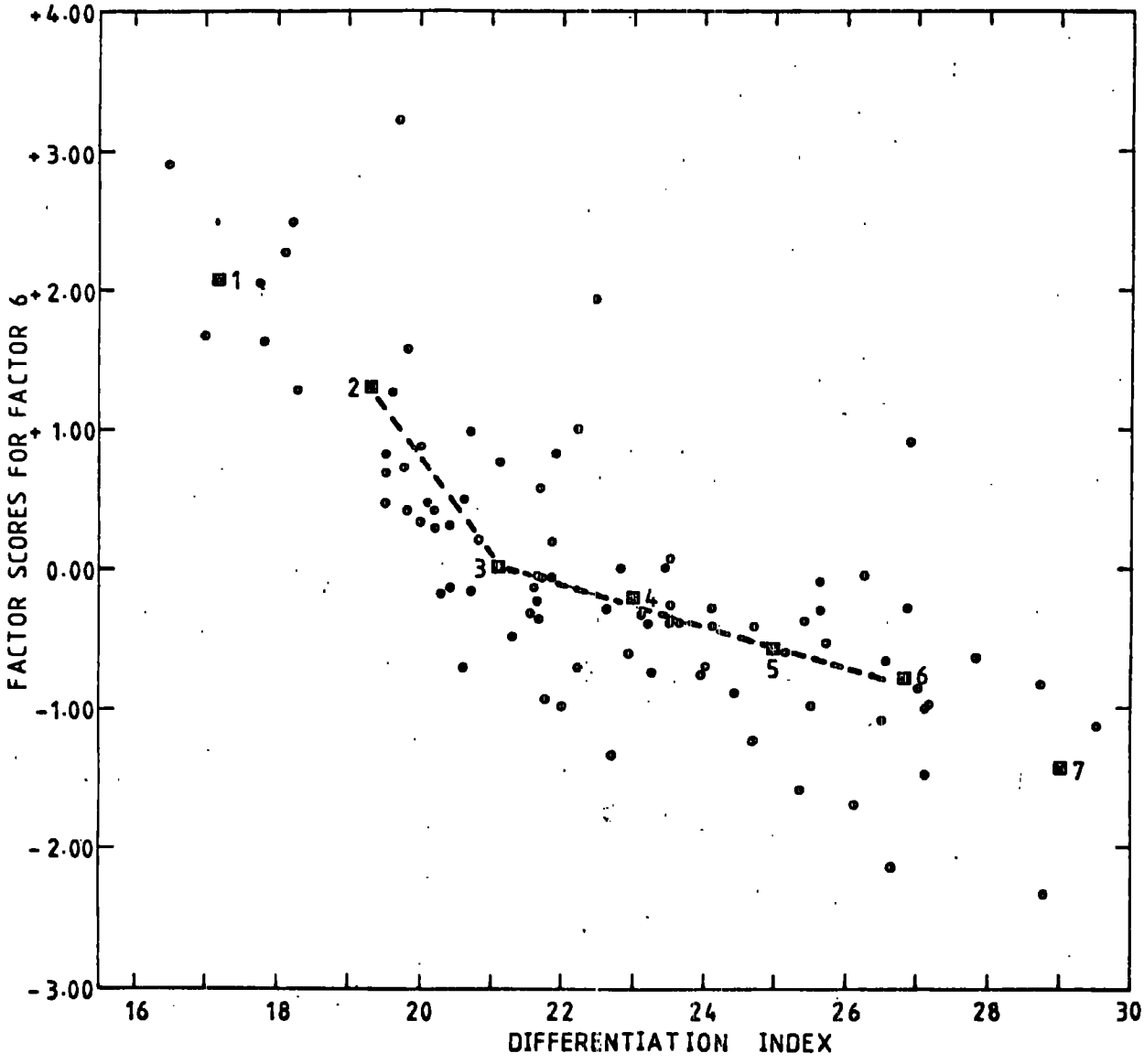
+4·00
+3·00
+2·00
+1·00
0·00
-1·00
-2·00
-3·00
FACTOR SCORES FOR FACTOR 6
16
18
20
22
24
26
28
30
DIFFERENTIATION INDEX
1
2
3
4
5
6
7

differentiation-index intervals of 2 (Table 2-5) have been plotted. It emerges that the negative trend consists of two slopes, and that the change in the direction of the trend takes place at a factor score of about 0.00 and a differentiation-index value of about 21. This feature could be attributed to the removal of magnesian minerals in the earlier stage, and of Na-Al minerals in the later stage, from the successive melts.

The factor scores for each sample are plotted on diagrams with Factor 1 and Factor 6 (Fig. 2-11), Factor 2 and Factor 6 (Fig. 2-12), Factor 3 and Factor 6 (Fig. 2-13), Factor 4 and Factor 6 (Fig. 2-14), Factor 5 and Factor 6 (Fig. 2-15), and Factor 7 and Factor 6 (Fig. 2-16) as axes. The points appear to scatter in any field, and the majority of them tend to cluster around null fields. The scattering of these points might be due to the limited compositional range of the studied lavas. However, when the factor scores of each factor are grouped according to differentiation-index intervals of 2 (Table 2-5), they appear to show trends with two different slopes, and the divergence of the trends occur around the null fields. This might be explicable on the same grounds as for the plot of factor scores for Factor 6 against differentiation index (see above).

The normative olivine-clinopyroxene-quartz plot, in

Table 2-5. Average values of factor scores for promax oblique primary pattern matrix according to their groupings based on differentiation-index intervals of 2

Group No.	1	2	3	4	5	6	7
Differentiation-index grouping	16-18	18-20	20-22	22-24	24-26	26-28	28-30
Abundance of Specimens	4	12	26	16	13	12	3
Factor 1	2.18	-0.40	0.20	-1.36	0.11	2.07	-0.02
Factor 2	0.52	-0.26	-0.08	-0.44	0.25	1.31	-0.20
Factor 3	0.21	-0.08	-0.66	-0.19	0.55	0.02	-0.48
Factor 4	0.17	-0.38	-0.16	-0.01	-0.75	-0.20	-0.09
Factor 5	-0.58	0.79	0.46	0.69	0.20	-0.55	0.42
Factor 6	-0.83	0.34	0.94	0.63	-0.04	-0.82	0.81
Factor 7	-1.82	-0.45	0.82	-0.21	-1.47	-1.42	0.60
Differentiation index	17.16	19.29	21.08	23.00	24.95	26.81	28.99

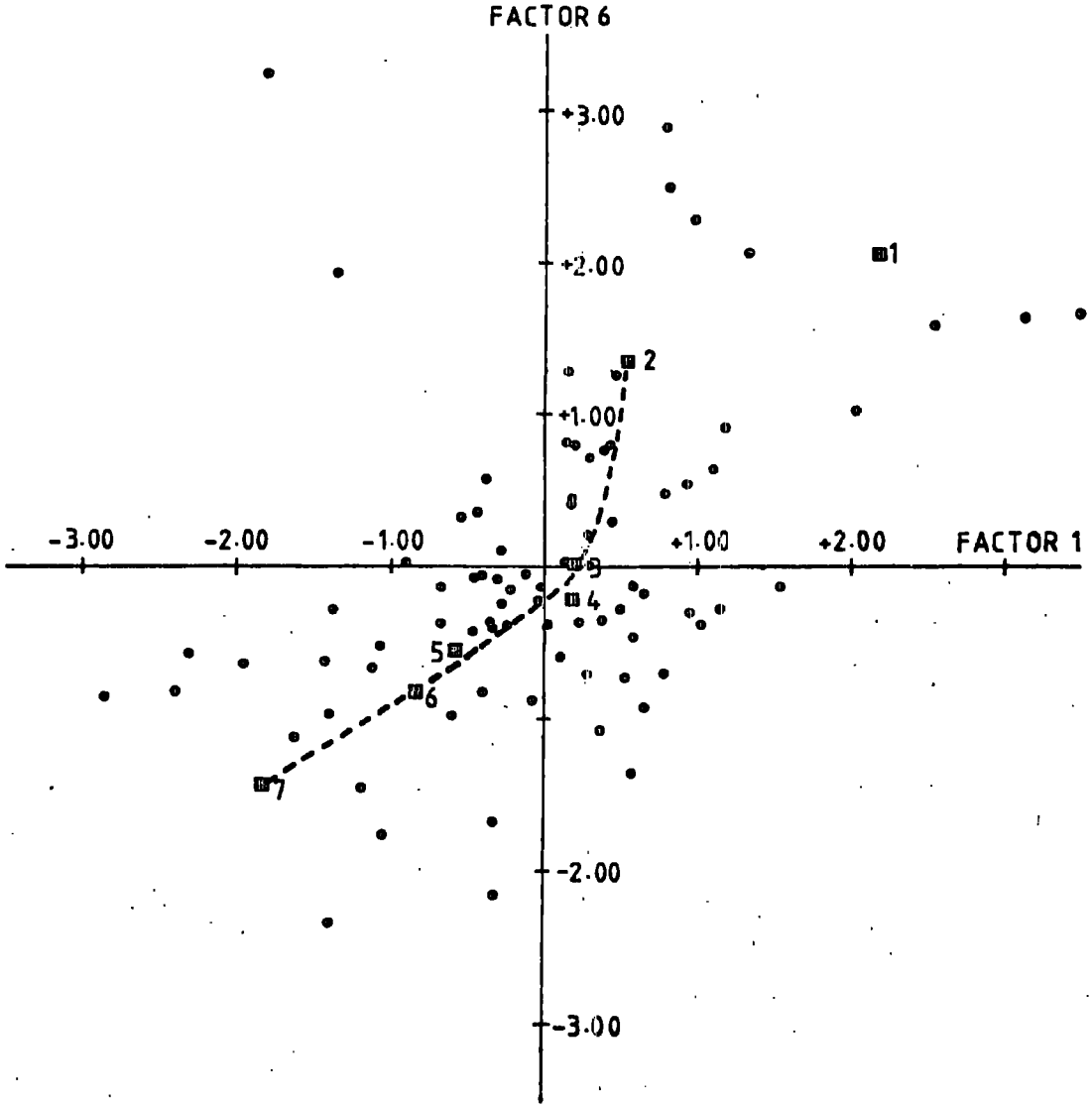
FACTOR 6
+3.00
+2.00
+1.00
-2.00
-3.00
-3.00
-2.00
-1.00
+1.00
+2.00
FACTOR 1
1
2
3
4
5
6
7

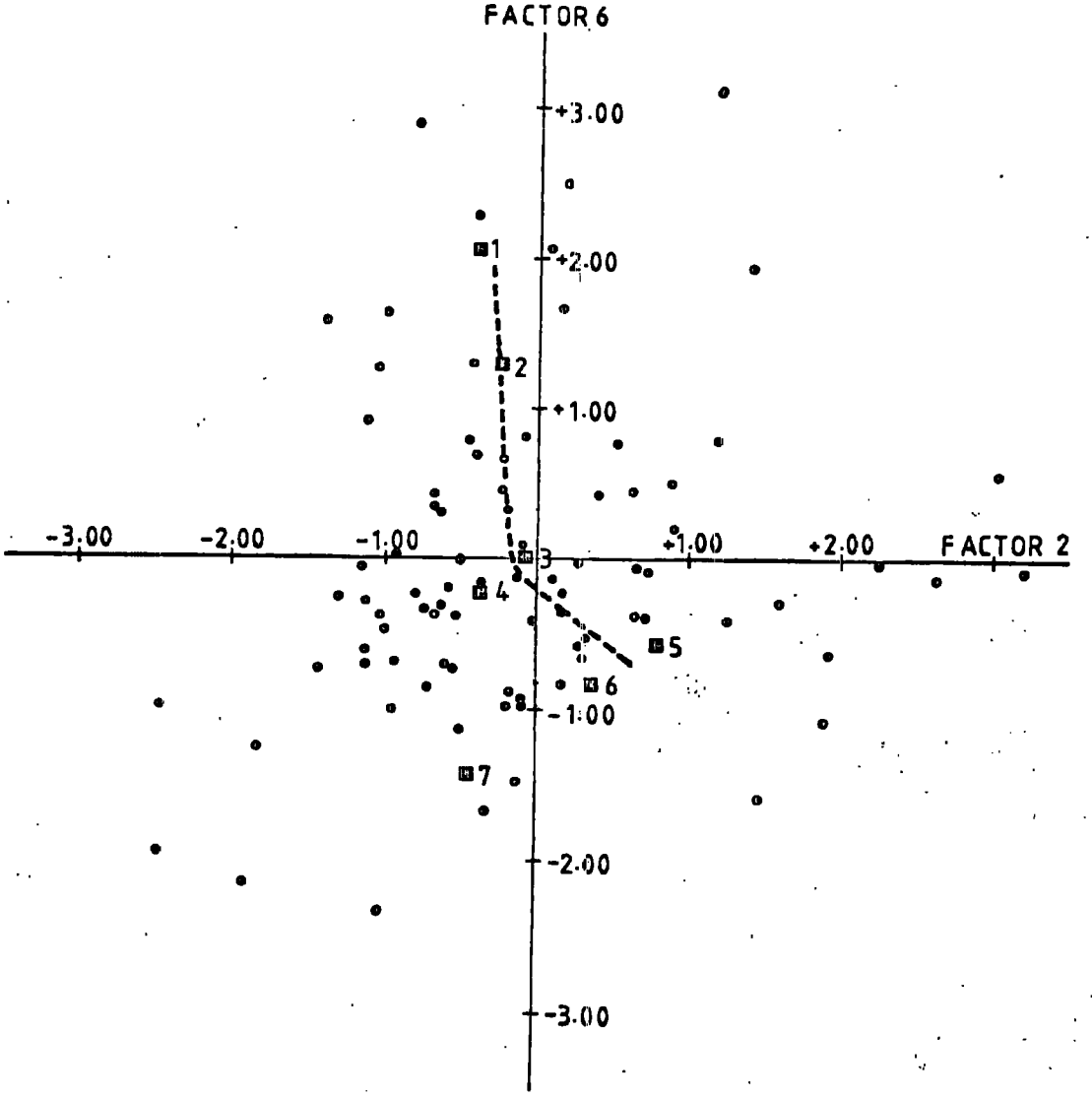
FACTOR 6
+3.00
+2.00
+1.00
-1.00
-2.00
-3.00
-3.00
-2.00
-1.00
+1.00
+2.00
FACTOR 2
1
2
3
4
5
6
7

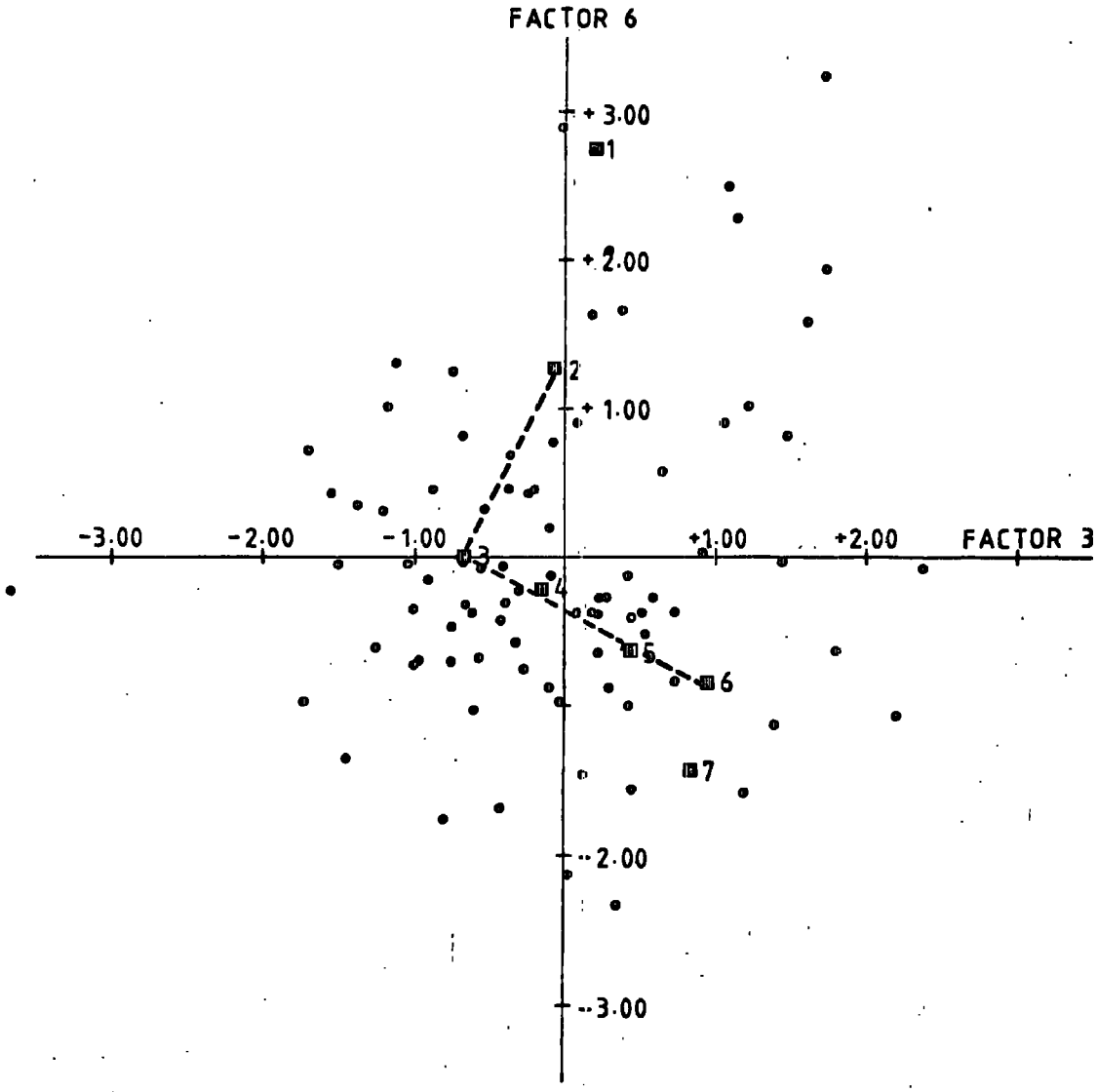
FACTOR 6
+ 3.00
1
+ 2.00
2
+ 1.00
-3.00
-2.00
-1.00
3
+1.00
+2.00
FACTOR 3
4
5
6
7
-2.00
-3.00

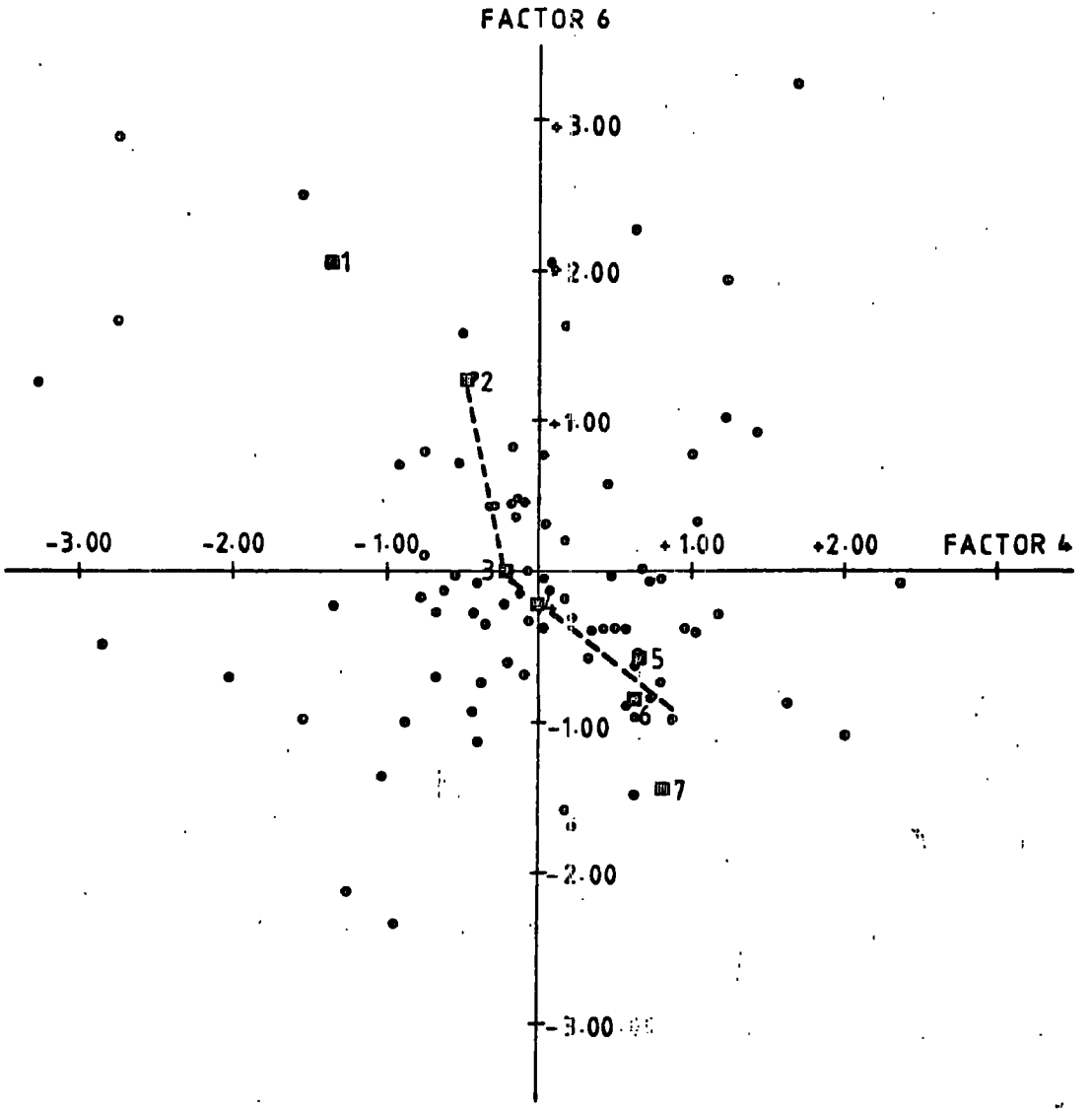
FACTOR 6
+3·00
+2·00
+1·00
-1·00
-2·00
-3·00
-3·00
-2·00
-1·00
+1·00
+2·00
FACTOR 4
1
2
3
5
6
7

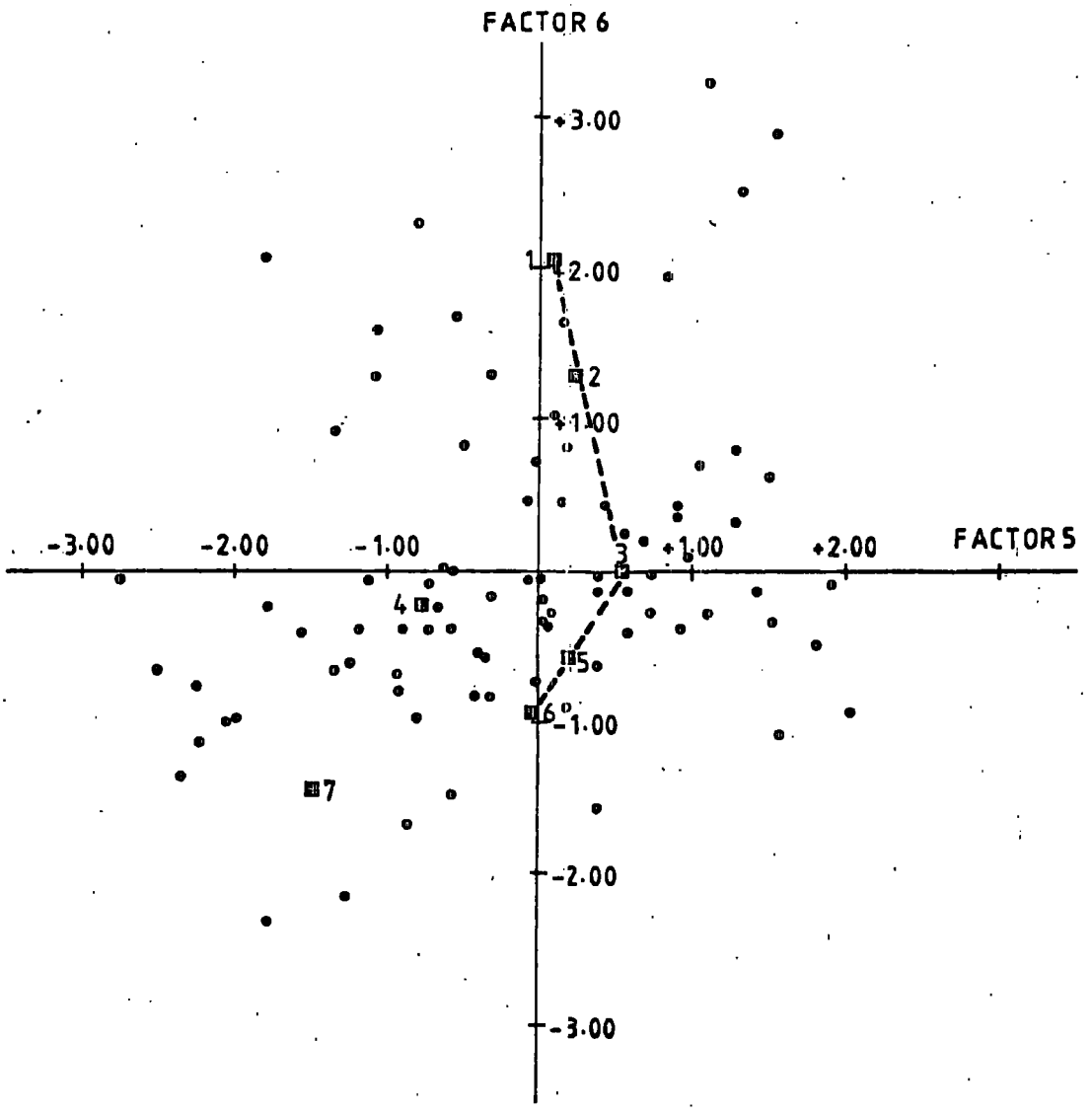
FACTOR 6
+3·00
+2·00
+1·00
-1·00
-2·00
-3·00
-3·00
-2·00
-1·00
+1·00
+2·00
FACTOR 5
1
2
3
4
5
6
7

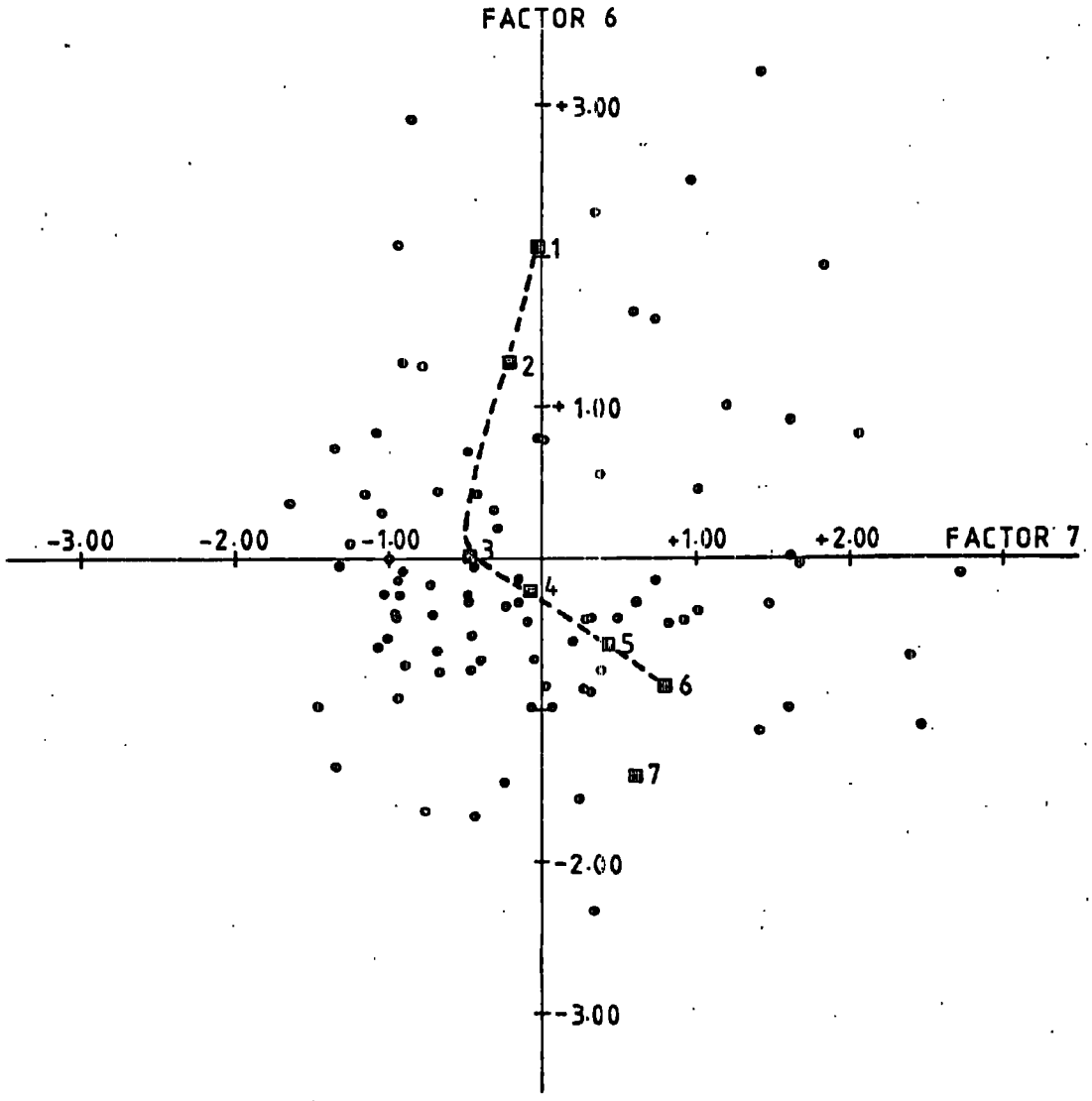
FACTOR 6
+3.00
+1.00
-2.00
-3.00
-3.00
-2.00
-1.00
+1.00
+2.00
FACTOR 7
1
2
3
4
5
6
7

terms of molecular percent (Fig. 2-17), demonstrates that most of the East Greenland basalts cluster around the critical plane of silica-saturation (Yoder and Tilley, 1962), and tend to form a broad band trending towards the quartz apex. This trend suggests that a low-pressure fractionation process might be involved in the geochemical variation of the studied samples.

According to Yoder and Tilley (1962), olivine, clinopyroxene and plagioclase can substitute for forsterite, diopside and the albite-anorthite series, respectively, in the iron-free system of diopside-forsterite-albite-anorthite. Thus all the analysed tholeiites are plotted on the quartz projection (weight percent) within the normative basalt tetrahedron (Yoder and Tilley, 1962) in Fig. 2-18, in which phase boundaries are from the experimental work on the iron-free system of Osborn and Tait (1952). It is obvious that the analysed samples lie close to the locus of liquid in equilibrium with olivine, plagioclase and spinel; and predominantly in the plagioclase field. Such a feature might be indicative of the principal phenocryst and/or microphenocryst assemblage as described in Chapter 3, i.e. the predominant, principal phenocryst and/or microphenocryst assemblage is plagioclase, and the olivine-plagioclase assemblage is much more common than that containing a significant amount of clinopyroxene phenocrysts and/or microphenocrysts.

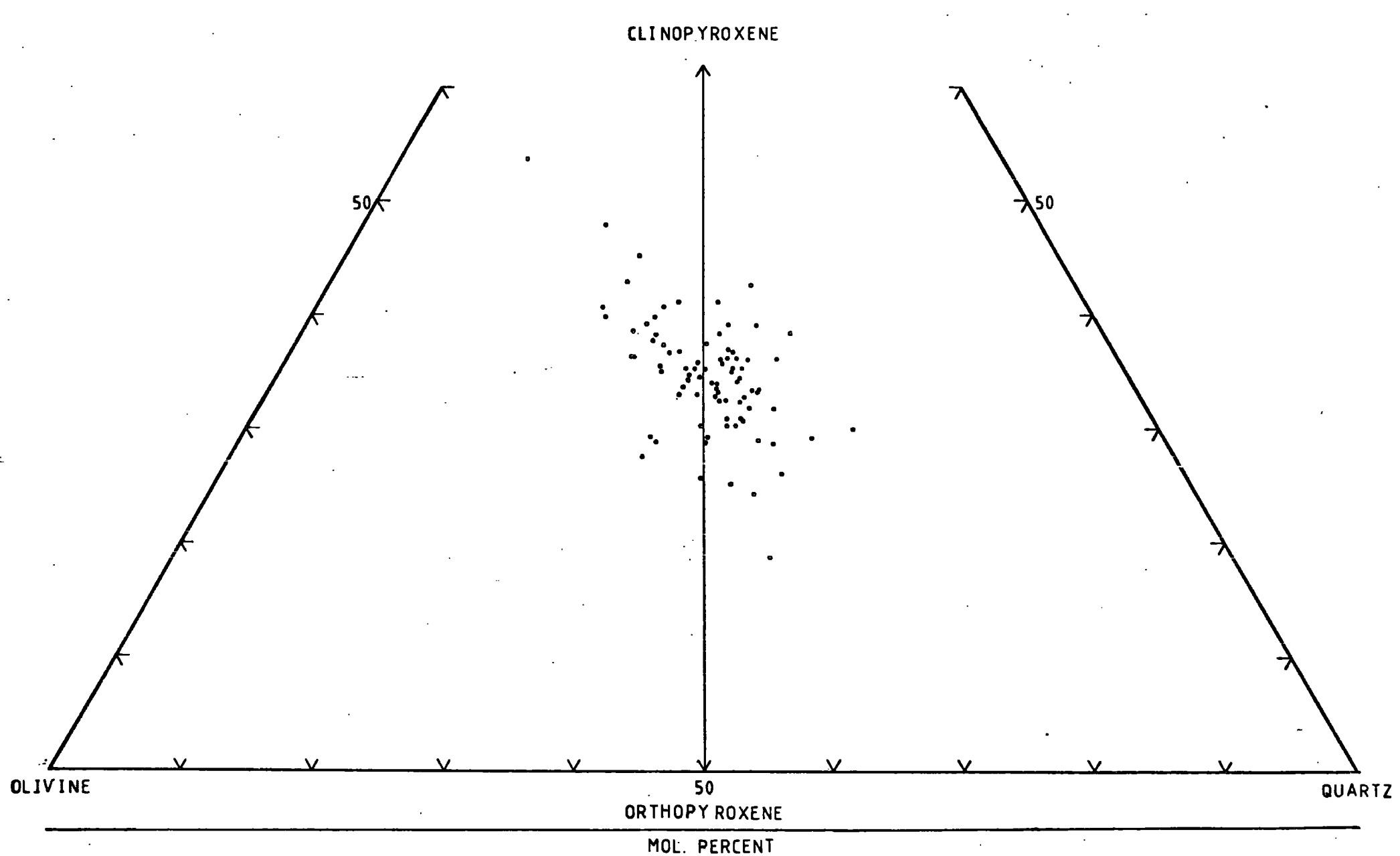
CLINOPYROXENE
50
50
OLIVINE
50
QUARTZ
ORTHOPYROXENE
MOL. PERCENT

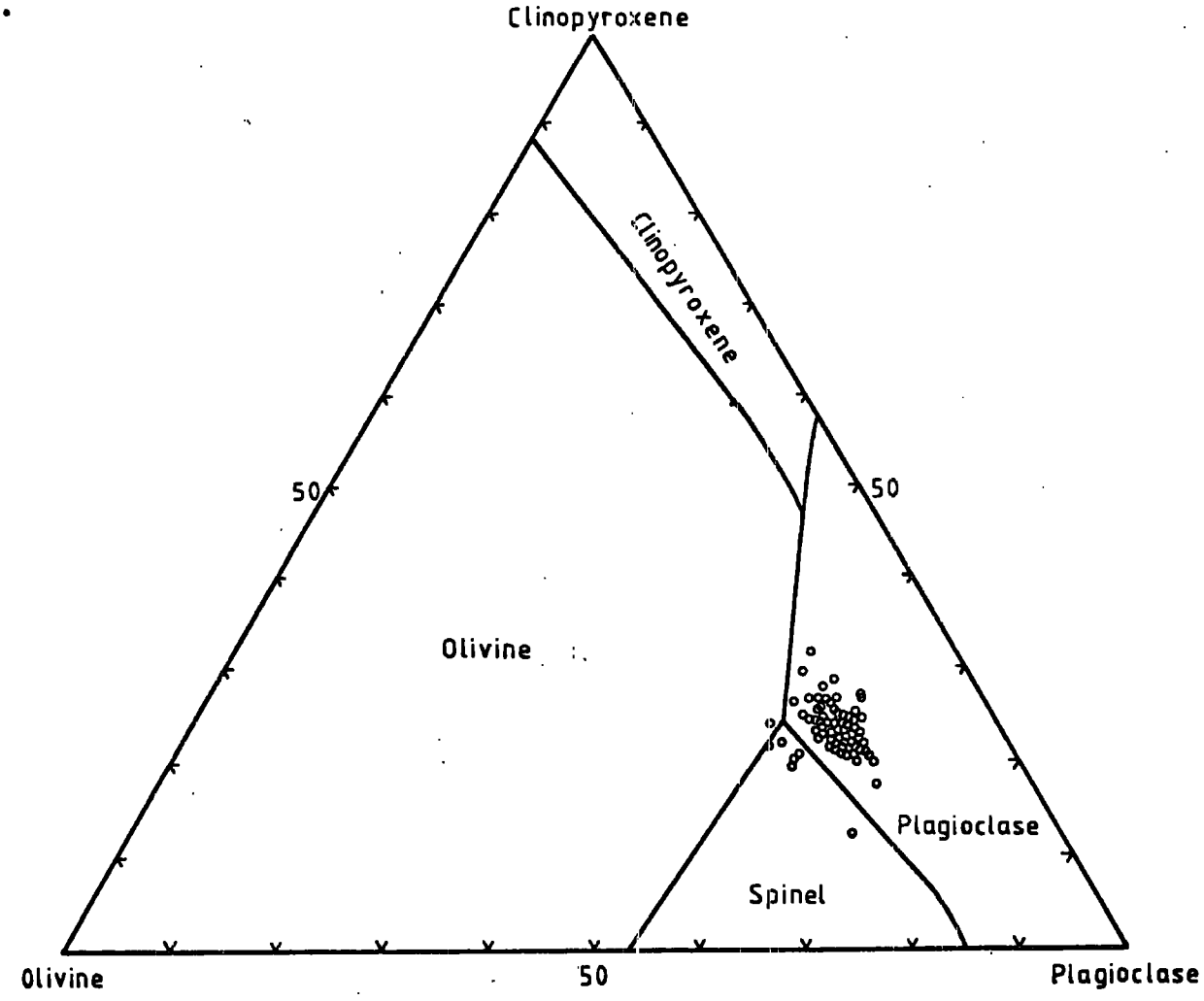
Clinopyroxene
Clinopyroxene
50
50
Olivine
Plagioclase
Spinel
Olivine
50
Plagioclase
WEIGHT PERCENT

Comparisons in the light of geochemical features of the analysed lavas have been drawn with other tholeiites in the North Atlantic Tertiary Igneous Province, and with ocean-floor tholeiites. The average values for major oxides, minor oxides and dispersed elements, including K/Rb, Sr/Rb and Na/K ratios, of the tholeiitic lavas from the research region, mid-west Iceland (Johannesson, 1975), Skye (I.T. Williamson, personal communication), and certain ocean floor regions (Engel et al., 1965) are given in Table 2-6. It is clearly seen that the average values for Al_2O_3, Cu and K/Rb ratio of the studied lavas are higher but for K_2O and Na/K are lower than those of the tholeiites from mid-west Iceland. In contrast, the average values for the East Greenland tholeiites are lower in Al_2O_3, Cu and K/Rb ratio, and high in K_2O and Na/K ratio, relative to those for the low-alkali tholeiites of Skye, and for ocean-floor tholeiites, except for Al_2O_3 and K/Rb values which appear to be similar in both the tholeiites of East Greenland and Skye. Nevertheless, when the average values for TiO_2 total iron, MnO, P_2O_5, Ba and Sr/Rb are taken into consideration, the average values for the analysed lavas are broadly comparable to those for the mid-west Icelandic lavas according to their both being higher in these values than the Skye and ocean-floor tholeiites. In other words, the East Greenland lavas bear a close relationship to the

Table 2-6. Average analyses for major and minor oxides (wt.%), and trace elements (ppm) of the analysed Tertiary tholeiitic lavas from East Greenland, compared with tholeiites from mid-west Iceland, Skye and parts of the ocean floor.

	1	2	3	4
SiO_2	48.16±0.68	49.65±1.03	46.78±0.37	49.92±0.51
TiO_2	2.70±0.37	2.83±0.54	0.98±0.10	1.51±0.50
Al_2O_3	15.28±0.15	14.24±0.46	15.64±0.46	17.24±2.36
Fe_2O_3	3.24±0.00	4.64±1.25	1.11±0.11	2.02±0.97
FeO	10.14±0.49	9.34±1.46	9.90±0.37	6.87±1.79
MnO	0.21±0.00	0.36±0.13	0.20±0.00	0.17±0.00
MgO	6.27±0.88	4.91±0.99	8.78±0.68	7.28±1.09
CaO	11.15±0.52	10.31±0.98	12.55±0.22	11.86±0.84
Na_2O	2.46±0.30	3.03±0.40	1.83±0.15	2.76±0.28
K_2O	0.22±0.09	0.46±0.18	0.11±0.00	0.16±0.07
P_2O_5	0.25±0.00	0.23±0.15	0.13±0.00	0.16±0.06
Ba	89±21	141±33	6±8	14±9
Nb	17±4	27±8	1±1	<30
Zr	167±32	197±55	36±6	95±43
Y	32±5	40±8	20±2	42±14
Sr	237±38	263±36	119±13	130±32
Rb	9±4	9±5	0	<10
Zn	90±12	124±14	68±6	*
Cu	241±36	135±58	164±75	77±7
Ni	90±34	36±16	160±31	97±25
Cr	139±53	*	421±25	297±95
K/Rb	207±19	435±27	∞	
Sr/Rb	27±10	24±7	∞	
Na/K	10±3	2±1	15±0	15±1

Key: 1. Average of 86 samples of analysed East Greenland tholeiites. 2. Average of 76 tholeiitic lavas from mid-west Iceland (Johannesson,1975). 3. Average of 16 low-alkali tholeiites from Skye (I.T.Williamson, pers. comm.). 4. Average of 10 samples of oceanic tholeiites dredged from the Atlantic and Pacific oceans (Engel et al., 1965). *No data available.

mid-west Icelandic lavas. Those differences between the average values for the tholeiitic lavas from East Greenland and from mid-west Iceland are probably due to different stages of fractionation, i.e. the differentiation indices and Fe-Mg ratios for the mid-west Icelandic tholeiites are generally higher (i.e. more advanced) than those for the East Greenland tholeiites.

Hart (1969) has shown that the patterns on a K/Rb-K diagram can show either a primary feature or a modified feature as the result of later alterations of submarine tholeiitic basalt magma. In the case of the primary feature, K/Rb ratios seem to be roughly constant throughout various values of K; in the other case the altered samples, owing to a low-grade metamorphism or an exchange in cations with sea water, appear to form a trend of decreasing K/Rb with increasing K contents. The K/Rb-K plot for the studied lavas (Fig. 2-19) reveals a trend of increasing K/Rb ratios in relation to their corresponding K contents. Hence, it strongly supports the view that the differentiation process took place during crystallisation.

An effective method for discriminating between oceanic basalts and non-oceanic basalts, based on a TiO_2-K_2O-P_2O_5 plot, has been proposed by Pearce et al. (1975). They have also shown, on such a diagram, that the tholeiites from Scoresby Sund have oceanic affinities although they have

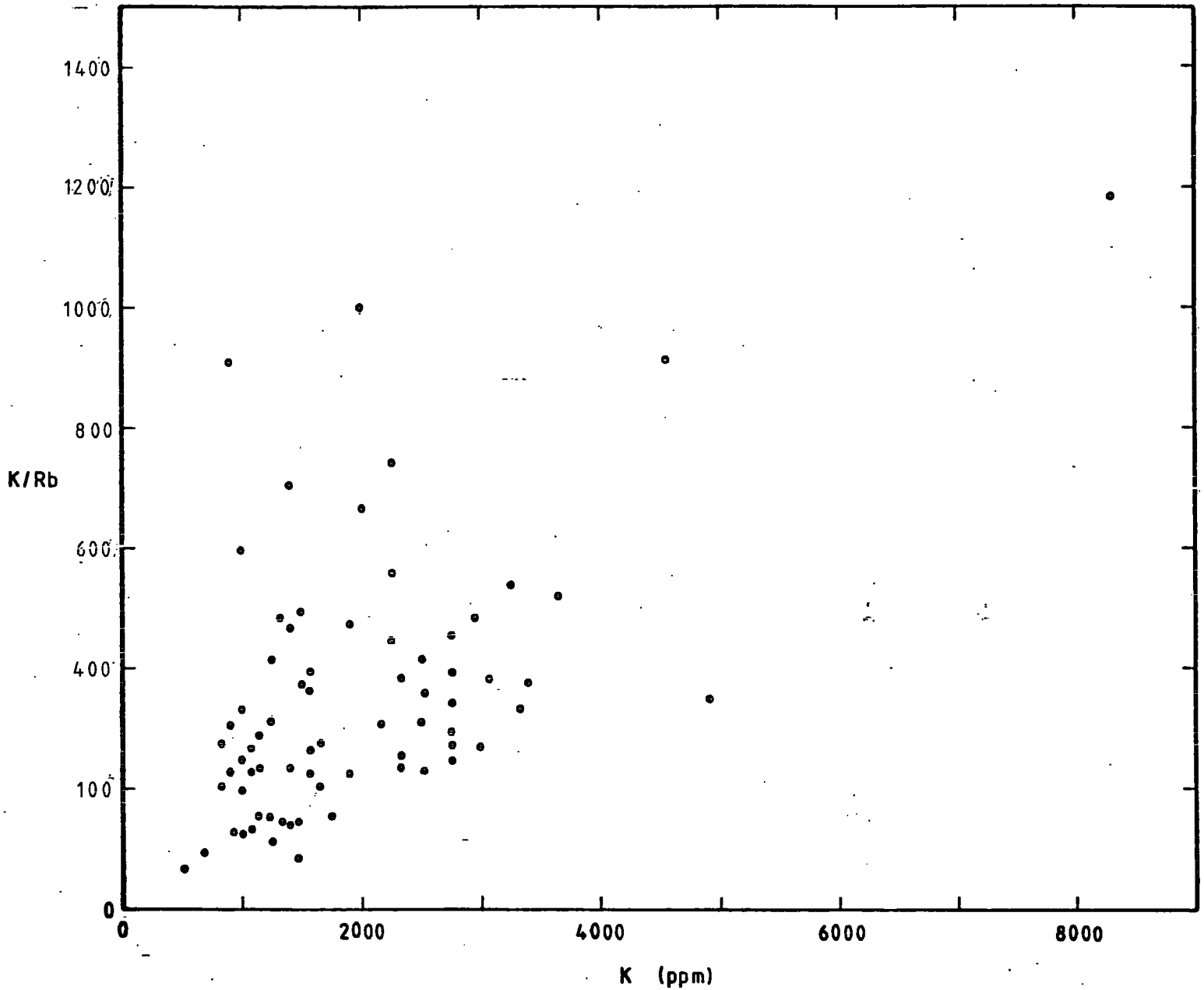
1400
1200
1000
800
600
400
100
0
K/Rb
0
2000
4000
6000
8000
K (ppm)

certain characteristics of continental plateau basalts. Fig. 2-20 is the TiO_2-K_2O-P_2O_5 diagram for the analysed samples, the mid-west Icelandic tholeiites, and the lavas along the Reykjanes Ridge and Neovolcanic zone of Iceland (Schilling, 1973). It can be deduced from this plot that all of these lavas are oceanic, and form a distinct trend. The trend appears to change its direction, from having a constant P_2O_5 relative to TiO_2 and K_2O to having a constant K_2O relative to P_2O_5 and TiO_2, at the following (approximate) coordinates: TiO_2, 78%; K_2O, 13%; P_2O_5, 9%. This might be one of the characteristic patterns of the tholeiites in the North Atlantic Tertiary Igneous Province.

Pearce and Cann (1973) have classified basic volcanic rocks, according to their geotectonic position, into a number of magma types and have proposed a classic flow diagram for distinguishing these magma types on the grounds of less mobile elements (Ti, Zr, Ni and Y; Cann, 1970) and Sr. In this study, the proposed classification scheme of Pearce and Cann (1973) has also been followed. It is found that the majority of the East Greenland tholeiites are "within plate" basalts, i.e. oceanic island or continental basalts (Fig. 2-21). On the same Ti/100 - Zr - Y.3 diagram, the mid-west Icelandic tholeiites, the tholeiitic lavas of Skye and the Atlantic ocean-floor tholeiites (Engel et al., 1965) have also been plotted. It is discerned that the mid-

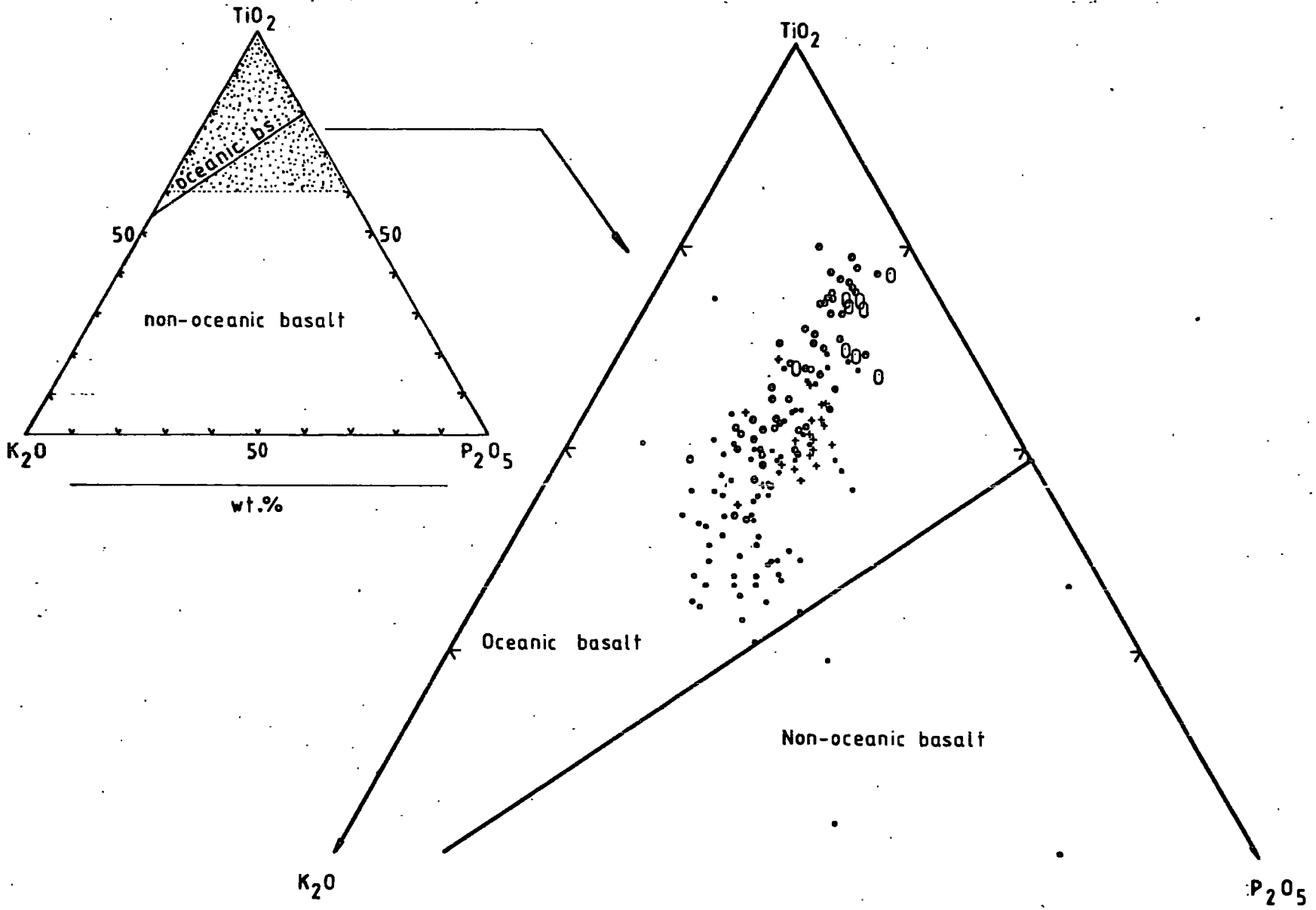
TiO2
oceanic bs
50
50
non-oceanic basalt
K2O
50
P2O5
wt.%
TiO2
Oceanic basalt
Non-oceanic basalt
K2O
P2O5

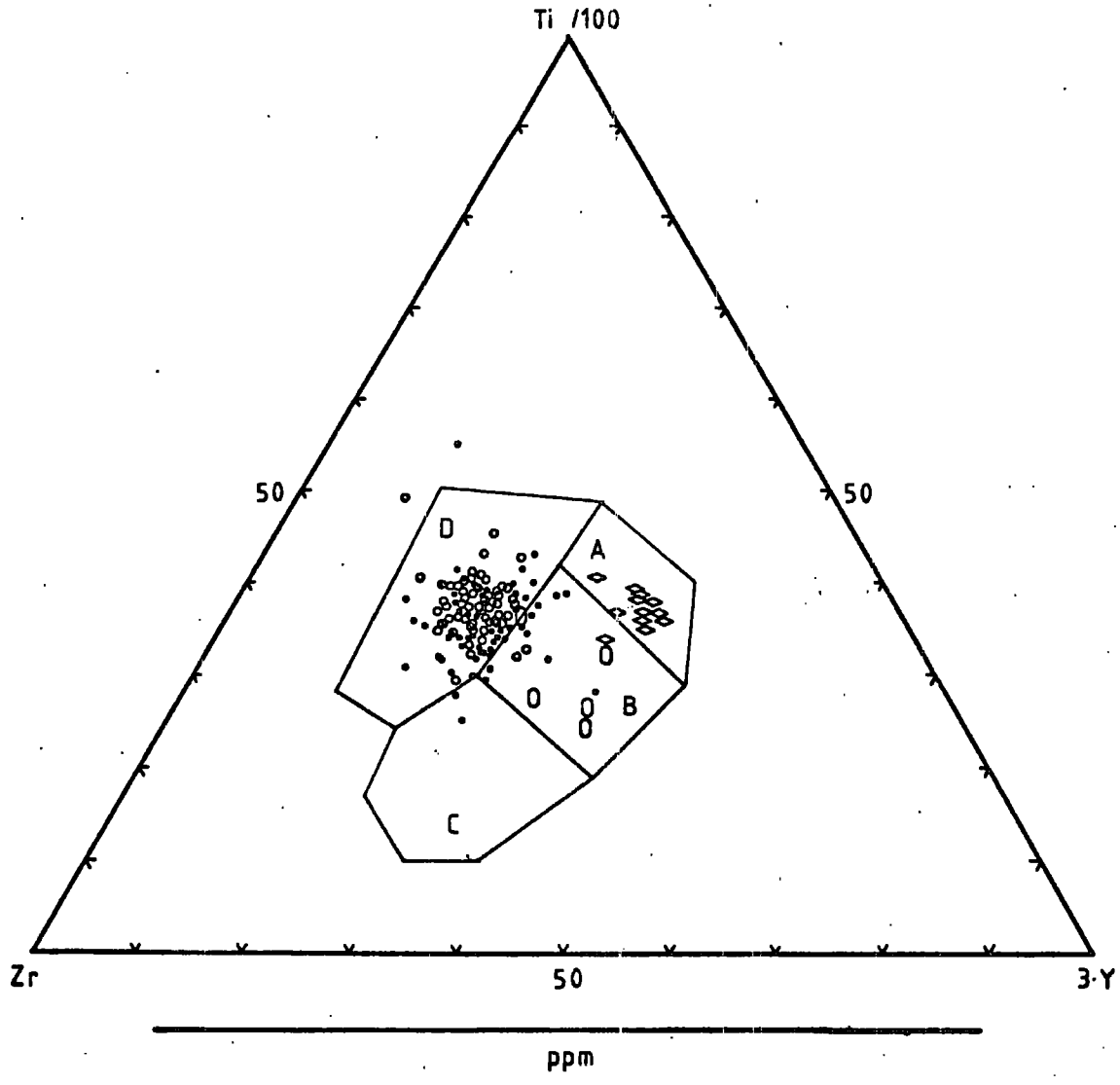
Ti /100
50
50
D
A
B
C
Zr
50
3·Y
ppm

west Icelandic tholeiites superimpose on the plotted East Greenland tholeiites, and that the tholeiites of Skye and of the Atlantic ocean floor fall within the ocean-floor basalt and the low-potassium tholeiite fields, respectively.

Schilling (1973) studied the geochemistry of the tholeiites occurring along the Reykjanes Ridge, extending to the middle Neovolcanic zone of Iceland, by plotting large incompatible elements (K and La) and minor elements (Ti and P), including $(La/Sm)_{E.F.}$ ratio, against latitude. The results of these plots give rise to three distinguishable types of the tholeiites: "primary hot mantle plume (PHPM)" - derived basalts, "depleted low velocity layer (DLVL)" - derived basalts, and "transitional" basalts. The PHMP - derived basalts are made up of all the land-exposed basalts, and have constant values of K, La, Ti, P and $(La/Sm)_{E.F.}$ ratio. The transitional basalts, which are believed to be the mixing products of the PHMP-derived and the DLVL-derived basalts, lie between the margin of Iceland and latitude about $60^{o}N$ along the Reykjanes Ridge, and show remarkable depletion in the large incompatible elements, minor elements, and $(La/Sm)_{E.F.}$ ratios relative to distance away from the land. The DLVL-derived basalts exist along the Reykjanes Ridge extending southwards from latitude $60^{o}N$, and have constant values of K, La, Ti, P and $(La/Sm)_{E.F.}$ ratio which are lower than those of the PHMP-derived basalts. Figs. 2-22 (a,b) show TiO_2-K_2O and P_2O_5-K_2O plots of the samples

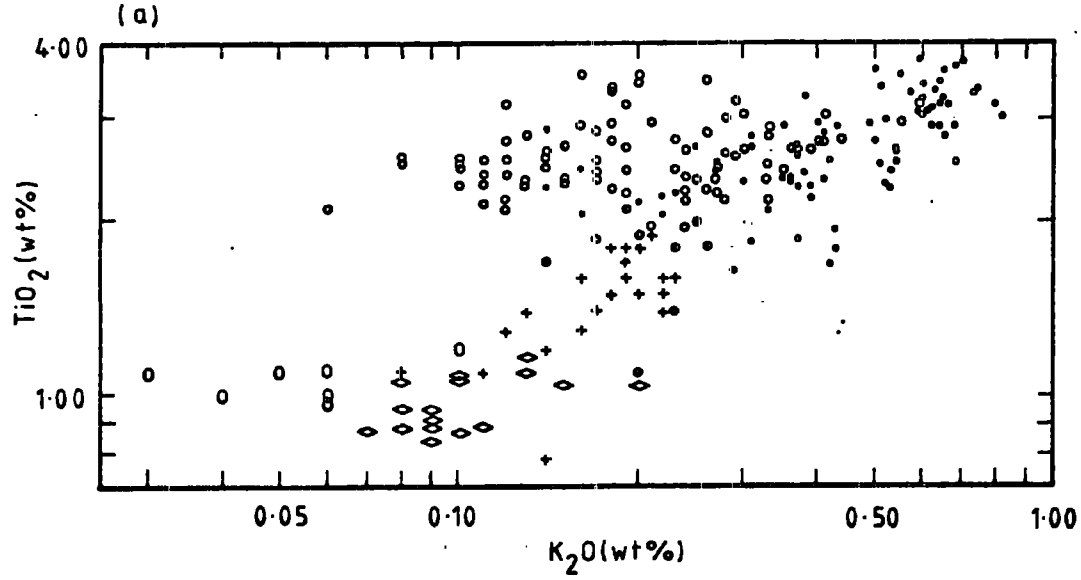
(a)
4·00
1·00
TiO_2(wt%)
0·05
0·10
0·50
1·00
K_2O(wt%)

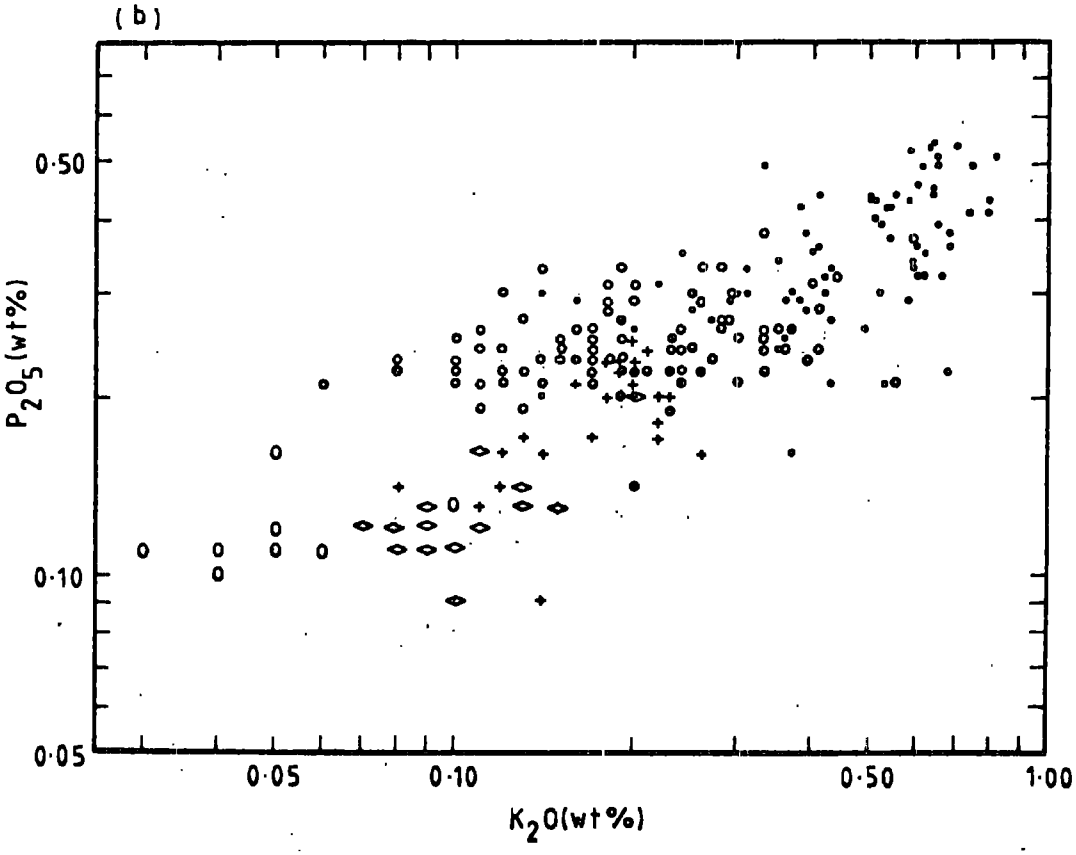
(b)
0·50
0·10
0·05
P_2O_5(wt%)
0·05
0·10
0·50
1·00
K_2O(wt%)

described in this thesis, the mid-west Icelandic tholeiitic lavas, the Skye tholeiitic lavas and the three types of tholeiites studied by Schilling (1973). It appears that the tholeiites from East Greenland and mid-west Iceland are similar to the PHMP-derived basalts whereas the Skye lavas seem to relate to either the transitional basalts of the mixing model or to the DLVL-derived basalts.

Extremely low amounts of incompatible elements (Ba, K, P, Sr, Rb and Zr) are regarded as the typical characteristics of ocean-ridge tholeiites (Engel et al., 1965; Gast, 1965; Kay et al., 1970). Fig. 2-23 is a plot of Rb versus Sr on a logarithmic scale for the tholeiites of East Greenland, mid-west Iceland, Skye, and the Reykjanes Ridge (O'Nions and Pankhurst, 1974). It is clearly seen that the tholeiites of East Greenland and mid-west Iceland are in unison, and form a trend of constant Sr values (about 250 ppm) with variable Rb values ranging from 1 to about 25 ppm. The tholeiites from the Reykjanes Ridge have lower Sr and Rb concentrations than those from East Greenland and mid-west Iceland. Furthermore, when the tholeiites existing along the Reykjanes Ridge are classified according to Schilling (1973), it is obvious that the DLVL-derived basalts and the transitional basalts are distinctly separated from each other on this Sr-Rb diagram. The low-alkali tholeiites from Skye have the lowest values of Rb in relation to other tholeiites and

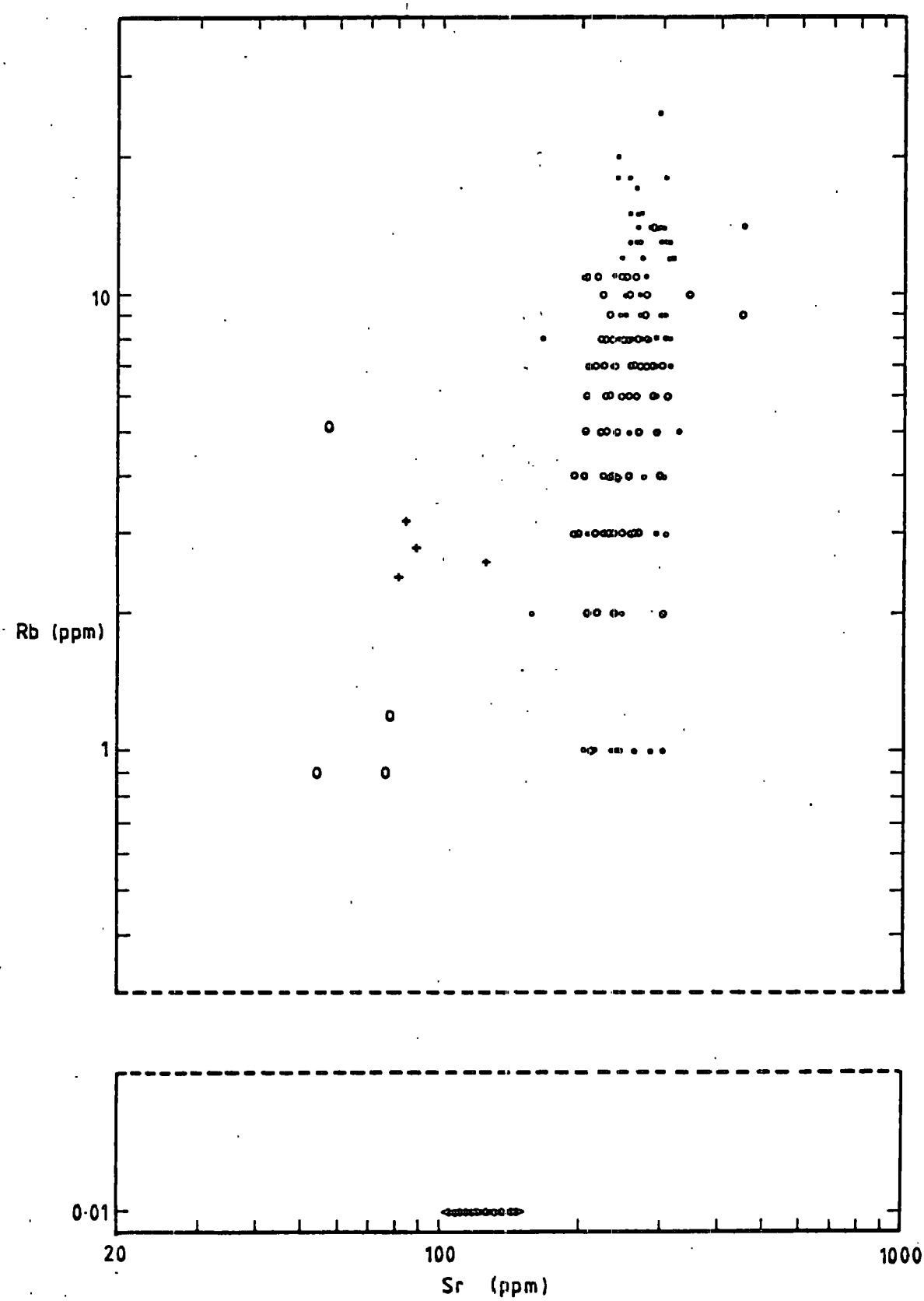
10
1
0·01
Rb (ppm)
20
100
1000
Sr (ppm)

have Sr values slightly higher than the transitional basalts but lower than the East Greenland and mid-west Icelandic tholeiites.

Fig. 2-24 shows a Ti-Zr plot for the tholeiites from East Greenland, mid-west Iceland, Skye, and the Atlantic ocean-floor (Engel et al., 1965). This plot reveals a strong positive correlation between Ti and Zr. The studied tholeiites appear to coincide with the mid-west Icelandic tholeiites. The Skye tholeiites seem to occupy the lowest end of the trend suggesting that they are not transitional basalts of the mixing-model type (Schilling, 1973) and that they might have the same origin as the ocean-floor tholeiites.

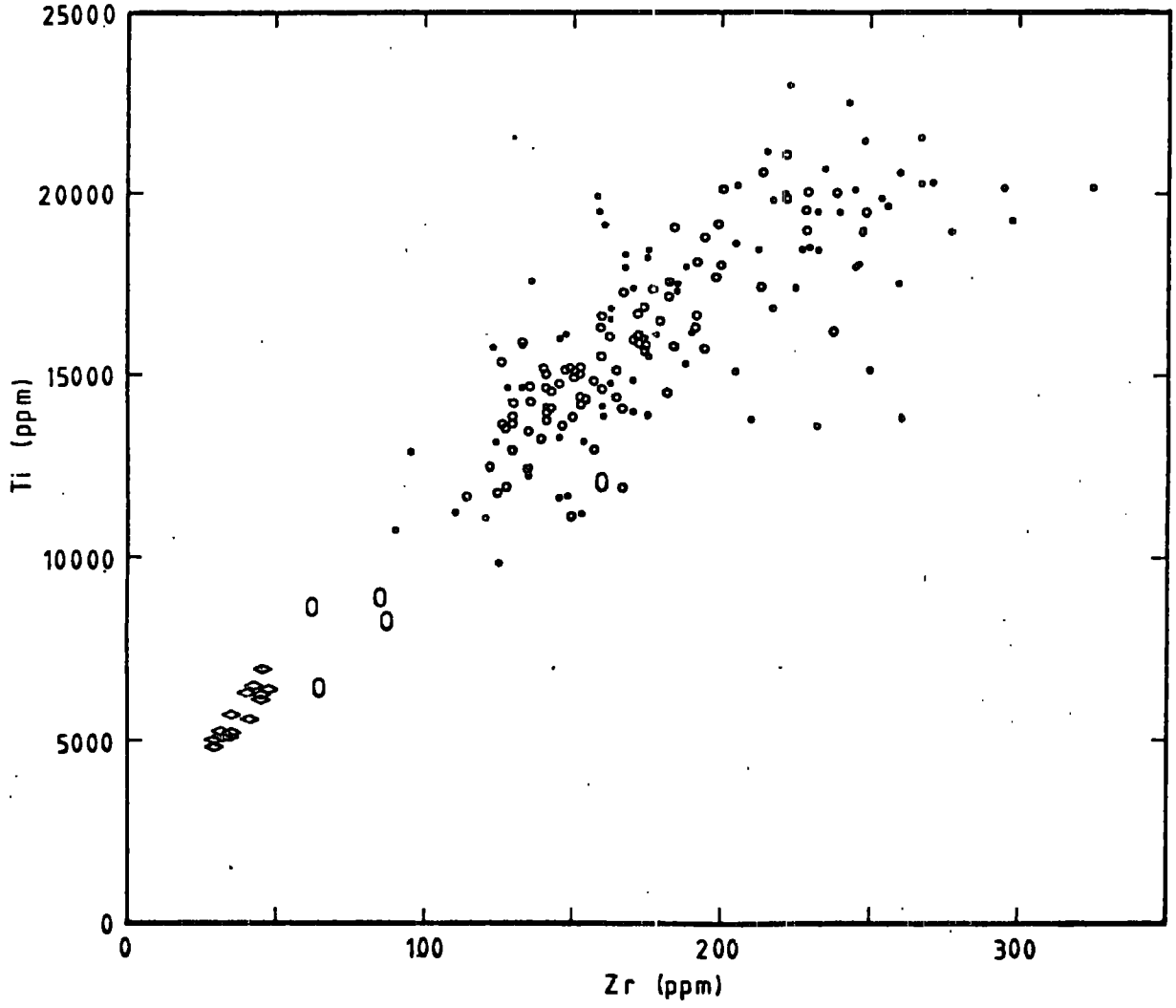
25000
20000
15000
10000
5000
0
Ti (ppm)
0
100
200
300
Zr (ppm)

CHAPTER 3

PETROGRAPHY

3.1. Classification

All the lavas of the five self-contained areas are mainly composed of plagioclase (average labradorite), clinopyroxene (augite) and Fe-Ti oxide phases, with small amounts of olivine and pigeonite. Interstitial, yellowish brown to brownish-red and greenish glass is sometimes found between the feldspar laths, excluding the pillow lavas where the groundmass is entirely glass. Thus the East Greenland lavas are classified as tholeiitic basalts according to the definition by Kennedy (1933). However, Macdonald and Katsura (1964) have pointed out that positive microscopic criteria for the distinction between tholeiitic and alkalic rocks are few, and should be used with great caution. Thus the chemical and quasi-chemical schemes of Macdonald and Katsura (1964) and of Yoder and Tilley (1962) were followed, as well as the quantitative mineralogical classification.

Fig. 3-1 shows total alkalis plotted against SiO_2, which is used by Macdonald and Katsura (1964), to discriminate between the Hawaiian tholeiitic and alkalic series. It reveals that all the analysed samples fall within the tholeiitic field.

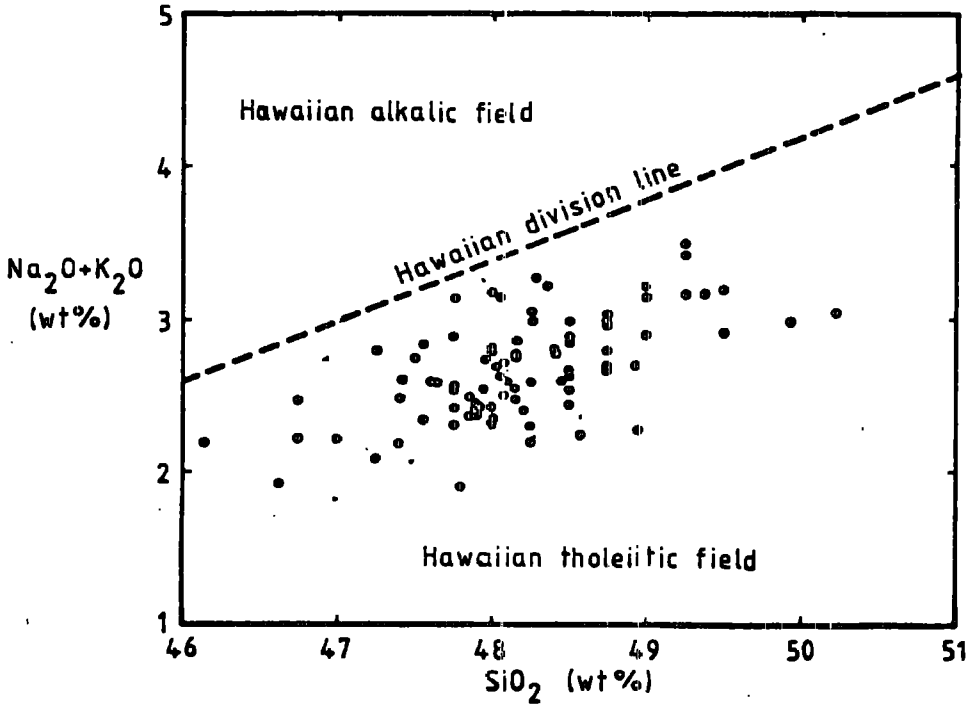
Hawaiian alkalic field
Hawaiian division line
Hawaiian tholeiitic field
Na_2O+K_2O (wt%)
SiO_2 (wt%)
5
4
3
2
1
46
47
48
49
50
51

Basalts can be best classified by using their normative minerals, i.e. clinopyroxene, orthopyroxene, plagioclase, olivine, quartz and nepheline which is the basis used by Yoder and Tilley (1962). In considering the analysed lavas, the abundances of normative hypersthene, quartz and olivine show that they are distinctly tholeiitic in composition and can be divided into two main groups, namely quartz tholeites and olivine tholeiites. When the relevant molecular proportions of the lavas are plotted on the ternary diagram (Fig. 3-2), which is the projection from the plagioclase apex onto the olivine-clinopyroxene-quartz plane of the basalt tetrahedron, most of them cluster around the trace of the critical plane of silica saturation. However, since these basalts have undergone alteration, the oxidation state must be considered because it influences the proportions of normative minerals. Fawcett et al. (1973) showed that if the chemical composition of a rock is calculated to normative compositions with differing ratios of FeO to Fe_2O_3, the percentage of normative quartz will decrease as the FeO/Fe_2O_3 ratio increases. In contrast, normative olivine will increase with increasing FeO/Fe_2O_3 ratio. Thus the original, unaltered (pre-oxidation) composition of the bulk of the lavas might be olivine-tholeiitic. In this account, the

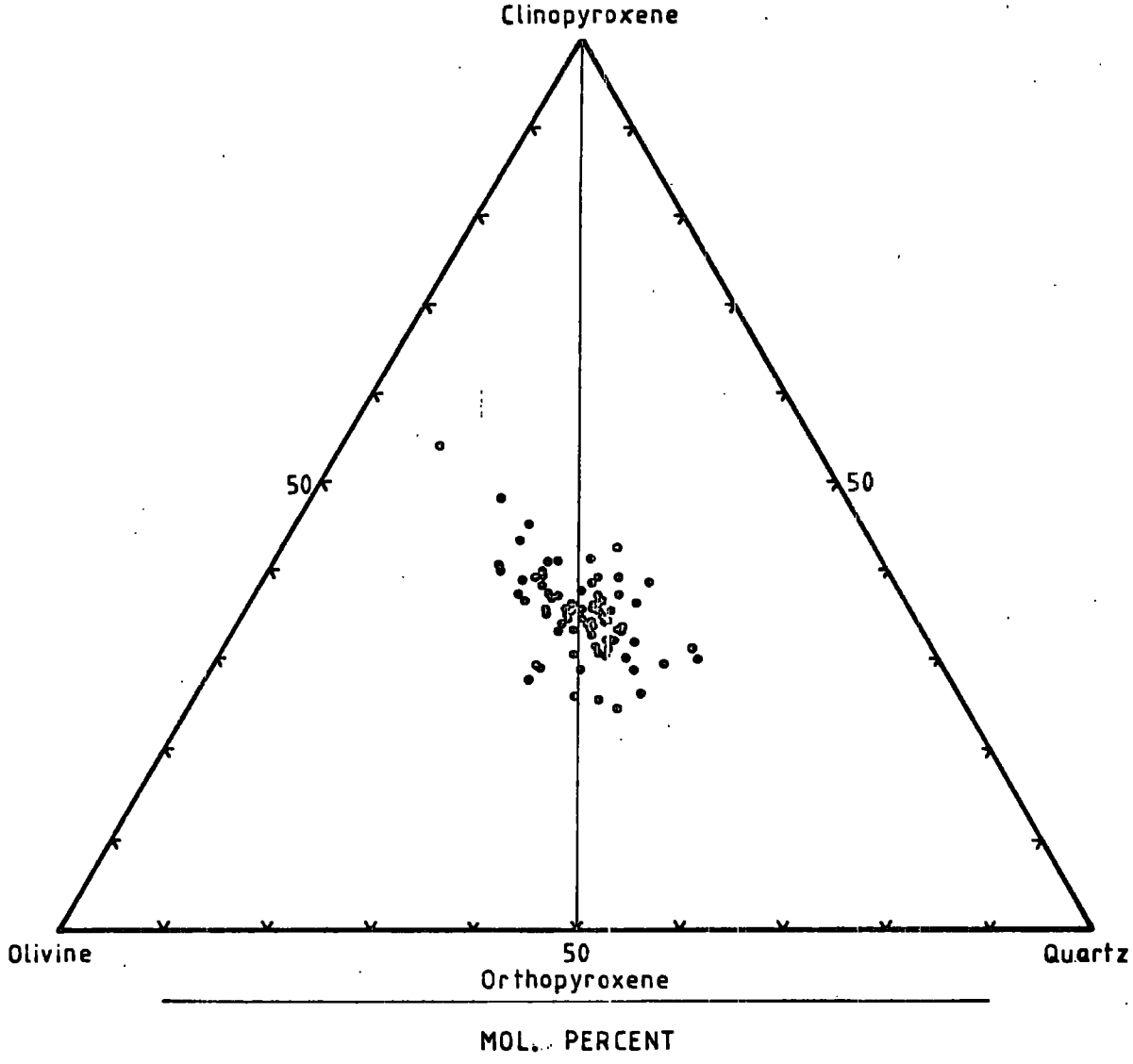
Clinopyroxene
50
50
Olivine
50
Orthopyroxene
Quartz
MOL. PERCENT

term tholeiite is used to cover both olivine tholeiite and quartz tholeiite because of the above reasons and the uncertainty of oxidation state.

The classifications in the light of normative compositions and chemical criteria are in broad agreement with the petrographic modal observations. Other important direct and indirect chemical characteristics of these basalts are their SiO_2 of 46-50%, a range of differentiation index (Thornton and Tuttle, 1960) of 16-30, and normative feldspars and modal feldspars more calcic than An_{50}.

3.2. Textures

In spite of their simple mineralogy, the described lavas show noteworthy varieties of textures, especially the degree of crystallinity and granularity which range from glassy up to coarse-grained (average groundmass grainsize of about 0.06-0.08 mm) types. Hence, these lavas are divided into four main groups on the grounds of their average groundmass grainsize, and of field observations (Emeleus, 1971), and then subdivided according to their amounts, types and sizes of phenocrysts and/or microphenocrysts together with their groundmass-mineral textures. The four main groups are pillow lavas and fine-grained, medium-grained, and coarse-grained basalts of which the average groundmass grainsizes

are about < 0.02 mm, 0.02-0.04 mm, and 0.06-0.08 mm, respectively. Throughout this account, the arbitrary value of 5% by volume of phenocrysts and/or microphenocrysts (R.N. Thompson et al., 1972) is used for distinguishing the lavas as phyric or aphyric. Those containing > 5% microphenocrysts and/or phenocrysts are called phyric lavas. The majority of these lavas are aphyric. The phenocryst and/or microphenocryst assemblages are plagioclase, plagioclase + olivine, plagioclase + olivine + augite, Fe-Ti oxides, or Fe-Ti oxides + plagioclase. The petrographic features of each specimen from the five self-contained areas are summarised in Table 3-1.

3.2.1. Pillow lavas

The general features of the pillow lavas are shown in Fig. 3-3. The groundmass consists of brownish, devitrified glass and where alteration has taken place, it produces opaque materials. Amygaloidal texture is common in two samples and the amygdale minerals are zeolites, apophyllite, calcite, amphibole, ?chlorophaeite and silica minerals.

Vitrophyric texture is common and is made up of plagioclase and olivine, with occasional augite microphenocrysts set in the glassy groundmass. The principal microphenocryst assemblages are plagioclase, and plagioclase + olivine. The plagioclase microphenocrysts are

Table 3-1. Petrographic features of the analysed samples from the five self-contained areas (a), (b), (e), (f) and (g)

Main Groups	Phyric or aphyric	Phenocryst and/or microphenocryst assemblages	Groundmass textures	Sample numbers and self-contained areas
Pillow lavas	Phyric	Plagioclase	Glassy	144007 (a) 143902 (d) 143903 (d)
		Plagioclase + olivines		
Fine-grained basalts	Phyric	Fe-Ti oxide microphenocrysts	Intergranular clinopyroxenes and plagioclase laths with occasional subophitic clinopyroxenes. Small amounts of interstitial glass and Fe-Ti oxides.	143844 (a) 143868 (a) 143896 (d) 143856 (f)
		Fe-Ti oxide and plagioclase microphenocrysts		143820 (a) 143841 (a) 143897 (d)
Medium-grained basalts	Aphyric	Sporadic plagioclase, olivine, clinopyroxene and Fe-Ti oxide microphenocrysts	Intergranular clinopyroxenes and plagioclase laths with occasional subophitic clinopyroxenes. Interstitial glass and Fe-Ti oxides are common.	143827 (a) 143825 (a) 143842 (a) 143866 (a) 143865 (a) 144008 (a) 144009 (a) 143837 (a) 143829 (b) 143810 (b)

Table 3-1 continued

Main Groups	Phyric or aphyric	Phenocryst and/or microphenocryst assemblages	Groundmass textures	Sample numbers and self-contained areas
Continued	Continued	Continued	Continued	143809 (b) 143808 (b) 143807 (b) 143804 (b) 143895 (d) 143894 (d) 143893 (d) 143892 (d) 143891 (d) 143890 (d) 143889 (d) 143887 (d) 143886 (d) 143862 (f) 143863 (f) 143860 (f) 143858 (f) 143957 (g) 143956 (g) 143955 (g) 143953 (g) 143951 (g) 143940 (g)

Table 3-1 continued

Main Groups	Phyric or aphyric	Phenocryst and/or microphenocryst assemblages	Groundmass textures	Sample numbers and self-contained areas
Continued	Continued	Continued	Continued	143855 (g) 143854 (g) 143853 (g) 143852 (g) 143851 (g) 143850 (g)
			Subophitic clinopyroxenes and plagioclase laths with occasional intergranular clinopyroxenes. Interstitial glass and Fe-Ti oxides are common.	143814 (a) 143830 (a)
	Phyric	Plagioclase with occasional olivine, clinopyroxene and Fe-Ti oxides.	Intergranular clinopyroxene and plagioclase laths with occasional subophitic clinopyroxene. Interstitial glass and Fe-Ti oxides are common.	143840 (a) 143871 (a) 143846 (b) 143845 (b) 143909 (d) 143885 (d) 143859 (f) 143857 (f) 143941 (g)
		Plagioclase + olivine with occasional clino-pyroxene and Fe-Ti oxides		144004 (a) 143806 (b) 143805 (b)

Table 3-1 continued

Main Groups	Phyric or aphyric	Phenocryst and/or microphenocryst assemblages	Groundmass textures	Sample numbers and self-contained areas
continued	continued	Plagioclase + clinopyroxene + olivine with occasional Fe-Ti oxides.	Continued	143882 (b)
		Big feldspar phenocrysts (up to 2cm in length) with occasional clinopyroxene, olivine and Fe-Ti oxides.		144006 (a) 143877 (b)
			Plagioclase laths and interstitial glass with occasional olivine, Fe-Ti oxides and clinopyroxene	143878 (b)
		Big feldspar phenocrysts (up to 2cm in length and olivine microphenocrysts with occasional clinopyroxene and Fe-Ti oxides	Intergranular clinopyroxene and plagioclase laths with occasional subophitic clinopyroxene. Interstitial glass and Fe-Ti oxides are common	143839 (a)
Coarse-grained basalts	Aphyric	Sporadic plagioclase, olivine, clinopyroxene and Fe-Ti oxides.	Intergranular clinopyroxene and plagioclase laths with occasional subophitic clinopyroxene. Interstitial glass and Fe-Ti oxdies are common	143828 (a) 143824 (a) 143843 (a)
			Subophitic clinopyroxene and plagioclase laths with occasional intergranular clinopyroxene. Interstitial glass and Fe-Ti oxides are common.	143831 (b) 143832 (b) 143881 (b) 143880 (b)

Table 3-1 continued

Main Groups	Phyric or aphyric	Phenocryst and/or microphenocryst assemblages	Groundmass textures	Sample numbers and self-contained areas
Continued	Continued	Continued	Continued	143876 (b) 143908 (d) 143888 (d) 143864 (f)
	Phyric	Big feldspar phenocrysts (up to 2cm in length) with occasional clino-pyroxene, olivine and Fe-Ti oxides.		143872 (a) 143870 (a) 143869 (a) 143899 (d) 143898 (d)
			Intergranular clinopyroxene and plagioclase laths with occasional subophitic clino-pyroxene. Interstitial glass and Fe-Ti oxides are common.	143873 (a) 143879 (b)

euhedral to subhedral, and exhibit oscillatory zoning. These microphenocrysts often cluster together forming glomeroporphyritic aggregates. The euhedral to anhedral olivine microphenocrysts are less abundant relative to the plagioclase microphenocrysts, and sometimes contain tiny grains of picotite. Pale greenish, clinopyroxene microphenocrysts are rare or absent; when they exist, they show subhedral to anhedral outlines. Hourglass structure and subophitic texture are also present in some clinopyroxene microphenocrysts.

3.2.2. Fine-grained basalts

Typically, all of these lavas show microprophyritic texture, and have an average groundmass grainsize of less than 0.02 mm (Fig. 3-4). The microphenocrysts are composed mainly of Fe-Ti oxides and plagioclase, with occasional pale-coloured clinopyroxenes. The Fe-Ti oxide microphenocrysts form numerous and evenly distributed, euhedral to subhedral crystals and have sizes of groundmass minerals being due to ease of nucleation (Carmichael, 1964). Oscillatory-zoned plagioclase microphenocrysts are subordinate to the Fe-Ti oxide microphenocrysts, and have sizes up to 0.05 mm. In general, the plagioclase microphenocrysts occur in glomeroporphyritic fashion, and have euhedral to subhedral outlines; sometimes, corroded crystals are

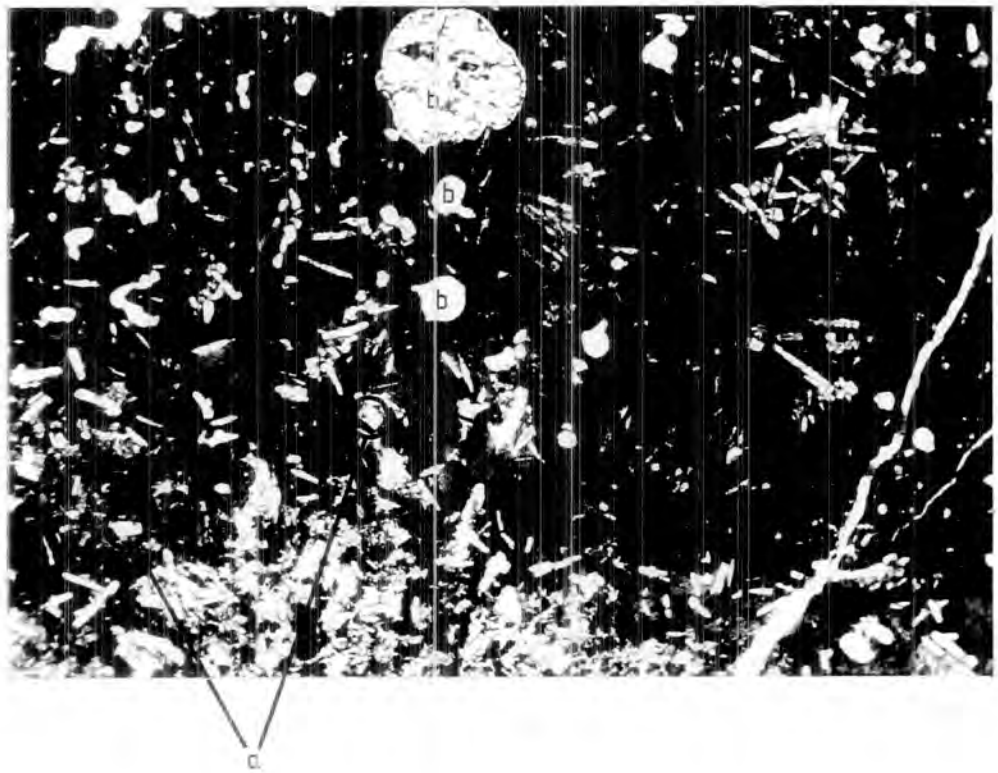
b
b
b
a

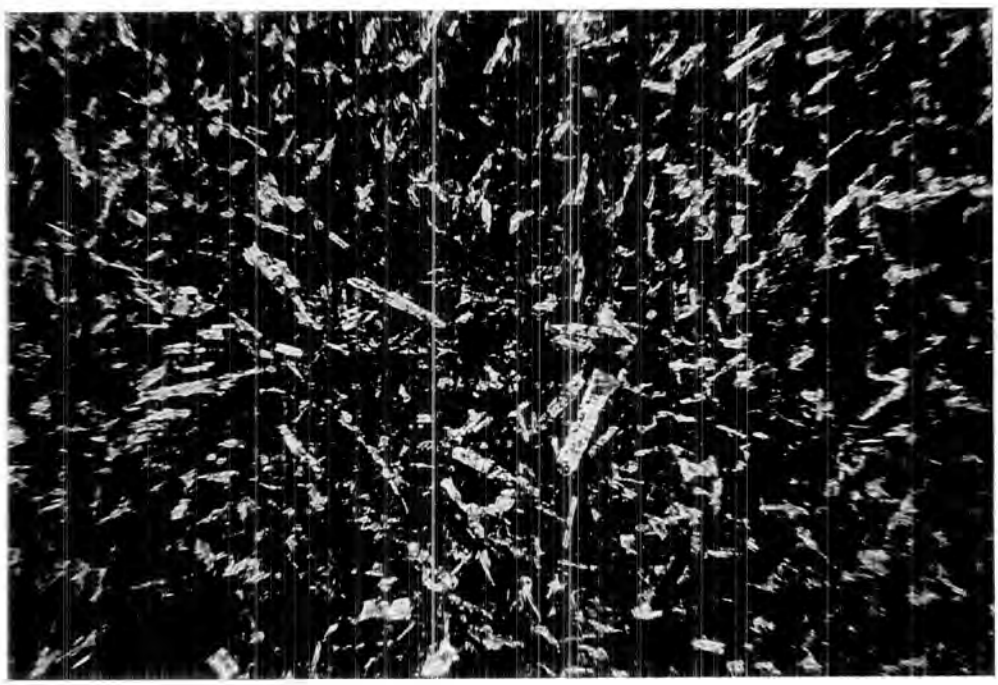

observed. Clinopyroxene microphenocrysts are rare or absent, and also show oscillatory zoning with anhedral-subhedral outlines. The characteristic microphenocryst assemblages are Fe-Ti oxides, and Fe-Ti oxides + plagioclase.

The groundmass chiefly consists of plagioclase laths and intergranular, with occasionally subophitic, clinopyroxenes. Olivines, interstitial Fe-Ti minerals and glass are much less common. The vesicles in these lavas are filled with chlorophaeite.

3.2.3. Medium-grained basalts

The majority of the studied samples belong to this group of which the average groundmass grainsize is about 0.02-0.04 mm. Apart from the groundmass grainsize, the differences between the fine-grained and the medium-grained basalts are that the proportions of interstitial glass and Fe-Ti oxides, and of intergranular olivines of the medium-grained groundmass are much greater than in the fine-grained groundmass. Fe-Ti oxide microphenocrysts are rare in the medium-grained lavas.

On the basis of the arbitrary value (5% by volume) of microphenocrysts and/or phenocrysts, the medium-grained basalts can be categorised as either phyric or aphyric lavas.

The aphyric lavas (Figs. 3-5, 3-6) consist mainly of plagioclase laths; intergranular, greenish clinopyroxenes with sparsely subophitic clinopyroxenes; interstitial Fe-Ti minerals, and brownish to greenish glass. Anhedral olivines are present in small amounts. In a few specimens, subophitic clinopyroxenes predominate over the intergranular clinopyroxenes. Two types of Fe-Ti oxides have been observed: a Ti-magnetite solid-solution and an ilmenite-hematite solid-solution. The Ti-magnetite solid-solution often forms irregular patches within interstices whereas the ilmenite-hematite solid-solution has needle- or blade-shaped crystals.

The phyric lavas have variable amounts and sizes of microphenocryst and phenocryst minerals. The principal mineral assemblages are plagioclase, plagioclase + olivine (Figs. 3-7, 3-8), and plagioclase + clinopyroxene + olivine. Plagioclase phenocrysts and/or microphenocrysts usually form stellate-glomeroporphyritic aggregates (Figs. 3-7, 3-8) and individual crystals are euhedral-anhedral with oscillatory zonation. Some of them have sieve texture and irregular outlines. The sizes of the plagioclase phenocrysts range up to 2 cm in length. Clinopyroxenes occurring as phenocrysts and/or microphenocrysts are anhedral-subhedral and have sizes of up to 0.9 mm in diameter. Oscillatory zoning and hour-

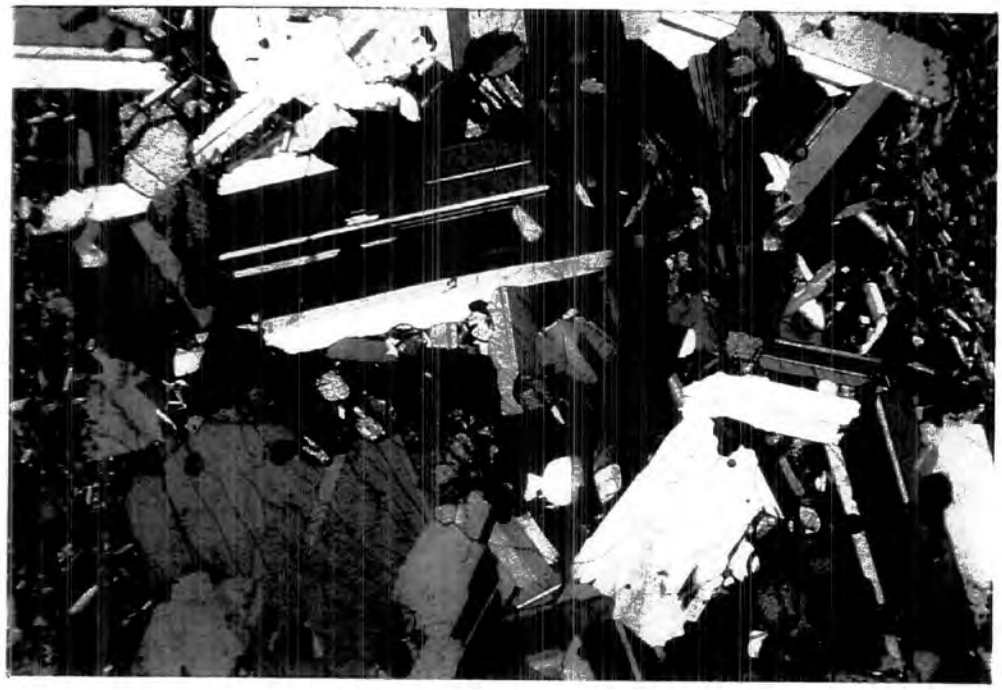

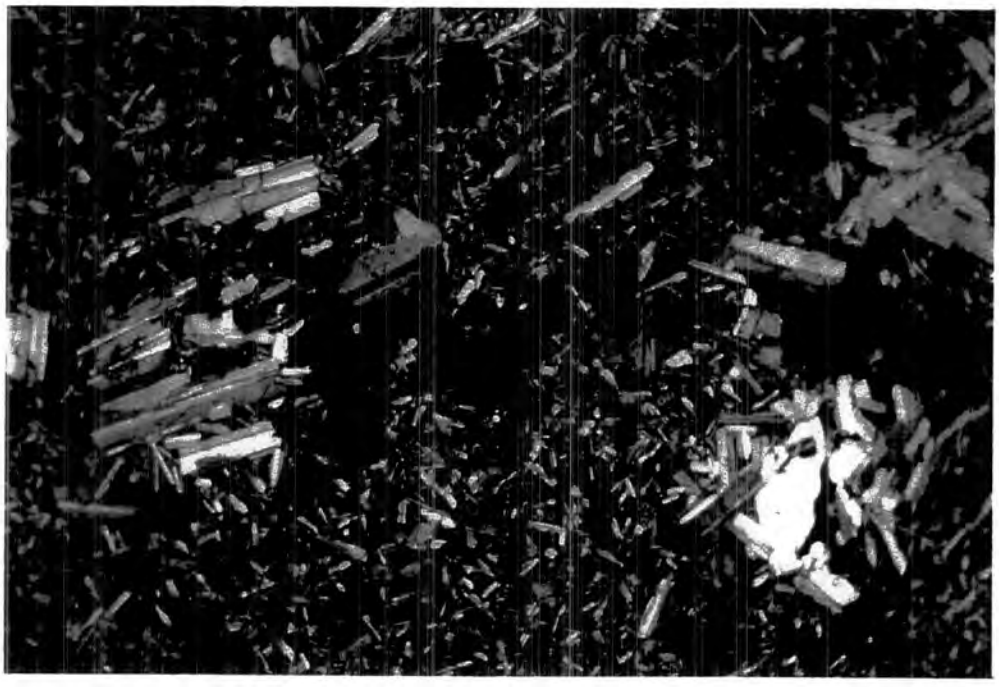

Fig. 3-7

Glomeroporphyritic textures of plagioclase-olivine phyric lava. The phenocrysts and/or microphenocrysts are made up of olivine and plagioclase. Sample no. 143805, crossed polars, x 25.

Fig. 3-8

Big-feldspar basalt of medium-grained type showing plagioclase and altered olivine (reddish brown) microphenocrysts. Sample no. 143839, crossed polars, x 25.

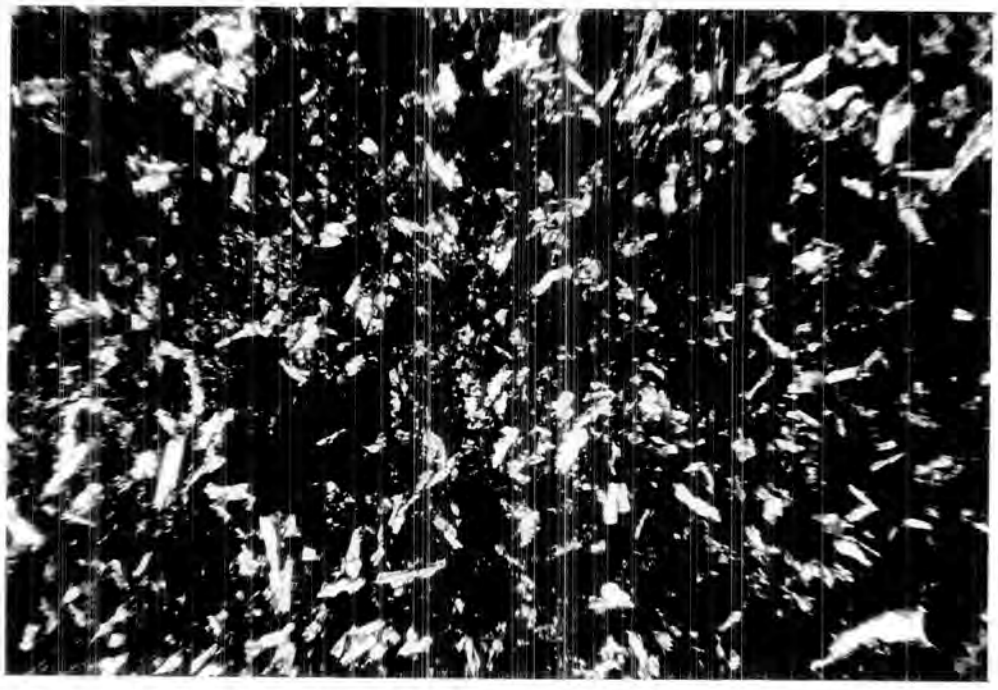

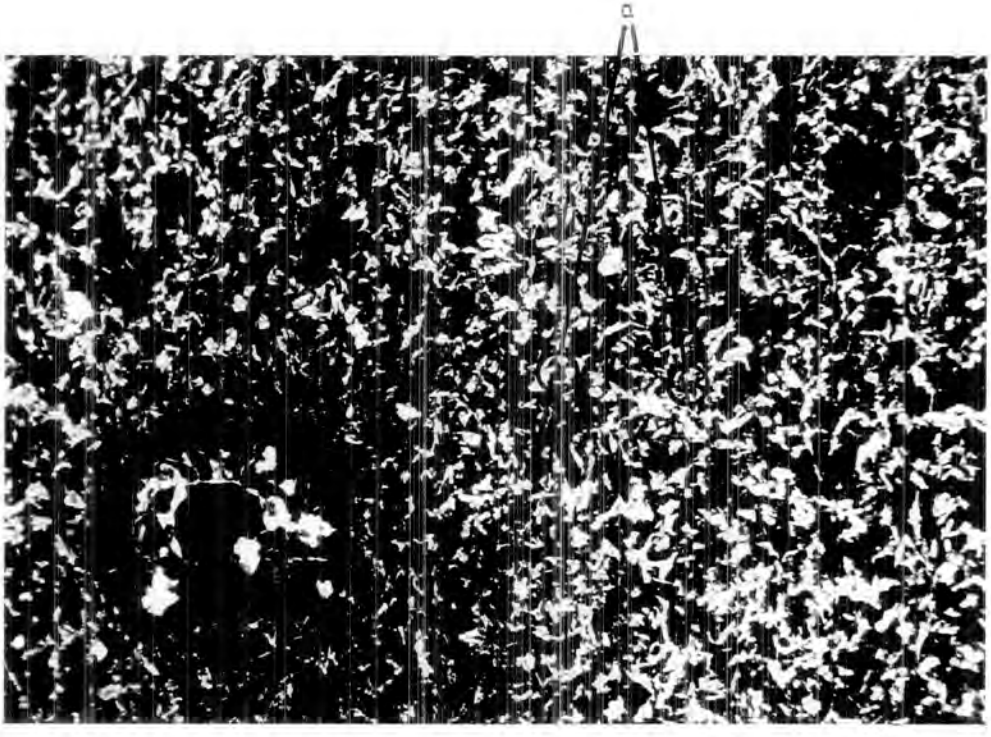
a

glass texture can be observed in some specimens. Olivine microphenocrysts and/or phenocrysts, ranging up to 0.9 mm in diameter, have anhedral-subhedral outlines, and sometimes occur in glomeroporphyritic fashion along with plagioclase microphenocrysts and/or phenocrysts. Fe-Ti oxide microphenocrysts are less common.

According to oxidation and alteration processes, most of the spinels show a variety of subsolidus textures when they are examined under reflected light. Fresh olivines and glass are rare, and are pseudomorphed by secondary minerals, such as iddingsite, chlorophaeite, amphibole, calcite and silica minerals, as found in vugs.

3.2.4. Coarse-grained basalts

The groundmasses of these lavas are variable from that of fine-grained basalts up to about 1 mm. The average groundmass grainsize is about 0.06-0.08 mm. The only significant phenocryst is plagioclase, and the clinopyroxene in the groundmass is predominantly subophitic to plagioclase (Figs. 3-9, 3-10,3-11). Intergranular clinopyroxene in the groundmass is found in a few samples (Fig. 3-12). Generally, the petrographic features of the coarse-grained basalts are similar to those of the medium-grained basalts except for the grainsizes, phenocryst mineral assemblages and the nature of pyroxene groundmass, as described above.


q
q
q
q
q

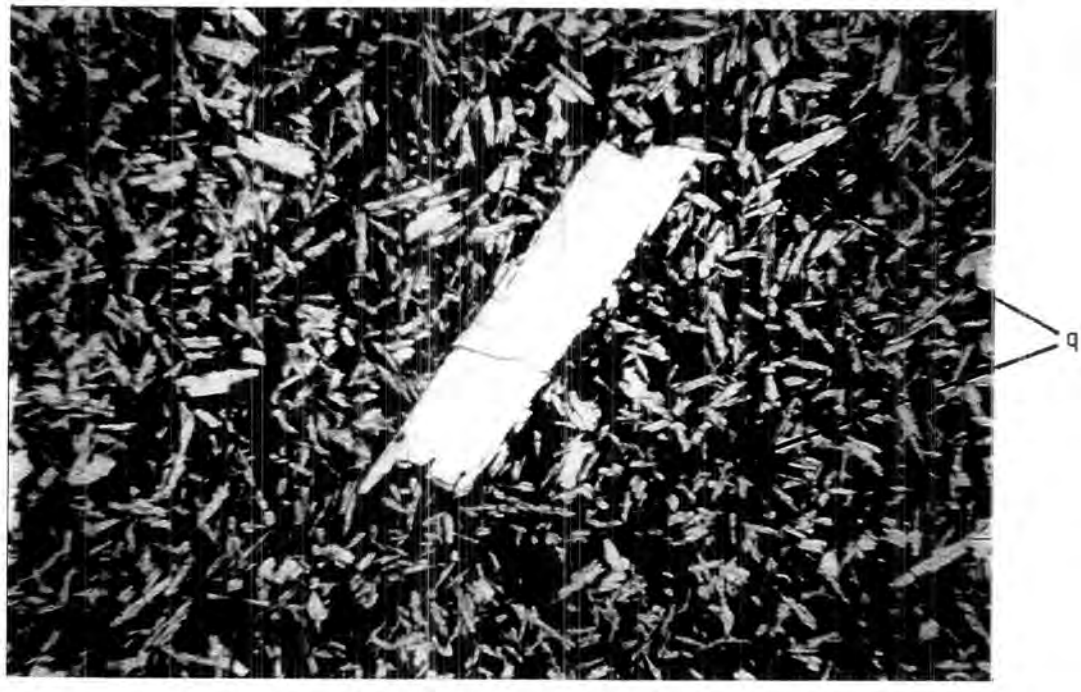
q

Fig. 3-11

Big-feldspar basalt of coarse-grained type displaying skeletal Fe-Ti oxide microphenocrysts. Sample no. 143872, ordinary light, x 45.

Fig. 3-12

Groundmass of big-feldspar basalt of coarse-grained type showing intergranular clinopyroxene groundmass and secondary calcite (a). Sample no. 143879, crossed polars, x 20.

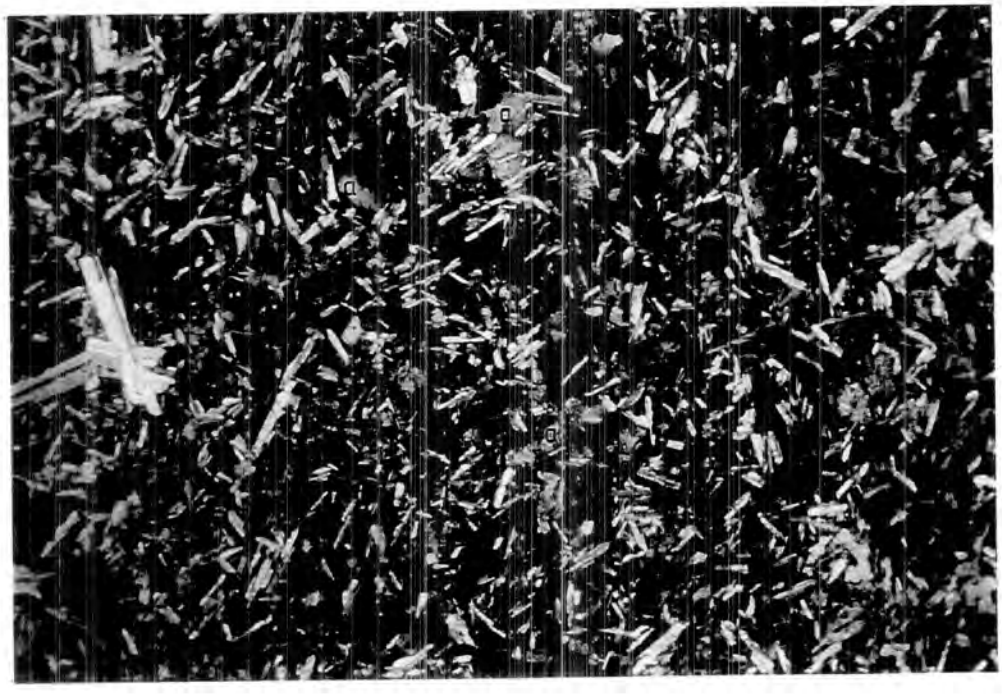

Judged from petrographic evidence, excluding Fe-Ti oxides, picotite was the earliest phase to crystallise. It was then followed by olivine, augite and plagioclase. The order of crystallization of the Fe-Ti oxides, especially those forming microphenocrysts, is difficult to delineate because there is no evidence to place them either before or after olivine. The inclusions of Fe-Ti oxides, which have euhedral or subhedral outlines, in the augite and plagioclase microphenocrysts and phenocrysts lead to the conclusion that they formed before the augite and plagioclase. The Fe-Ti oxides occurring as interstitial minerals, as well as the interstitial glass, were last to form from the magma.

3.3. Comparisons

Comparisons between the tholeiites in this study and the tholeiites described by Fawcett et al. (1973), in the light of the petrographic evidence, have been made. It appears that both sets of observations are broadly comparable. The basalts consist chiefly of plagioclase, clinopyroxene and Fe-Ti oxide phases with sporadic olivine and pigeonite. Most of them are aphyric lavas; sometimes, plagioclase and clinopyroxene occur as phenocrysts and/or microphenocrysts.

However, significant differences between the two

studies exist. Firstly, a considerable amount of olivine microphenocrysts has been observed in many of the thin sections studied here; also, tiny grains of picotite have been observed in some olivine grains in this study. Such observations have not been reported by Fawcett et al. (1973). Secondly, the Fe-Ti oxide phases described in this thesis can be divided into two stages of occurrence: the earlier and late stages. In the case of the earlier stage, a Ti-magnetite solid solution occurs as microphenocrysts whereas in that of the late stage, a Ti-magnetite solid solution forms ragged, large grains filling interstices. These interpretations are not concordant with those of Fawcett et al. who depicted the subhedral crystals of Fe-Ti oxides as a groundmass phase. Finally, one of the amygdale minerals in this study was identified by X-ray diffraction as apophyllite.

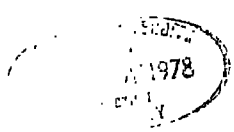

CHAPTER 4

MINERALOGY

4.1. Methods

A number of elements in feldspars (Si, Ti, Al, Fe, Mn, Mg, Ca, Na, Cr and K), pyroxenes (Si, Ti, Al, Cr, Fe, Mn, Mg, Ca and Na), Fe-Ti minerals (Si, Ti, Al, Cr, Fe, Mn, Mg and Ca), and olivines (Si, Ti, Al, Cr, Fe, Mn, Mg, Ca and Ni) were determined by using an electron microprobe analyser (Cambridge Scientific Instrument Company "Geoscan - Mk.II"). Samples were prepared as polished thin sections and were coated at the same time as the standards. Standards used were jadeite for Na and Al, wollastonite for Ca and Si, alkali feldspar for K, TiO_2 for Ti, Cr_2O_3 for Cr, MgO for Mg, MnO for Mn, Ni metal for Ni, and Fe metal for Fe.

All analyses were performed with a wavelength-dispersive system, under high-vacuum conditions, at an accelerating voltage of 15 Kv and a probe current of 0.04 μA on a Faraday cage. The electron beam was focussed to a spot of 2-5 μm in diameter, and $W_{K\alpha}$ radiation was used in analysing all elements. Analysing crystals and proportional counter voltages used for analysing various elements were: KAP (1710 V) for Si, Al, Mg and Na; LiF (1570 V) for Fe, Mn, Cr, Ti, Ca and Ni; and PET (1640 V) for K. Four 10-second count accumulations were made for

the peak and background of each element.

The general method outlined by Sweatman and Long (1969) was followed in data processing with the aid of an on-line Varian, 620/L-100 computer. The programme "Tim-3" (written by Dr. A. Peckett) performs the corrections for atomic number (electron back-scattering and electron retardation), mass absorption and fluorescence effects, on peak and background data of standards and samples.

All the mineral analyses made in this study are listed in Appendix.

4.2. Plagioclase

Plagioclase is a predominant constituent of the East Greenland tholeiitic basalts, occurring both as phenocrysts and microphenocrysts and as a groundmass phase. The plagioclase phenocrysts and microphenocrysts often show complex zonation and occur either as discrete crystals or in stellate, glomeroporphyritic aggregates. In general, they have euhedral-subhedral outlines; sometimes, anhedral outlines and sieve texture are observed. The groundmass plagioclases usually form small, lath-shaped crystals.

Plagioclase analyses were carried out on 17 rocks (which have differentiation-index values ranging from 17.01 to 27.07). Eighty-five random point analyses on plagioclase crystals (phenocrysts, microphenocrysts and

groundmass) and 14 systematic point analyses on one big-plagioclase crystal (5 x 18 mm) in sample number 143878 were made. The analyses of all the plagioclases are tabulated in Table A-4 and Table A-5 (Appendix).

The variations in terms of albite, anorthite and orthoclase components (molecular ratios) are shown in Fig. 4-1. The analysed plagioclases define a distinct, linear trend from $An_{83.4}Ab_{16.3}Or_{0.3}$ to $An_{27.3}Ab_{68.7}Or_{4.0}$. In general, these results are comparable to those given by Fawcett et al. (1973) except for K_2O contents. The upper and lower limits of K_2O from the work of Fawcett et al. are lower than those in this study.

One big-plagioclase crystal (5 x 18 mm) was systematically analysed, based on distance intervals of 0.2-0.4mm, from core to margin in the direction nearly perpendicular to its length. The analyses are listed in Table A-5 (Appendix), and the pattern of oscillatory zoning is presented on an anorthite content - distance diagram (Fig. 4-2). Since there is little agreement among petrologists as to the causes of oscillatory zoning and insufficient data in this study to add to the solution, no conclusions as to the cause of the pattern are drawn. Fawcett et al. (1973) considered the process of diffusion - controlled growth described by Bottinga et al. (1966) as the possible cause for oscillatory-zoned plagioclases in

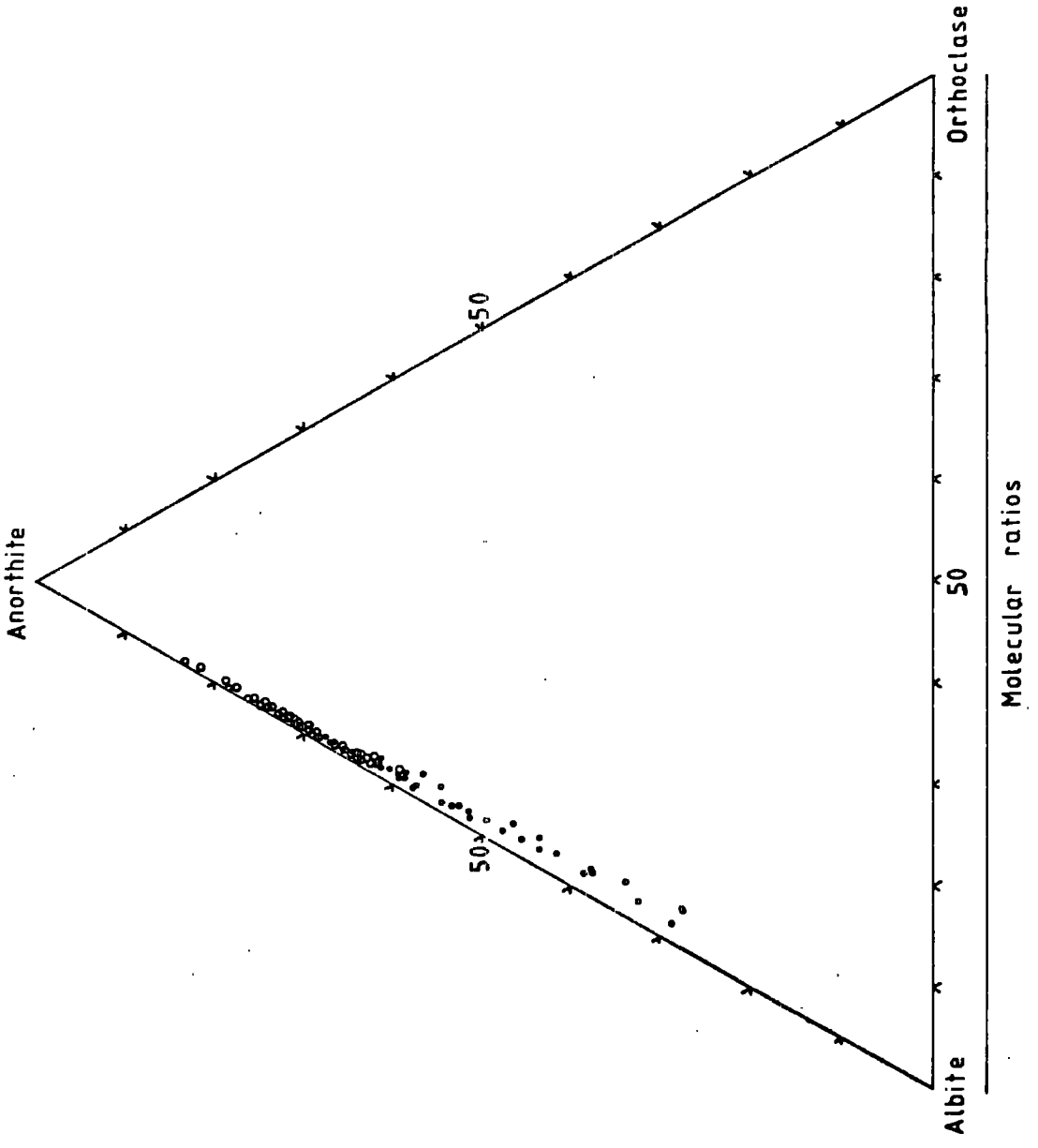
Anorthite
Orthoclase
Albite
50
50
50
Molecular ratios

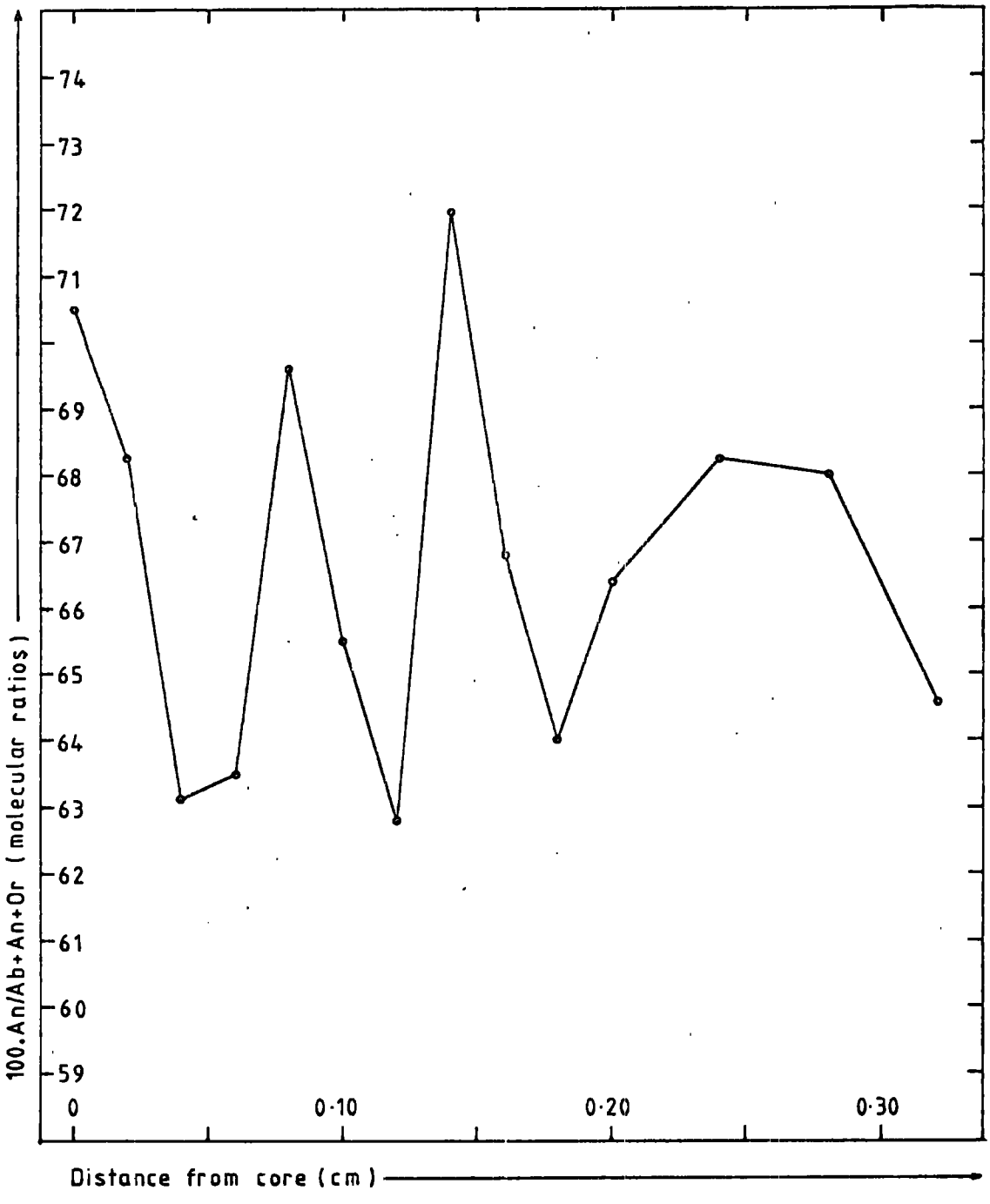
74
73
72
71
69
68
67
66
65
64
63
62
61
60
59
0
0·10
0·20
0·30
100.An/Ab+An+Or (molecular ratios)
Distance from core (cm)

related basalts of this region.

4.3. Pyroxenes

The majority of the pyroxenes found in the East Greenland tholeiites are augites; uniaxial pigeonite is also observed microscopically, in small amounts. The augite occurring as a groundmass phase can be divided, on the basis of their relationships to groundmass plagioclase, into two types: intergranular augite and subophitic augite. In general, the intergranular augite is a typical characteristic of the fine-grained and medium-grained basalts whereas the subophitic augite characterises the coarse-grained basalts. Augite is also found as phenocrysts and microphenocrysts but their proportions are subordinate to plagioclase and olivine phenocrysts and/or microphenocrysts. The augite phenocrysts and microphenocrysts often show euhedral to subhedral outlines; oscillatory zoning and hourglass texture is seen in some specimens.

Sixty-seven point analyses on pyroxene crystals, occurring either as phenocrysts and microphenocrysts or as a groundmass constituent in 16 rocks (differentiation-index values ranging from 17.01 to 27.07), were made. The analytical data are given in Table A-6 (Appendix).

All the analyses are plotted, on the basis of molecular percent, on the quadrilateral $CaMgSi_2O_6$ -

$CaFeSi_2O_6$ - $Mg_2Si_2O_6$ - $Fe_2Si_2O_6$ (Fig. 4-3). It appears that nearly all the analyses fall within the augite field. Most of the analyses follow the equilibrium fractionation trend of the Skaergaard pyroxenes (Brown, 1967); a trace of the metastable (supercooled) trend (Brown, 1967) is also observed. No pigeonite was detectable during analysis. However, Fawcett et al. (1973) have analysed about 550 pyroxenes in the East Greenland tholeiites and detected pigeonite, and more pronounced metastable trends to sub-calcic augite. The differences between the two sets of studies are attributed to the shortage of data in the mineralogical part of this study.

4.4. Olivine

Olivine occurs either as microphenocrysts and phenocrysts or as a groundmass phase. Although the groundmass olivine is present in small proportions, the olivine phenocrysts and microphenocrysts appear to occur in considerable amounts ($\geq$5% by volume) in some samples. Normally, the olivine phenocrysts and microphenocrysts have anhedral to subhedral outlines except for the olivine microphenocrysts in pillow lavas which are euhedral to anhedral. Sometimes, they form glomeroporphyritic aggregates along with plagioclase phenocrysts and/or microphenocrysts. The olivine occurring as a groundmass phase is generally anhedral and is less abundant in the

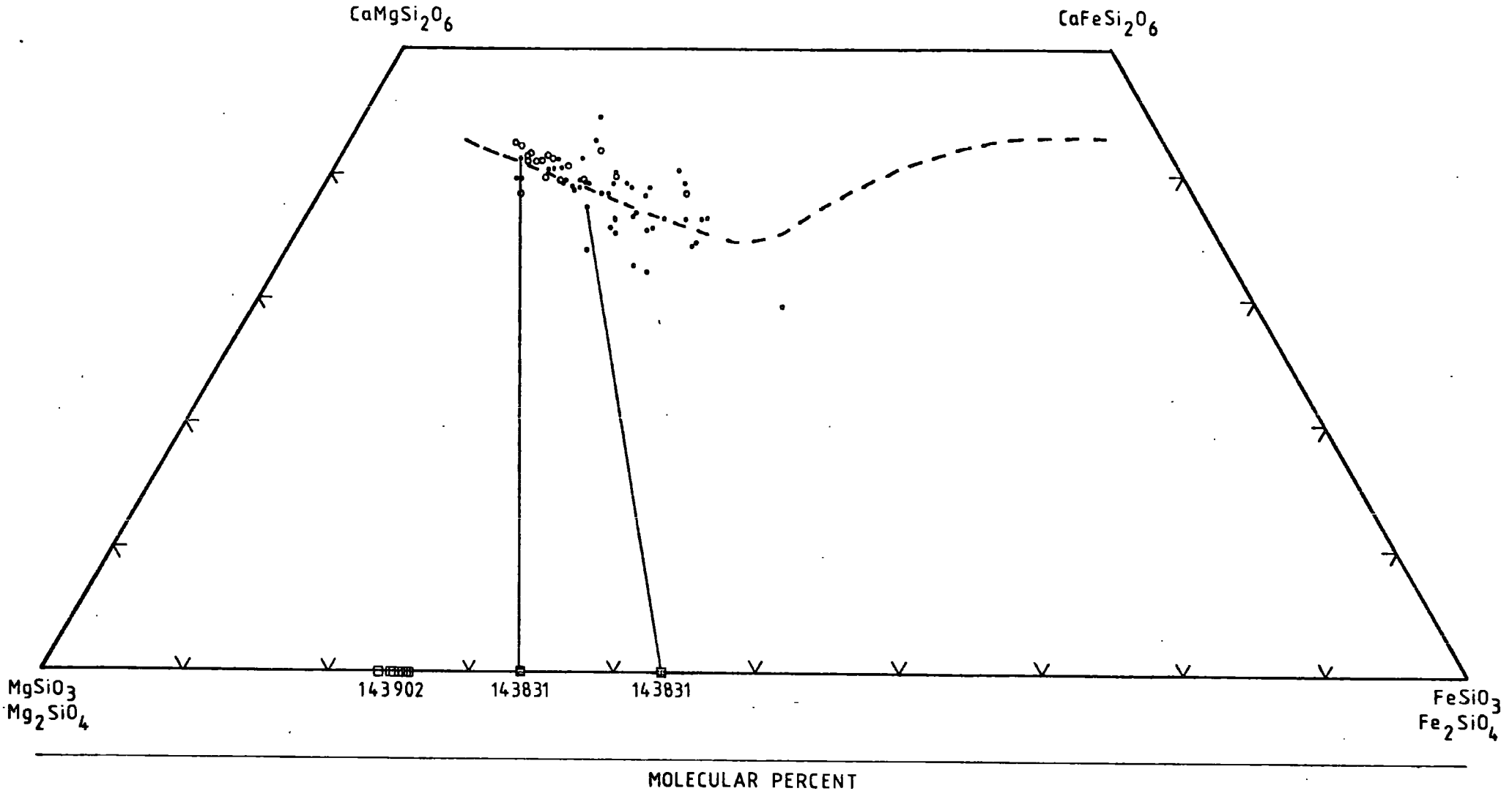
$CaMgSi_2O_6$
$CaFeSi_2O_6$
$MgSiO_3$
Mg_2SiO_4
143902
143831
143831
$FeSiO_3$
Fe_2SiO_4
MOLECULAR PERCENT

fine-grained tholeiites than in the medium-grained and coarse-grained tholeiites.

Since the studied tholeiites have been subjected to secondary alteration processes, it was very difficult to find fresh olivine crystals for analysis. However, two of the selected specimens contain unaltered olivine crystals; thus 2 analyses of the groundmass olivines (sample no. 143831) and 6 analyses of olivine microphenocrysts (sample no. 143902) were carried out. It appears that the groundmass olivines are hyalosiderites ($Fo_{56.5}$ to $Fo_{66.6}$) whereas the olivine microphenocrysts are chrysolites ($Fo_{74.4}$ to $Fo_{76.4}$). The analytical data (Table A-7; Appendix) have been plotted on Fig. 4-3 in terms of their Fo and Fa contents; the tie-lines between the coexisting pairs of groundmass olivines and clinopyroxenes in sample number 143831 are also shown.

4.5. Iron-titanium oxides

Coexisting iron-titanium oxide phases (titaniferous magnetite and ilmenite) have been observed throughout the tholeiitic suite from East Greenland except for the pillow lavas. The titaniferous magnetite is present as either a microphenocryst phase or a groundmass phase. The titaniferous magnetites occurring as microphenocrysts usually have euhedral to subhedral shapes whereas the groundmass phase exhibits ragged outlines. These features, again,

can be used as petrographic criteria for differentiating between the fine-grained tholeiites and the medium-grained and coarse-grained tholeiites. Titaniferous magnetite microphenocrysts are much more common in the fine-grained tholeiites whereas interstitial titaniferous magnetites are abundant in the medium-grained and coarse-grained tholeiites. The ilmenites usually form needle- or blade-shaped crystals.

In many of the described tholeiites, the spinel phase (titaniferous magnetite) has been subsequently oxidised, resulting in a variety of subsolidus exsolution textures (cf. Buddington and Lindsley, 1964). Only in six samples are the spinel phases rather homogeneous and 12 analyses were made; the results are given in Table A-8 (Appendix).

In spite of being subjected to alteration processes, the needle- or blade-shaped ilmenite crystals do not show exsolution textures or other heterogeneity. Nevertheless, due to their small sizes it was impossible to analyse the ilmenites in some specimens. Thus only 18 ilmenite crystals from nine specimens were analysed; the analytical results are listed in Table A-9 (Appendix). No analyses have been made on the ilmenites which are the products of subsequent oxidation.

The analyses of both titaniferous magnetites and ilmenites in four specimens (sample nos. 143806, 143814, 143830 and 144008), where fresh coexisting pairs are

available, have been recalculated to check their quality (cf. Carmichael, 1967a). The recalculated results, including their compositions in terms of the molecular percent of ulvöspinel in the titaniferous magnetite and of R_2O_3 in the ilmenite (Carmichael, 1967a), are given in Tables 4-1 and 4-2. It appears that the totals of the recalculated ilmenite analyses (Table 4-2) are satisfactory and that the totals of the spinel phases (Table 4-1) are satisfactory only on the ulvöspinel basis but not on the ilmenite basis. However, temperatures and oxygen fugacities were estimated from the curves of Buddington and Lindsley (1964). The temperatures and oxygen fugacities, together with the differentiation-index values of the host rocks are also given in Table 4-2.

Fig. 4-4 shows the plots of all analysed Fe-Ti minerals in terms of the molecular percent of the ulvöspinel and R_2O_3; tie-lines delimiting the range of compositions in each specimen which contains fresh pairs of titaniferous magnetites and ilmenites, are also shown.

The temperatures and oxygen fugacities indicated by the oxide equilibrium data are plotted in Fig. 4-5. All the points appear to lie between the curves representing quartz-fayalite-magnetite and wüstite-magnetite buffers at one atmosphere total pressure (Eugster and Wones, 1962). Although these spinel-ilmenite phase equilibria data were

Table 4-1 Analyses of titaniferous magnetites in those analysed tholeiites containing fresh pairs of titaniferous magnetites and ilmenites

Wt.%	143806a	143806b	143814a	143814b	143814c
SiO_2	0.20	0.37	0.22	0.15	0.67
TiO_2	22.79	24.41	24.88	25.31	25.34
Al_2O_3	2.43	1.83	1.55	1.76	1.50
Cr_2O_3	0.51	0.04	0.06	0.05	0.06
FeO	69.50	69.15	69.55	68.83	69.10
MnO	0.38	0.41	0.86	0.49	0.54
MgO	1.04	1.28	0.31	0.61	0.45
CaO	0.01	0.06	0.10	0.10	0.22
Total	96.86	97.55	97.53	97.30	97.88

Recalculated analyses

Ilmenite basis					
Fe_2O_3	56.70	55.04	53.86	52.90	52.39
FeO	18.48	19.62	21.08	21.23	21.96
Recalculated total	102.54	103.06	102.92	102.60	103.13
Ulvöspinel basis					
Fe_2O_3	20.99	19.13	18.31	17.34	16.63
FeO	50.61	51.94	53.07	53.23	54.14
Recalculated total	98.96	99.47	99.36	99.04	99.55
Molecular percent					
Ulvöspinel	64.54	69.33	70.75	71.68	73.36

Table 4-1 (continued)

Wt.%	143830a	143830b	144008a	144008b
SiO_2	0.46	0.37	0.47	0.58
TiO_2	26.51	27.20	24.50	25.69
Al_2O_3	2.14	2.02	1.96	1.41
Cr_2O_3	0.16	0.13	0.26	0.19
FeO	65.79	67.00	68.30	67.34
MnO	1.16	0.96	0.69	1.08
MgO	1.32	1.37	1.96	1.51
CaO	0.16	0.20	0.13	0.17
Total	97.70	99.25	98.27	97.97

Recalculated analyses

Ilmenite basis				
Fe_2O_3	50.16	50.86	55.64	52.84
FeO	20.66	21.23	18.24	19.79
Recalculated total	102.73	104.34	103.85	103.26

Ulvöspinel basis				
Fe_2O_3	14.20	14.36	19.23	16.79
FeO	53.01	54.08	51.00	52.23
Recalculated total	99.12	100.69	100.20	99.65

*Molecular percent

Ulvöspinel	75.38	75.84	68.99	73.37

*Based on the calculation method of Carmichael (1967a)

Table 4-2 Analyses of ilmenites in those analysed tholeiites containing fresh pairs of titaniferous magnetites and ilmenites, including the estimated temperatures and oxygen fugacities, and the differentiation-index values of the host rocks.

Wt.%	143806a	143806b	143814a	143814b
SiO_2	0.33	0.50	0.31	0.69
TiO_2	50.16	49.85	50.10	50.15
Al_2O_3	0.22	0.25	0.12	0.17
Cr_2O_3	-	-	-	0.01
FeO	46.63	47.14	47.58	46.40
MnO	0.44	0.42	0.69	0.45
MgO	1.40	0.63	0.59	0.56
CaO	0.08	0.22	0.24	0.23
Total	99.26	99.01	99.63	98.66
		Recalculated analyses		
Fe_2O_3	4.64	3.93	4.69	2.48
FeO	42.45	43.60	43.35	44.17
Recalculated total	99.72	99.40	100.09	98.91
Molecular percent R_2O_3	4.70	4.00	4.62	2.62
Temp. (°C)	950	940	950	880
fO_2 (bars)	10^{-12}	$10^{-12.5}$	$10^{-12.4}$	$10^{-14.1}$
Differentiation index	27.07		26.24	

Table 4-2 (continued)

Wt.%	143830a	143830b	144008a	144008b
SiO_2	0.64	0.23	0.60	0.36
TiO_2	49.16	49.98	49.78	50.30
Al_2O_3	0.39	0.03	0.29	0.35
Cr_2O_3	0.11	0.08	0.12	0.09
FeO	47.12	47.51	45.44	44.70
MnO	0.64	0.68	0.50	0.63
MgO	0.51	-	2.11	2.02
CaO	0.34	0.24	0.20	0.33
Total	98.91	98.75	99.04	98.78
		Recalculated analyses		
Fe_2O_3	4.60	3.65	4.97	4.11
FeO	42.98	44.22	40.96	41.00
Recalculated total	99.37	99.11	99.53	99.19
*Molecular percent				
R_2O_3	5.06	3.62	5.20	4.48
**Temp (^oC)	1050	1090	975	1010
**fO_2 (bar)	$10^{-10.75}$	10^{-10}	$10^{-11.75}$	$10^{-11.5}$
Differentiation index	19.47		23.22	

*Based on the calculation method of Carmichael (1967a)

**Based on the Fe-Ti oxide equilibration curves of Buddington and Lindsley (1964).

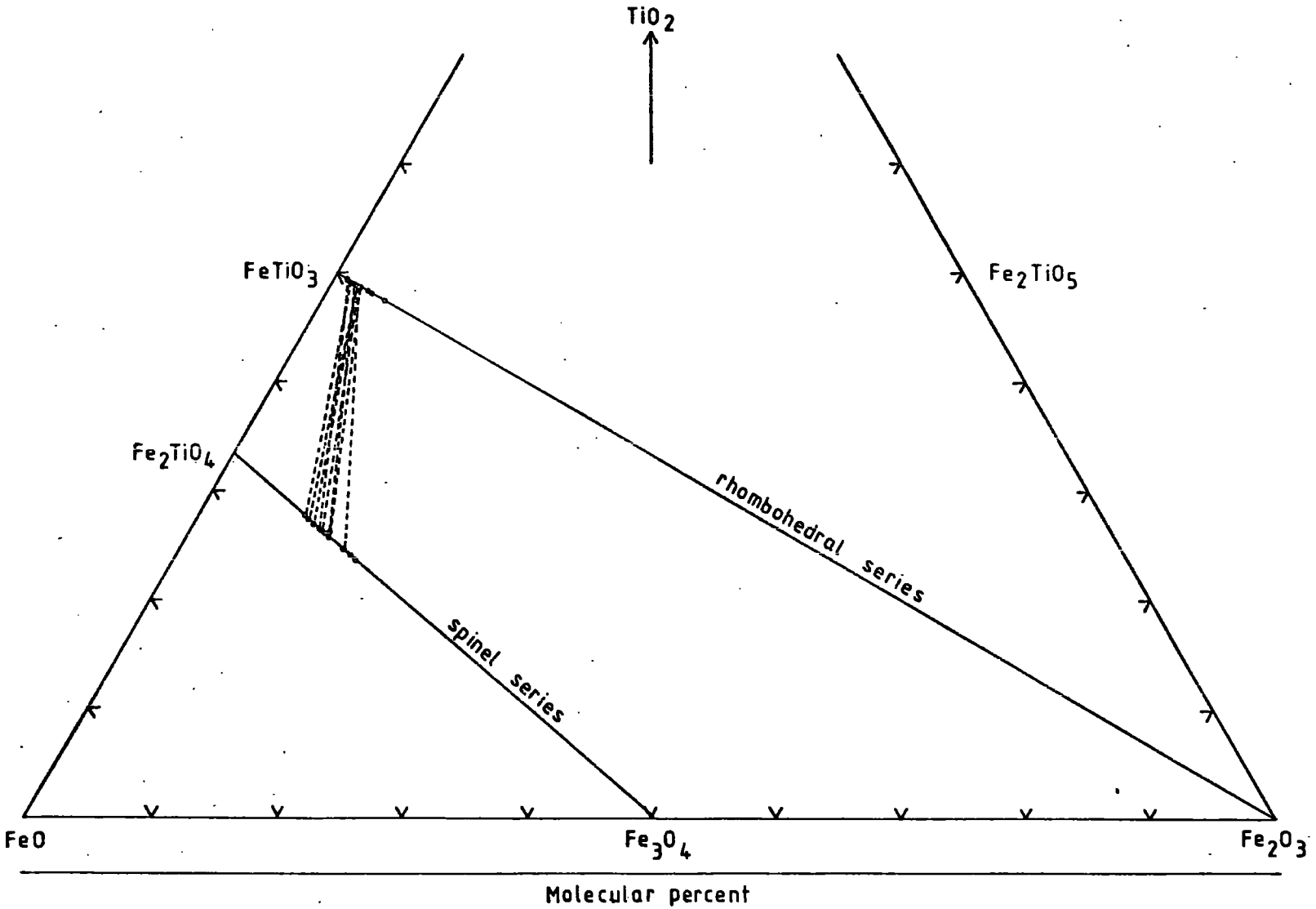
TiO2
FeTiO3
Fe2TiO5
Fe2TiO4
rhombohedral series
spinel series
FeO
Fe3O4
Fe2O3
Molecular percent

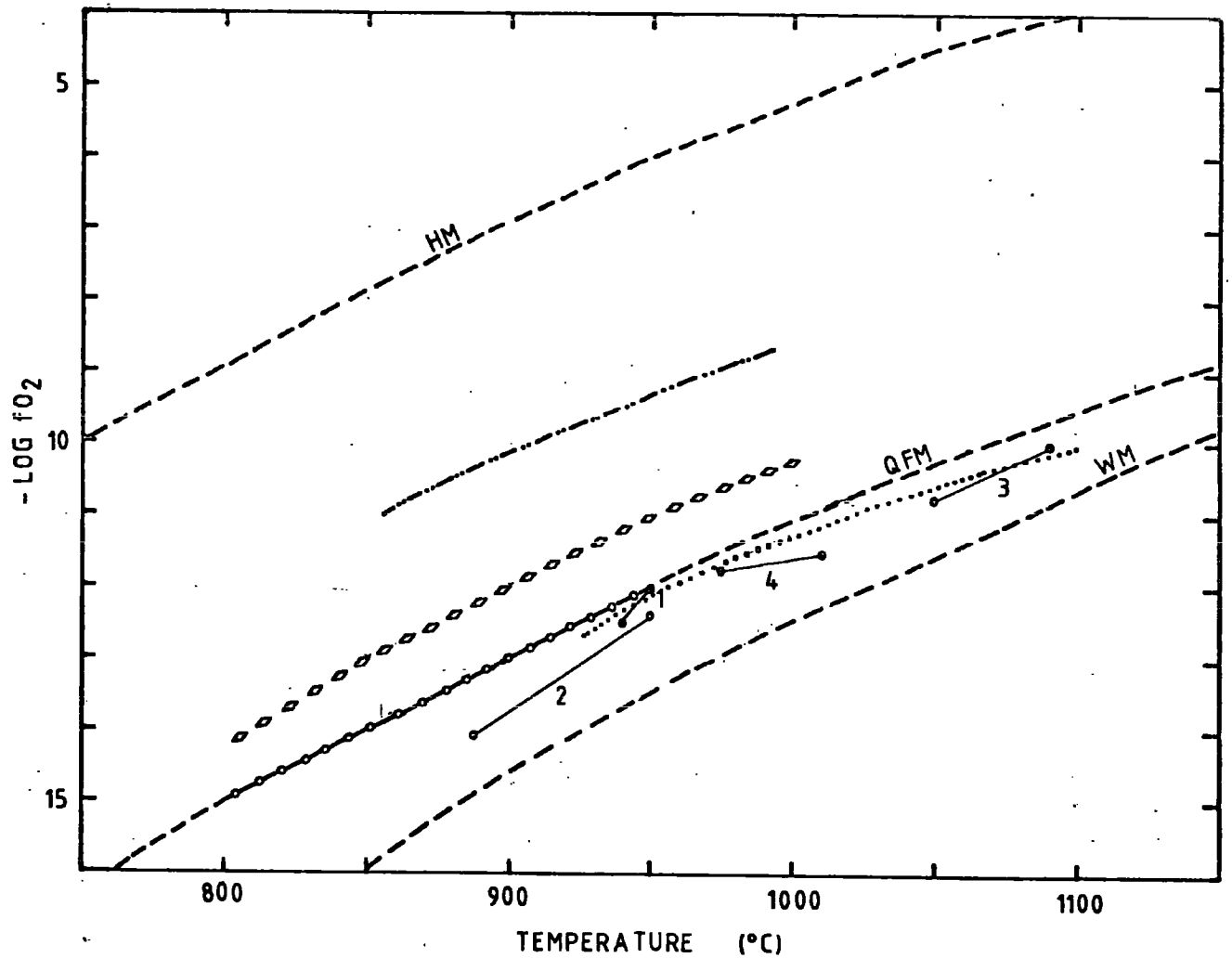
5
10
15
- LOG fO2
HM
QFM
WM
1
2
3
4
800
900
1000
1100
TEMPERATURE (°C)

obtained from only four specimens, the general conclusion can be drawn that there is a smooth, progressive decrease in oxygen fugacity and temperature with differentiation index (see caption to Fig. 4-5) and that the oxygen fugacities are slightly lower than those of the tholeiitic suite of Thingmuli (Carmichael, 1967b).

CHAPTER 5

SUMMARY

5.1. Field relations

The 2,660m-thick basalt pile in the research region represents one of the higher parts of the whole basalt sequence in East Greenland. It rests on Lower Cretaceous sediments and is overlain by sediments of the Kap Dalton Formation. The great majority of basalts appear to have been extruded under subaerial conditions. The evidence of subaqueous eruptions are occasionally observed. The northwestern part of the research region consists of flat-lying flows whereas in the southern and southeastern parts, flows are disturbed by a system of normal faults striking approximately WSW-ENE and downthrowing to the south. The flows in the faulted areas dip southerly or southeasterly at angles of up to 20^{o}. No dykes or intrusions have been recorded. The lavas have been categorised into five main groups: pillow lavas; big-feldspar basalts; coarse-grained, non-porphyritic basalts; medium- to fine-grained, porphyritic basalts; medium- to fine-grained, sparsely porphyritic and non-porphyritic basalts. The lavas were grouped by Dr. C.H. Emeleus, based on geological and geographical boundaries, into a number of self-contained areas and then the correlation between successions of the self-contained areas were made by

linking recognizable horizons and large-scale features. That correlation is supported by the geochemical evidence provided by this study.

5.2. Chemical, petrographical and mineralogical relations

Chemically, all the analysed lavas can be classified as tholeiites according to the classification schemes of Yoder and Tilley (1962) and of Macdonald and Katsura (1964); in terms of geotectonic position, they are oceanic island basalts (Pearce and Cann, 1973; Pearce et al., 1975). The general geochemical features are enrichment in TiO_2, FeO, Fe_2O_3, Zn and Cu but depletion in K_2O, Ba, Sr and Rb relative to those of world-wide distribution (Manson, 1967; Prinz, 1967). However, the compositional ranges are rather narrow and consequently, poorly defined trends are obtained as shown in many of the diagrams in Chapter 2.

For comparative purposes, the data on the Tertiary tholeiites from mid-west Iceland (Johannesson, 1975), which are believed to have the same origin (primary hot mantle plume) as those of East Greenland (Brooks, 1973b; Schilling and Noe-Nygaard, 1974) are also plotted along with the East Greenland data. The results of plotting both sets of data reveal much more pronounced trends which consist of two different slopes and the trends appear to diverge at a differentiation-index value of 21 (Figs. 2-1, 2-5). These features imply two different episodes of

fractionation. From the FeO + MgO against FeO/MgO diagram, which is used by Macdonald and Katsura (1964) to show fractionation patterns of the Hawaiian tholeiitic series, it is clear that the studied tholeiites approximately occupy the position where the change in the Hawaiian tholeiitic trends occur. Thus, the ill-defined trends for the East Greenland tholeiites are attributed to the two stages of mineral separation from the successive liquids as well as to the limited compositional ranges. According to low-pressure crystallisation (petrographic criteria), the deduction can be made from various diagrams, although they are not in agreement in every detail, that the trend is controlled largely by olivine fractionation in the initial stage and subsequently by plagioclase fractionation.

Comparison between bivariate analysis and multivariate analysis was performed. It appears that either bivariate plots or multivariate plots may give similar results, e.g. MgO decreases whereas Na_2O increases with differentiation index. However, the multivariate analysis shows the sympathetic behaviour between Na_2O and Al_2O_3, and a distinctive trend can be obtained by plotting factor scores for each sample of Factor 6 (MgO, positive pole; Na_2O and Al_2O_3, negative pole) against their relevant differentiation-index values (Fig. 2-10). Furthermore, the trend obtained by plotting the average factor score, on the basis of diff-

erentiation-index groupings, against the average differentiation-index, supports the two episodes of fractionation. The divergence of trend seems to occur at around factor-score and differentiation-index values of 0.00 and 21, respectively. Although the plots of the factor scores for other factors against those for Factor 6 are scattered (Figs. 2-11, 2-12, 2-13, 2-14, 2-15, 2-16), the two different patterns can also be seen if the scores are grouped on the same basis as mentioned above. Thus, in the case of such a narrow compositional range, R-mode factor analysis is much more suitable for showing chemical relationships than bivariate analysis.

Petrographically, all the studied tholeiites consist mainly of plagioclase (average labradorite), augite and Fe-Ti oxide minerals with small amounts of olivine, pigeonite and interstitial glass except for pillow lavas where the groundmass is entirely glass. These tholeiites can be divided, in terms of an average groundmass grainsize and of field evidence, into four main groups (pillow lavas, fine-, medium- and coarse-grained basalts) and then subdivided according to the amounts and sizes of phenocrysts and/or microphenocrysts.

The pillow lavas are composed chiefly of devitrified glass and have a vitrophyric texture. The principal microphenocryst assemblages are plagioclase and plagioclase +

olivine. Some olivine microphenocrysts contain tiny picotite grains.

The fine-grained basalts often show microporphyritic texture. The groundmass phase is predominantly plagioclase and intergranular, with occasional subophitic, clinopyroxenes. Olivine, interstitial Fe-Ti oxide minerals and glass are much less common. The characteristic microphenocryst assemblages are Fe-Ti oxides and Fe-Ti oxides + plagioclase.

The medium-grained basalts occur as either phyric or aphyric types. The groundmass consists mainly of plagioclase, intergranular clinopyroxenes with occasional subophitic clinopyroxenes, and interstitial Fe-Ti oxide minerals. Olivine and interstitial glass are much more common than in the fine-grained basalts. In a few specimens, subophitic clinopyroxenes predominate over intergranular clinopyroxenes. The significant phenocryst and/or microphenocryst assemblages are plagioclase, plagioclase + olivine and plagioclase + clinopyroxene + olivine. Some plagioclase phenocrysts have sizes up to 2cm in length.

The coarse-grained basalts have similar features to the medium-grained basalts, excluding the average groundmass grainsize, texture of the clinopyroxene groundmass and nature of the phenocryst assemblage. Most of the clinopyroxene groundmass is subophitic to plagioclase; inter-

granular clinopyroxenes are abundant in a few samples. Plagioclase is the only principal phenocryst assemblage in these rocks. It is likely that the coarse-grained basalts are the late-differentiate rocks of the sampled suite.

The amygdale minerals present in the studied tholeiites are zeolites, apophyllite, calcite, amphibole, chlorophaeite and silica minerals.

The criteria for oxidation and alteration processes affecting the described tholeiites are a variety of sub-solidus textures in the spinel phase and the relative scarcity of fresh olivines and glass. However, the pattern on the K-K/Rb diagram (Fig. 2-19) suggests that these processes have less influence on the geochemical patterns than do the crystal fractionation processes.

From petrographic observations, the order of crystallisation started with picotite and was then followed by olivine, augite and plagioclase. The Fe-Ti oxide microphenocrysts might have formed simultaneously with picotite and/or olivine. The interstitial Fe-Ti oxides and glass were the last phases to crystallise from the magma. Such a pattern suggests that the tholeiites of East Greenland crystallised under low-pressure conditions (Yoder and Tilley, 1962).

The geochemical features can be related to petrography

by plotting the normative constituents of the studied tholeiites on the ternary diagram (Fig. 2-18) representing the olivine-clinopyroxene-plagioclase plane of the basalt tetrahedron (Yoder and Tilley, 1962) in which field boundaries are taken from the work on the iron-free system by Osborn and Tait (1952). The position of the plotted samples, lying close to the locus of liquid in equilibrium with olivine, plagioclase and spinel, and predominantly in the plagioclase field, is in accordance with the predominant, principal phenocryst and/or microphenocryst assemblage (plagioclase) and with the olivine (?containing picotite) - plagioclase assemblage which predominates over the assemblage containing a significant amount of clinopyroxene.

Mineralogically, the compositions of feldspar vary from $An_{83.4}Ab_{16.3}Or_{0.3}$ to $An_{27.3}Ab_{68.7}Or_{4.0}$. The upper and lower limits of anorthitic contents, including K_2O contents, for the analysed feldspars are slightly higher than those given by Fawcett et al. (1973). The great majority of the clinopyroxenes are augite and they appear to follow the equilibrium trend of the Skaergaard suite; only a trace of the metastable trend has been observed. Neither pigeonite nor subcalcic augite was detectable during probe analysis. However, Fawcett et al. (1973) have detected pigeonite, subcalcic augite and various pronounced metastable trends. Eight analyses of olivine crystals in two samples were made.

The microphenocrysts seem to have chrysolitic compositions ($Fo_{74.4}$ - $Fo_{76.4}$) whereas the groundmass olivines are hyalosiderites ($Fo_{56.5}$ - $Fo_{66.6}$). The iron-titanium oxide minerals, both titaniferous magnetites and ilmenites, were analysed and the temperatures and oxygen fugacities for the analysed samples which contain the two fresh oxide phases have been estimated from the oxygen fugacity - temperature equilibration curves of Buddington and Lindsley (1964). The data points lie between the curves of the quartz-fayalite-magnetite and wüstite-magnetite buffers and there is a smooth, progressive decrease in oxygen fugacity and temperature with host-rock differentiation index. The oxygen fugacities are only slightly lower than those of the Thingmuli tholeiitic suite at the same ranges of temperature.

5.3. Basalt comparisons

Comparisons, in terms of geochemistry, have drawn with certain Tertiary tholeiitic lavas from Skye (I.T. Williamson, personal communication), mid-west Iceland (Johannesson, 1975) and the Atlantic ocean floor (Engel et al. 1965). It is obvious that the studied tholeiites are similar to the mid-west Icelandic tholeiites in many respects. The mid-west Icelandic tholeiites seem to correspond to the late-fractionation trend of the East Greenland tholeiites which is largely controlled by plagioclase fractionation. It is

not implied that the mid-west Icelandic tholeiites are the differentiated products of the East Greenland tholeiite magmas but that the relationship indicates similarities in source material and fractionation processes. Johannesson (1975) concluded that the quartz tholeiites and olivine tholeiites in mid-west Iceland are the products of partial melting of the Earth's upper mantle at different depths (rather than due to plagioclase fractionation) because there is no significant Eu anomaly in the Icelandic basalts (Shimokawa and Masuda, 1972; O'Nions and Grönvold, 1973) and samples which are high in Al_2O_3 are high in MgO. However, the average REE pattern of the tholeiites from Wiedemann Fjord in East Greenland (Brown and Whitley, 1976) is similar to that of the Tertiary Icelandic basalts. Thus, from the evidence presented in this study and the geochemical break between quartz tholeiites and basaltic icelandite in mid-west Iceland, the absence of significant Eu anomalies in both sets of data is probably an indication of the fractionation process during rapid ascent of magma rather than of partial melting at different depths. That is, the quartz tholeiites were differentiated from the parental olivine tholeiites and they are the final products of high-level crystal fractionation.

Comparisons are also made with the tholeiites occurring along the Reykjanes Ridge and the middle Neovolcanic zone of

Iceland (Schilling, 1973; O'Nions and Pankhurst, 1974). It appears that the East Greenland tholeiites as well as the mid-west Icelandic tholeiites have the same characteristics as those from the middle Neovolcanic zone of Iceland which are believed to be PHMP (primary hot mantle plume)-derived basalts (Schilling, 1973).

The results of comparisons made by plotting the tholeiitic lavas from East Greenland, mid-west Iceland and Skye on a total alkalis versus silica diagram (Fig. 2-3,a) and total alkalis versus Fe/Mg ratio diagram (Fig. 2-3,b) give rise to distinctive patterns. In Fig. 2-3,a, the pattern conforms with the Hebridean tholeiitic trend (Holland and Brown, 1972) and it extends that trend to a silica value of 46%. Nevertheless, in Fig. 2-3,b, the trend is not conformable with the Hebridean tholeiitic trend (Holland and Brown, 1972) between Fe/Mg ratios of 0.65 and 0.75 although it appears to be in harmony with that trend for higher values of Fe/Mg ratio. These patterns might be characteristic of the tholeiites in the North Atlantic Tertiary Igneous Province. The plots for the tholeiitic lavas from East Greenland and mid-west Iceland on a TiO_2-P_2O_5-K_2O diagram (Fig. 2-20) also give a distinct pattern. It, again, might be one of the characteristic patterns for this region.

5.4. Origin of the basalts

It is widely accepted that basaltic magmas are derived

from the Earth's upper mantle (peridotitic composition) by partial melting processes. Recent experimental work on either natural rocks or related synthetic rocks at various pressure and temperatures (Yoder and Tilley, 1962; Green and Ringwood, 1967; Green et al., 1967; Green, 1971; O'Hara, 1965; O'Hara and Yoder, 1967; O'Hara, 1968) reveal that the products from partial melting of the Earth's upper mantle (primary magma) are dependent on the pressure regime at the site of melting and that subsequent primary magma fractionation can produce different types of derivative magma under variously decreasing pressure regimes. Although there is general agreement about the partial melting phenomenon, the arguments concerning the products of these melting processes still remain, relative to the materials chosen for representing the Earth's upper mantle in experimental studies. One school of thought (Green and Ringwood, 1967; Green et al., 1967; Green 1971) regards pyrolite (1 part of basalt + 3 parts of peridotite) as the best source material whereas the other school (O'Hara, 1965, 1968; O'Hara and Yoder, 1967) have used various mixes of natural minerals separated from a garnet peridotite and an eclogite as the source material. However, these experiments can only explain different basaltic types in terms of the major elements. The differences in minor elements, trace elements and isotopic compositions in

basaltic rocks of similar major element contents are still to be explained.

In the case of tholeiites occurring along the Reykjanes Ridge and in the Neovolcanic zone of Iceland, the origin of regional and temporal variations in chemistry have been widely discussed in the literature and are considered to be related to the nature of the underlying mantle (Schilling, 1973; O'Hara, 1973, 1975; Flower et al., 1975; Sigvalderson et al., 1974; O'Nions et al., 1976). O'Nions et al. (1976) have reviewed the various source models (homogeneous single source, two-source mixing and inhomogeneous single source) to explain the variations in their isotopic data which encompass the whole area of Iceland and the Reykjanes Ridge. They draw conclusions as follows:

1. In the case of a homogeneous single source model, neither extensive crystal fractionation (O'Hara, 1973, 1975) nor variable degrees of partial melting with disequilibrium of phlogopite (Flower et al., 1975; Sigvalderson et al., 1974) can alone explain the chemical differences between the Icelandic and the Atlantic-ridge basalts.

2. The two-source mixing model for basalts in the Iceland-Reykjanes Ridge system of Schilling (1973) is not supported by Sr-isotope data.

3. The equilibrium partial melting of geochemically heterogeneous segments, i.e. local chemical variation,

either vertical or horizontal, within the Earth's upper mantle, seems preferable to account for the chemical differences. Some of these heterogeneities have existed for a long period of time ($\sim 10^9$ years) and may have resulted from one or more fractionation events.

Thus the similarities in geochemical features between the East Greenland tholeiites and the mid-west Icelandic tholeiites, including the tholeiites of the Icelandic middle Neovolcanic zone, and their close proximity in relation to sea-floor spreading imply that the East Greenland tholeiites are derived from the products of partial melting of one segment of the mantle containing relatively high amounts of incompatible elements.

The generation of the tholeiitic magmas in East Greenland can be explained by the model of Green (1971). It would begin with upwelling of relatively undepleted Earth's mantle material and thinning of the continental crust on the present seaward side of the Blosseville coast, causing extensive fracture systems (see Soper et al., 1976; Brown and Whitley, 1976). The initial partial melting of the mantle would take place at a depth of about 70km with a high degree of melting, giving rise to picritic lava which was extruded rapidly to the Earth's surface via the fractures (see Brooks et al., 1976). Subsequently, lower degrees of partial melting occurred at a shallow depth (i.e. $<$ 15km),

giving rise to olivine tholeiitic lavas with low normative olivine contents. The partial melting during this episode took place over a large area, producing voluminous tholeiitic lavas which then ascended rather slowly relative to the picritic lavas, as indicated by the crystal-liquid fractionation patterns imposed upon the tholeiitic magmas.

REFERENCES

Anwar, Y.M. (1955). Geological investigation in East Greenland. Part V. Petrography of the Prinsen af Wales Bjerge lavas. Medd. om Grønland, Bd. 135, Nr.1, 1-31.

Beckinsale, R.D., Brooks, C.K. and Rex, D.C. (1970). K-Ar ages for the Tertiary of East Greenland. Bull. geol. Soc. Denmark, 20, 27-37.

Bottinga, Y., Kudo, A. and Well, D. (1966). Some observations on oscillatory zoning and crystallization of magmatic plagioclase. Am. Min., 51, 792-806.

Brooks, C.K. (1973a). Tertiary of Greenland - a volcanic and plutonic record of continental break-up. Am. Assoc. Petroleum Geol. Mem. 19, 150-160.

Brooks, C.K. (1973b). Rifting and doming in southern east Greenland. Nature Phys. Sci., 244, 23-40.

Brooks, C.K. (1976). The Fe_2O_3/FeO ratio of basalt analyses: an appeal for a standardized procedure. Bull. geol. Soc. Denmark, 25, 117-120.

Brooks, C.K., Nielsen, T.F.D., and Petersen, T.S. (1976). The Blosseville coast basalts of East Greenland: their occurrence, composition and temporal variations. Contr. Mineral. Petrol., 58, 279-292.

Brown, G.M. (1967). Mineralogy of basaltic rocks. In H.H. Hess and A. Poldervaart (eds.), Basalts, The Poldervaart treatise on rocks of basaltic composition, 1, 103-162.

Brown, G.M., Emeleus, C.H., Holland, J.G. and Phillips, R. (1970). Petrographic, mineralogic and X-ray fluorescence analysis of Lunar igneous-type rocks and spherules. Science, 167, 599-601.

Brown, P.E. and Whitley, J.E. (1976). Eastern Greenland basalts and their supposed plume origin. Nature, 260, 232-234.

Buddington, A.F. and Lindsley, D.H. (1964). Iron-titanium oxide mineral and synthetic equivalents. J. Petrology, 5, 310-357.

Cann, J.R. (1970). Rb, Sr, Y, Zr and Nb in some ocean floor basaltic rocks. Earth Planet. Sci. Lett. 10, 7-11.

Carmichael, I.S.E. (1964). The Petrology of Thingmuli, a Tertiary Volcano in Eastern Iceland. J. Petrology, 5, 435-460.

Carmichael, I.S.E. (1967a). The iron-titanium oxides of salic volcanic rocks and their associated ferromagnesian silicates. Contr. Mineral. Petro., 14, 36-64.

Carmichael, I.S.E. (1967b). The mineralogy of Thingmuli, a Tertiary volcano in Eastern Iceland. Am. Min.,52, 1815-1841.

Chayes, F. (1960). On correlation between variables of constant sum. J. Geophys. Res., 65, 4185-4193.

Emeleus, C.H. (1971). Geology of Savoia Halvø between Kap Brewster and about 23°W, Unpublished, 1-27.

Engel, A.E.J., Engel, C.G. and Havens, R.G. (1965). Chemical characteristics of oceanic basalts and the upper mantle. Geol. Soc. Am. Bull., 76, 719-734.

Eugster, H.P. and Wones, D.R. (1962). Stability relations of the ferruginous biotite, annite. J. Petrology, 3, 82-125.

Fawcett, J.J., Rucklidge, J.C. and Brooks, C.K. (1966). Geological expedition to the Tertiary basalt region of Scoresby Sund, East Greenland. Nature, 212, 603-604.

Fawcett, J.J., Brooks, C.K. and Rucklidge, J.C. (1973). Chemical petrology of Tertiary flood basalts from the Scoresby Sund area, Medd. om Grønland, Bd.195, Nr.6, 1-54.

Flanagan, F.J. (1973). 1972 values for international geochemical reference standards. Geochim. Cosmochim. Acta, 37, 1189-1200.

Flower, M.F.J., Schmincke, H.U. and Thompson, R.N. (1975). Phlogopite stability and the $^{87}Sr/^{86}Sr$ step in basalts along the Reykjanes Ridge. Nature, 254, 404-406.

Gast, P.W. (1965). Terrestrial ratio of potassium to rubidium and the composition of the Earth's mantle. Science, 147, 858-860.

Gill, R.C.O. (1972). The geochemistry of the Grønnedal-Ika alkaline complex, South Greenland. Unpublished Ph.D. Thesis, Univ. of Durham, 298 pp.

Green, D.H. (1971). Composition of basaltic magmas as indicators of conditions of origin: application to oceanic volcanism. Phil. Trans. Roy. Soc. Lond., A.268, 707-725.

Green, D.H. and Ringwood, A.E. (1967). The genesis of basaltic magmas. Contr. Mineral. Petrol., 15, 103-190.

Green, T.H., Green, D.H. and Ringwood, A.E. (1967). The origin of high-alumina basalts and their relationships to quartz tholeiites and alkali basalts. Earth Planet. Sci. Lett., 2, 41-51.

Hallam, A. (1975). Alfred Wegener and the hypothesis of continental drift. Sci. Am., 232, Nr.2, 88-97.

Hart, S.R. (1969). K, Rb, Cs contents and K/Rb, K/Cs ratios of fresh and altered submarine basalts. Earth Planet. Sci. Lett., 6, 295-303.

Heirtzler, J.R. (1968). Sea-floor spreading. Sci. Am., 219, Nr.6, 60-70.

Hendrickson, A.E. and White, P.O. (1964). Promax: a quick method for rotation to oblique simple structure. Br. J. Statist. Psychol., 17, 65-70.

Holland, J.G. and Brindle, D.W. (1966). A self-consistent mass absorption correction for silicate analysis by X-ray fluorescence. Spectrochim. Acta, 22, 2083-2093.

Holland, J.G. and Brown, G.M. (1972). Hebridean tholeiitic magmas: a geochemical study of the Ardnamurchan cone sheets. Contr. Mineral. Petrol., 37, 139-160.

Holmes, A. (1918). The basaltic rocks of the Arctic region. Min. Mag., 18, 180-223.

Johannesson, H. (1975). Structure and petrochemistry of the Reykjadalur central volcano and the surrounding areas, Midwest Iceland. Unpublished Ph.D. thesis, Univ. of Durham, 273 pp.

Kay, R., Hubbard, N.J. and Gast, P.W. (1970). Chemical characteristics and origin of oceanic ridge volcanic rocks. J. Geophys. Res., 75, 1585-1613.

Kennedy, W.Q. (1933). Trends of differentiation in basaltic magma. Am. J. Sci., ser.5, 25, 239-256.

Lambert, R.St.J. and Holland, J.G. (1974). Yttrium geochemistry applied to petrogenesis utilizing calcium-yttrium relationships in minerals and rocks. Geochim. Cosmochim. Acta, 38, 1393-1414.

Macdonald, G.A. (1969). Composition and origin of Hawaiian lavas. Geol. Soc. Am. Mem., 116, 477-522.

Macdonald, G.A. and Katsura, T. (1964). Chemical composition of Hawaiian lavas. J. Petrology 5, 82-133.

Manson, V. (1967). Geochemistry of basalts: major elements. In H.H. Hess and A. Poldervaart (eds.), Basalts, The Poldervaart treatiese on rocks of basaltic composition, 1, 215-269.

O'Hara, M.J. (1965). Primary magmas and the origin of basalts. Scott. J. Geol., 1, 19-40.

O'Hara, M.J. (1968). The bearing of phase equilibria studies in synthetic and natural systems on the origin and evolution of basic and ultrabasic rocks. Earth-Sci. Rev., 4, 69-133.

O'Hara, M.J. (1973). Non-primary magmas and dubious mantle plume beneath Iceland. Nature, 243, 507-508.

O'Hara, M.J. (1975). Is there an Icelandic mantle plume? Nature, 253, 708-710.

O'Hara, M.J. and Yoder, H.S. Jr. (1967). Formation and fractionation of basic magmas at high pressure. Scott. J. Geol., 3, 67-117.

O'Nions, R.K. and Grönvold, K. (1973). Petrogenetic relationships of acid and basic rocks in Iceland: Sr-isotope and rare-earth elements in late and post glacial volcanic rocks. Earth Planet. Sci. Lett., 19, 13-21.

O'Nions, R.K. and Pankhurst, R.J. (1974). Petrogenetic singificance of isotope and trace element variations in volcanic rocks from the mid-Atlantic. J. Petrology, 15, 603-634.

O'Nions, R.K., Pankhurst, R.J. and Grönvold, K. (1976). Nature and development of basalt magma sources beneath Iceland and the Reykjanes Ridge. J. Petrology, 17, 315-338.

Osborn, E.F. and Tait, D.B. (1952). The system diopside-forsterite-anorthite. Am. J. Sci., Bowen volume, 413-433.

Pearce, J.A. and Cann, J.R. (1973). Tectonic settling of basic volcanic rocks determined using trace element analyses. Earth Planet. Sci. Lett., 19, 290-300.

Pearce, J.A. and Flower, M.F.J. (1977). The relative importance of petrogenetic variables in magma genesis at accreting plate margins: a preliminary investigation. J. Geol. Soc. Lond., 134, 103-127.

Pearce, T.H., Gorman, B.E. and Birkett, T.C. (1975) The TiO_2-K_2O-P_2O_5 diagram: a method of discriminating between oceanic and non-oceanic basalts. Earth Planet. Sci. Lett., 24, 419-426.

Prinz, M. (1967). Geochemistry of basalts: trace elements. In H.H. Hess and A. Poldervaart (eds.), Basalts, The Poldervaart treatise on rocks of basaltic composition, 1, 271-323.

Reeves, M.J. (1971). Geochemistry and mineralogy of British Carboniferous seatearths from northern coalfields. Unpublished Ph.D. Thesis, Univ. of Durham, 184 pp.

Rucklidge, J. (1966). Observations of hollows in the snow surface of Torv Gletscher, East Greenland. J. Glaciology, 6, 446-449.

Schilling, J-G. (1973). Iceland mantle plume: Geochemical study of Reykjanes Ridge. Nature, 242, 565-571.

Schilling, J-G. and Noe-Nygaard, A. (1974). Faeroe-Iceland Plume: rare-earth evidence. Earth Planet. Sci. Lett., 24, 1-14.

Scrutton, R.A. (1973). The age relationship of igneous activity and continental break up. Geol. Mag., 110, 227-234.

Shimokawa, T. and Masuda, A. (1972). Rare-earths in Icelandic neovolcanic rocks. Contr. Mineral. Petrol., 37, 39-46.

Sigvaldason, G.E., Steinthorsson, S. and Oskarsson, N. (1974). Compositional variation in recent Icelandic tholeiites and the Kverkfjöll hot spot. Nature, 251, 579-582.

Spencer, D.W. (1966). Factor analysis. Woods Hole Oceanographic Institution, Mass., Paper 66-39.

Spencer, D.W. (1967). Factor analysis II: A description of the application of oblique solutions. Woods Hole Oceanographic Institution, Mass., Paper 67-59.

Soper, N.J., Higgins, A.C., Downie, C., Matthews, D.W. and Brown, P.E. (1976). Late Cretaceous - Early Tertiary stratigraphy of the Kangerdlugssuaq area, east Greenland, and the age of opening of the north-east Atlantic. J. geol. Soc. Lond., 132, 85-104.

Sweatman, T.R. and Long, J.V.P. (1969). Quantitative electron-probe microanalysis of rock-forming minerals. J. Petrology, 10, 332-379.

Tarling, D.H. (1967). The palaeomagnetic properties of some Tertiary lavas from East Greenland. Earth Planet. Sci. Lett., 3, 81-88.

Thompson, G., Shido, F. and Miyashiro, A. (1972). Trace element distributions in fractionated oceanic basalts. Chem. Geol., 9, 89-97.

Thompson, R.N., Esson, J. and Dunham, A.C. (1972). Major element chemical variation in the Eocene lavas of the Isle of Skye, Scotland. J. Petrology, 13, 219-253.

Thornton, C.P. and Tuttle, O.F. (1960). Chemistry of igneous rocks I. Differentiation index. Am. J. Sci., 258, 664-684.

Tilley, C.E., Yoder, H.S. and Schairer, J.F. (1967). Melting relations of volcanic rock series. Yb. Carnegie Inst. Wash., 65, 260-269.

Wager, L.R. (1934). Geological investigations in East Greenland. Part I. General geology from Angmagssalik to Kap Dalton. Medd. om Grønland, Bd. 105, Nr.2, 1-46.

Wager, L.R. (1935). Geological investigations in East Greenland. Part II. Geology of Kap Dalton. Medd. om Grønland, Bd.105, Nr.3, 1-32.

Wager, L.R. (1947). Geological investigations in East Greenland. Part IV. The stratigraphy and tectonics of Knud Rasmussens Land and the Kangerdlugssuaq region. Medd. om Grønland, Bd.134, Nr.5, 1-64.

Watkins, W.D., Gunn, B.M. and Coy-yll, R. (1970). Major and trace element variations during the initial cooling of an Icelandic lava. Am. J. Sci., 268, 24-49.

Watt, W.S. (1969). An investigation of the Tertiary basalts in Scoresby Sund. In Report of Activities, 1968. Rapp. Grønlands geol. Unders., Nr.15, 22-23.

Yoder, H.S., Jr. and Tilley, C.E. (1962). Origin of Basalt Magmas: An experimental study of natural and synthetic rock systems. J. Petrology, 3, 342-532.

APPENDIX

TABLE A-1 MAJOR, MINOR AND TRACE ELEMENT ANALYSES OF THE STUDIED THOLEIITES(FE2O3*=TOTAL FE)

	143804	143805	143806	143807	143808	143809	143810	143814	143820	143824
PERCENT										
SIO2	49.15	49.09	49.05	48.39	49.22	48.10	48.15	48.92	48.87	48.35
AL2O3	16.14	16.20	15.71	15.46	15.18	15.02	14.86	14.36	14.65	13.38
FE2O3	3.10	3.00	3.12	3.08	3.19	3.20	3.31	3.55	3.40	3.56
FEO	9.65	9.32	9.71	9.63	10.00	10.00	10.31	11.09	10.56	11.09
MGO	4.91	5.47	5.65	6.53	5.12	6.66	6.84	4.86	5.58	1.98
CAO	10.33	10.67	10.29	10.98	10.06	11.80	11.26	10.68	10.78	10.27
NA2O	2.99	2.79	2.83	2.58	2.90	2.21	2.19	2.53	2.78	2.05
K2O	0.44	0.37	0.40	0.28	0.59	0.12	0.10	0.18	0.24	0.14
TIO2	2.78	2.64	2.73	2.61	3.18	2.39	2.53	3.33	2.64	2.62
P2O5	0.32	0.26	0.31	0.27	0.37	0.24	0.25	0.29	0.26	0.33
MNO	0.19	0.19	0.19	0.18	0.19	0.24	0.18	0.21	0.24	0.22
S	-	0.01	-	-	-	0.03	0.02	0.01	-	-
FE2O3*	13.79	13.32	13.87	13.75	14.26	14.28	14.73	15.83	15.09	15.84
PPM										
BA	109	86	111	103	137	74	64	110	108	95
NB	14	12	16	17	22	17	16	24	16	17
ZR	193	175	192	175	249	155	164	228	173	195
Y	41	32	30	30	39	27	29	36	37	31
SR	256	264	252	268	286	268	259	259	207	243
RB	7	8	10	6	14	5	3	7	2	4
ZN	94	76	85	83	104	82	92	99	97	99
CU	280	245	224	191	262	205	223	241	239	292
NI	89	108	93	122	91	117	124	34	42	108
CR	86	105	97	117	64	132	109	72	78	90

TABLE A-1 MAJOR,MINOR AND TRACE ELEMENT ANALYSES OF THE STUDIED THOLEIITES(FE2O3*=TOTAL FE)

	143825	143827	143828	143829	143830	143831	143832	143837	143839	143840
PERCENT										
SIO2	47.62	47.76	48.48	48.13	47.56	48.37	48.20	48.10	48.26	48.21
AL2O3	14.67	14.05	13.78	15.50	15.05	15.08	15.22	15.45	15.48	14.99
FE2O3	3.77	3.91	3.63	3.37	3.20	3.28	3.31	3.22	3.31	3.27
FEO	11.70	11.90	11.20	10.47	9.97	10.22	10.28	10.05	10.32	10.18
MGO	4.55	4.78	6.74	5.83	7.42	6.12	6.30	6.17	5.69	6.72
CAO	10.54	10.62	10.27	10.62	11.33	11.16	11.28	11.39	10.79	11.38
NA2O	2.89	2.69	2.27	2.50	2.22	2.47	2.42	2.57	2.70	2.30
K2O	0.26	0.20	0.18	0.33	0.12	0.15	0.17	0.25	0.30	0.10
TIO2	3.44	3.52	2.92	2.80	2.72	2.69	2.66	2.34	2.67	2.44
P2O5	0.29	0.31	0.31	0.22	0.22	0.23	0.24	0.24	0.25	0.21
MNO	0.25	0.25	0.21	0.21	0.19	0.21	0.20	0.21	0.21	0.21
S	0.01	-	-	-	0.01	0.01	0.03	-	-	-
FE2O3*	16.72	17.08	16.03	14.96	14.24	14.60	14.69	14.35	14.74	14.54
PPM										
BA	108	95	96	125	70	77	87	78	126	67
NB	25	25	21	15	13	15	16	14	18	13
ZR	216	223	214	173	160	172	167	143	171	139
Y	45	47	39	35	28	33	32	32	22	31
SR	255	252	261	237	253	261	252	214	250	196
RB	7	8	7	7	4	11	6	7	8	4
ZN	103	104	101	104	98	75	85	88	97	97
CU	325	370	281	225	190	223	212	252	259	207
NI	99	39	87	68	92	69	66	114	76	129
CR	31	32	80	97	135	111	108	73	59	89

TABLE A-1 MAJOR, MINOR AND TRACE ELEMENT ANALYSES OF THE STUDIED THOLEIITES(FE2O3*=TOTAL FE)

	143841	143842	143843	143844	143845	143846	143850	143851	143852	143853
PERCENT										
SIO2	50.23	48.28	49.19	49.49	48.12	48.38	48.41	47.75	48.08	48.33
AL2O3	14.76	15.38	15.26	15.17	15.51	16.30	14.84	14.74	15.10	14.72
FE2O3	3.30	3.15	3.28	3.15	3.34	2.93	3.52	3.55	3.46	3.66
FEO	10.28	9.84	10.19	9.82	10.41	9.14	10.93	11.03	10.78	11.38
MGO	4.84	6.90	4.84	6.16	5.74	6.57	5.39	6.18	5.44	4.74
CAO	10.41	11.66	11.01	10.62	10.83	11.62	10.75	10.92	10.91	10.10
NA2O	2.69	2.32	2.85	2.66	2.53	2.43	2.64	2.42	2.66	2.96
K2O	0.36	0.06	0.33	0.27	0.26	0.24	0.17	0.13	0.16	0.26
TIO2	2.68	2.01	2.50	2.23	2.82	1.95	2.87	2.79	2.91	3.28
P2O5	0.24	0.21	0.25	0.23	0.22	0.24	0.26	0.27	0.26	0.33
MNO	0.20	0.19	0.20	0.19	0.21	0.19	0.21	0.21	0.22	0.22
S	-	-	-	-	-	-	-	-	-	-
FE2O3*	14.68	14.05	14.56	14.03	14.87	13.06	15.62	15.76	15.40	16.26
PPM										
BA	96	63	92	72	110	104	83	62	87	121
NB	15	12	16	12	20	16	17	14	20	26
ZR	163	117	150	128	174	144	183	173	177	229
Y	32	26	32	31	31	30	37	33	40	45
SR	205	214	218	206	250	237	228	225	236	221
RB	11	3	11	5	11	2	6	5	3	7
ZN	80	73	87	76	112	73	100	85	95	107
CU	294	211	265	244	269	239	189	222	203	362
NI	98	120	89	42	145	142	22	15	72	47
CR	79	110	76	76	103	142	69	58	71	57

TABLE A-1 MAJOR, MINOR AND TRACE ELEMENT ANALYSES OF THE STUDIED THOLEIITES (FE2O3*=TOTAL FE)

	143854	143855	143856	143857	143858	143859	143860	143862	143863	143864
PERCENT										
SIO2	48.07	47.42	47.96	47.95	47.85	47.76	47.91	48.16	48.16	47.91
AL2O3	15.64	15.84	14.62	16.68	15.01	14.95	15.03	15.40	15.09	15.83
FE2O3	3.20	3.27	3.22	3.01	3.25	3.37	3.34	2.16	3.34	3.24
FEO	9.98	10.16	10.05	9.38	10.09	10.50	10.37	10.64	10.40	10.12
MGO	6.54	6.47	6.96	6.06	6.84	6.64	6.59	6.43	5.91	6.50
CAO	11.37	11.42	11.26	11.42	11.57	11.51	11.42	11.63	11.53	11.20
NA2O	2.32	2.44	2.34	2.49	2.30	2.21	2.25	2.52	2.41	2.30
K2O	0.18	0.17	0.21	0.27	0.19	0.10	0.12	0.24	0.14	0.15
TIO2	2.27	2.39	2.55	2.34	2.44	2.52	2.54	2.39	2.58	2.32
P2O5	0.23	0.23	0.22	0.23	0.23	0.22	0.22	0.22	0.23	0.24
MNO	0.20	0.20	0.22	0.18	0.22	0.20	0.21	0.20	0.20	0.19
S	-	-	-	-	0.02	0.01	-	-	-	0.01
FE2O3*	14.25	14.52	14.35	13.40	14.42	15.00	14.82	13.96	14.86	14.45
PPM										
BA	90	77	92	116	92	64	113	86	56	89
NB	13	10	17	15	14	15	25	16	12	16
ZR	147	136	182	141	143	148	239	130	126	150
Y	33	33	31	30	28	31	44	26	27	35
SR	203	197	244	243	229	233	226	222	220	232
RB	4	3	11	3	6	4	8	3	5	3
ZN	80	84	91	76	83	84	113	77	74	85
CU	258	205	222	224	193	198	188	209	194	190
NI	77	76	42	96	87	67	101	105	89	102
CR	146	152	157	150	165	69	70	136	69	145

TABLE A-1 MAJOR, MINOR AND TRACE ELEMENT ANALYSES OF THE STUDIED THOLEIITES(FE2O3*=TOTAL FE)

	143865	143866	143868	143869	143870	143871	143872	143873	143876	143877
PERCENT										
SIO2	48.83	49.00	48.10	47.87	46.81	47.66	47.08	48.03	47.79	48.75
AL2O3	14.99	15.24	16.02	15.29	14.70	15.40	14.80	15.23	14.00	15.34
FE2O3	3.37	3.13	3.20	3.36	3.47	3.23	3.23	3.50	3.21	3.32
FEO	10.47	9.75	9.95	10.46	10.80	10.06	10.06	10.85	10.02	10.35
MGO	5.41	6.07	5.37	5.93	7.65	6.55	8.41	4.79	8.82	5.03
CAO	10.83	11.28	11.25	10.57	10.64	11.56	11.08	11.15	11.28	10.30
NA2O	2.72	2.66	2.83	2.49	1.94	2.49	1.82	2.73	1.83	2.77
K2O	0.29	0.24	0.35	0.18	0.29	0.08	0.39	0.33	0.08	0.20
TIO2	2.60	2.17	2.44	3.36	3.20	2.51	2.66	2.90	2.55	3.42
P2O5	0.27	0.26	0.26	0.28	0.30	0.23	0.23	0.26	0.22	0.29
MNO	0.21	0.19	0.21	0.20	0.19	0.21	0.22	0.21	0.18	0.21
S	-	-	-	-	-	0.03	-	0.02	0.02	-
FE2O3*	14.96	13.93	14.22	14.94	15.43	14.37	14.37	15.51	14.31	14.78
PPM										
BA	104	98	88	102	101	62	122	98	56	137
NB	15	15	12	28	25	18	14	8	14	18
ZR	160	167	154	230	200	152	133	167	139	240
Y	33	32	31	36	32	32	26	33	23	44
SR	227	235	207	299	278	233	208	288	255	272
RB	8	3	6	7	7	7	6	6	4	9
ZN	87	89	83	117	110	85	68	98	76	105
CU	263	273	219	326	300	268	200	265	165	277
NI	87	89	98	152	107	80	61	42	194	118
CR	94	98	73	114	244	139	129	68	218	144

TABLE A-1 MAJOR,MINOR AND TRACE ELEMENT ANALYSES OF THE STUDIED THOLEIITES(FE2O3*=TOTAL FE)

	143878	143879	143880	143881	143882	143885	143886	143887	143888	143889
PERCENT										
SIO2	46.62	48.58	48.56	47.19	48.11	47.40	48.44	48.10	47.41	48.05
AL2O3	13.97	14.52	14.73	14.27	15.73	15.28	14.90	15.79	15.52	14.66
FE2O3	3.49	3.06	3.11	3.52	3.10	3.39	3.18	3.09	3.22	3.63
FEO	10.84	9.56	9.70	10.94	9.67	10.58	9.93	9.61	10.05	11.30
MGO	6.48	7.37	6.04	7.71	6.56	6.35	6.35	6.72	7.78	5.01
CAO	12.71	11.81	12.34	10.64	11.47	11.52	11.64	11.78	11.30	10.22
NA2O	1.76	2.08	2.17	1.97	2.33	2.38	2.42	2.44	2.07	2.82
K2O	0.16	0.17	0.11	0.12	0.10	0.11	0.17	0.17	0.12	0.33
TIO2	3.55	2.42	2.40	3.14	2.51	2.53	2.54	1.87	2.09	3.26
P2O5	0.23	0.25	0.24	0.30	0.23	0.26	0.21	0.22	0.23	0.38
MNO	0.18	0.17	0.18	0.18	0.19	0.19	0.21	0.21	0.20	0.24
S	0.01	-	0.01	0.01	0.01	-	-	-	-	-
FE2O3*	15.49	13.65	13.86	15.63	13.81	15.11	14.18	13.73	14.35	16.14
PPM										
BA	135	99	51	77	61	81	61	74	97	73
NB	18	14	13	16	10	15	13	16	16	17
ZR	210	182	165	195	153	141	149	150	136	150
Y	37	31	45	34	34	29	31	29	29	31
SR	286	275	266	247	258	232	243	218	238	244
RB	6	10	3	3	3	4	3	2	5	6
ZN	94	75	70	87	82	83	75	92	83	104
CU	228	152	220	218	197	252	183	183	179	390
NI	167	137	124	138	90	51	64	71	92	84
CR	262	213	192	308	110	63	117	143	168	56

TABLE A-1 MAJOR, MINOR AND TRACE ELEMENT ANALYSES OF THE STUDIED THOLEIITES (FE2O3* = TOTAL FE)

	143890	143891	143892	143893	143894	143895	143896	143897	143898	143899
PERCENT										
SIO2	47.60	47.90	47.93	48.14	48.06	49.62	48.50	49.38	47.69	48.15
AL2O3	15.68	14.98	15.38	14.97	15.49	14.85	15.62	14.70	14.52	15.80
FE2O3	3.30	3.15	3.22	3.17	3.13	3.29	3.28	3.22	3.61	3.11
FEO	10.29	9.81	10.07	9.91	9.76	10.25	10.22	10.02	11.23	9.67
MGO	6.14	7.00	6.81	6.63	7.03	5.53	5.22	5.85	6.03	5.97
CAO	11.64	12.01	11.43	12.01	11.47	10.57	10.89	10.72	10.74	10.95
NA2O	2.48	2.30	2.34	2.37	2.42	2.86	2.78	2.84	2.24	2.60
K2O	0.13	0.13	0.10	0.11	0.21	0.33	0.23	0.33	0.19	0.28
TIO2	2.29	2.32	2.29	2.29	1.98	2.18	2.78	2.47	3.18	3.01
P2O5	0.22	0.19	0.23	0.19	0.22	0.26	0.24	0.24	0.33	0.26
MNO	0.21	0.21	0.19	0.21	0.22	0.26	0.21	0.21	0.22	0.19
S	0.01	-	0.01	-	-	-	-	-	0.01	-
FE2O3*	14.70	14.02	14.38	14.15	13.94	14.64	14.60	14.32	15.04	13.82
PPM										
BA	49	65	66	58	77	103	97	83	97	114
NB	10	15	10	11	13	13	21	15	25	28
ZR	130	130	130	126	124	158	159	158	230	214
Y	30	30	28	29	28	41	29	32	45	33
SR	204	211	195	209	204	159	229	207	232	303
RB	4	8	3	7	5	8	9	10	4	9
ZN	84	84	91	85	79	100	99	98	98	92
CU	239	226	238	212	234	239	241	257	243	264
NI	103	107	108	84	100	68	80	73	58	66
CR	64	145	64	152	104	59	99	52	126	154

TABLE A-1 MAJOR, MINOR AND TRACE ELEMENT ANALYSES OF THE STUDIED THOLEIITES (FE2O3*=TOTAL FE)

	143902	143903	143908	143909	143940	143941	143951	143953	143955	143956
PERCENT										
SIO2	47.35	46.14	46.67	48.84	47.56	48.03	47.86	48.00	48.14	48.40
AL2O3	13.37	14.52	15.05	15.30	15.23	16.04	15.29	14.84	15.71	15.01
FE2O3	3.36	3.34	3.37	3.12	3.33	3.10	3.19	3.20	3.11	3.45
FEO	10.50	10.41	10.51	9.70	10.07	9.67	9.93	9.96	9.69	10.75
MGO	7.10	7.98	7.87	6.20	6.15	6.15	6.55	7.13	6.26	5.63
CAO	11.25	11.94	10.54	11.32	11.88	11.42	11.89	11.65	11.61	10.73
NA2O	2.98	1.89	2.06	2.54	2.59	2.46	2.26	2.21	2.54	2.59
K2O	0.28	0.30	0.41	0.15	0.27	0.23	0.11	0.14	0.24	0.18
TIO2	3.18	3.03	3.03	2.38	2.47	2.45	2.11	2.46	2.26	2.76
P2O5	0.33	0.21	0.28	0.25	0.23	0.25	0.21	0.21	0.24	0.28
MNO	0.25	0.20	0.20	0.20	0.21	0.19	0.20	0.20	0.19	0.21
S	0.05	0.03	0.01	-	-	-	-	-	-	0.01
FE2O3*	14.99	14.87	15.01	13.86	14.38	13.81	14.19	14.23	13.84	15.35
PPM										
BA	63	83	84	65	98	92	75	74	93	94
NB	27	26	22	18	11	19	19	12	18	17
ZR	186	192	193	152	145	152	123	136	134	180
Y	36	32	29	31	28	31	26	25	30	38
SR	241	262	448	220	230	238	211	222	231	231
RB	10	6	9	8	4	4	1	4	3	3
ZN	98	95	95	77	84	86	75	84	107	96
CU	304	296	246	224	198	228	161	215	205	260
NI	160	123	129	80	49	71	77	85	94	96
CR	241	236	203	124	112	152	145	116	124	75

TABLE A-1 MAJOR, MINOR AND TRACE ELEMENT ANALYSES OF THE STUDIED THOLEIITES(FE2O3*=TOTAL FE)

	143957	144004	144006	144007	144008	144009
PERCENT						
SIO2	47.89	48.41	48.56	47.14	48.71	48.10
AL2O3	15.12	15.39	15.46	13.79	15.40	15.45
FE2O3	3.19	3.29	3.16	3.59	3.16	3.22
FEO	9.54	10.25	9.85	11.16	9.86	10.05
MGO	6.91	5.58	6.58	6.54	6.19	6.17
CAO	11.94	11.03	11.09	11.55	11.21	11.29
NA2O	2.31	2.70	2.39	2.24	2.61	2.57
K2O	0.12	0.19	0.15	0.55	0.19	0.25
TIO2	2.17	2.69	2.31	2.96	2.23	2.34
P2O5	0.21	0.25	0.25	0.21	0.23	0.24
MNO	0.20	0.21	0.20	0.25	0.21	0.21
S	-	-	0.01	0.01	-	-
FE2O3*	14.20	14.64	14.07	15.94	14.08	14.35
PPM						
BA	66	86	102	128	95	78
NB	13	17	21	19	14	14
ZR	129	184	141	199	140	143
Y	29	32	26	34	28	32
SR	199	288	193	291	230	214
RB	2	7	4	5	6	7
ZN	90	99	84	103	78	88
CU	182	283	200	253	222	292
NI	46	54	108	65	103	114
CR	148	72	85	67	117	73

TABLE A-2 CIPW NORMS AND DIFFERENTIATION-INDEX VALUES OF THE STUDIED THOLEIITES

	143804	143805	143806	143807	143808	143809	143810	143814	143820	143824
CZ	0.80	0.80	0.70	-	1.50	0.40	0.90	3.70	0.70	1.50
CR	2.60	2.20	2.40	1.70	3.50	0.70	0.60	1.10	1.40	0.80
AB	25.30	23.60	24.00	21.80	24.50	18.70	18.50	21.40	23.50	17.30
AN	29.30	30.60	29.00	29.80	26.70	30.70	30.40	27.20	26.80	26.90
DI	16.30	16.90	16.40	18.70	17.10	21.50	19.40	19.70	20.60	17.90
HY	15.10	15.90	17.10	17.10	15.20	18.20	19.80	14.60	16.40	24.60
OL	-	-	-	0.90	-	-	-	-	-	-
MT	4.50	4.30	4.50	4.50	4.60	4.60	4.80	5.20	4.90	5.20
IL	5.30	5.00	5.20	5.00	6.00	4.50	4.80	6.30	5.00	5.00
AP	0.80	0.60	0.70	0.60	0.90	0.60	0.60	0.70	0.60	0.80
PY	-	-	-	-	-	0.10	-	-	-	-
D.I.	28.7	26.6	27.1	23.5	29.5	19.8	20.0	26.2	25.7	19.7

TABLE A-2. CIPW NORMS AND DIFFERENTIATION-INDEX VALUES OF THE STUDIED THOLEIITES

	143825	143827	143828	143829	143830	143831	143832	143837	143839	143840
QZ	0.50	1.70	2.20	0.50	-	0.80	0.10	-	-	0.40
OR	1.60	1.20	1.10	2.00	0.70	0.90	1.00	1.50	1.80	0.60
AB	24.50	22.80	19.20	21.20	18.70	20.90	20.50	21.70	22.90	19.40
AN	26.30	25.70	26.90	30.10	30.70	29.60	30.20	29.90	29.20	30.30
DI	20.00	20.70	18.10	17.40	19.60	19.90	19.90	20.50	18.70	20.30
HY	14.50	14.90	21.00	18.20	18.40	17.50	18.50	14.10	16.50	19.20
OL	-	-	-	-	1.50	-	-	2.60	0.50	-
MT	5.50	5.70	5.30	4.90	4.60	4.80	4.80	4.70	4.80	4.70
IL	6.50	6.70	5.50	5.30	5.20	5.10	4.50	4.40	5.10	4.60
AP	0.70	0.70	0.70	0.50	0.50	0.50	0.60	0.60	0.60	0.50
FY	-	-	-	-	-	-	0.10	-	-	-
D.I.	26.5	25.7	22.5	23.6	19.5	22.6	21.6	23.2	24.7	20.4

TABLE A-2 CIPW NORMS AND DIFFERENTIATION-INDEX VALUES OF THE STUDIED THOLEIITES

	143841	143842	143843	143844	143845	143846	143850	143851	143852	143853
QZ	3.80	-	1.00	1.00	0.50	-	1.30	0.40	0.60	1.20
OR	2.20	0.40	2.00	1.60	1.60	1.40	1.00	0.80	1.00	1.60
AB	22.80	19.60	24.10	22.50	21.40	20.50	22.40	20.50	22.50	25.10
AN	27.10	31.40	28.20	28.60	30.20	32.90	28.10	28.90	28.80	26.10
DI	19.00	20.50	20.50	18.50	18.10	19.00	19.40	19.30	19.50	18.10
HY	14.70	18.20	14.10	18.40	17.50	15.20	16.60	19.00	16.50	15.70
OL	-	1.00	-	-	-	2.50	-	-	-	-
MT	4.80	4.60	4.70	4.60	4.80	4.30	5.10	5.10	5.00	5.30
IL	5.10	3.80	4.70	4.20	5.30	3.70	5.40	5.30	5.50	6.20
AP	0.60	0.50	0.60	0.60	0.50	0.60	0.60	0.60	0.60	0.80
PY	-	-	-	-	-	-	-	-	-	-
D.I.	28.7	20.0	27.1	25.2	23.5	22.0	24.7	21.7	24.1	27.8

TABLE A-2 CIPW NORMS AND DIFFERENTIATION-INDEX VALUES OF THE STUDIED THOLEIITES

	143854	143855	143856	143857	143858	143859	143860	143862	143863	143864
CZ	-	-	-	-	-	0.20	0.40	-	0.60	-
OR	1.10	1.00	1.30	1.60	1.10	0.60	0.70	1.40	0.80	0.90
AB	19.60	20.60	19.80	21.00	19.40	18.70	19.00	21.30	20.40	19.40
AN	31.70	31.80	28.80	33.50	30.10	30.60	30.60	30.00	29.90	32.40
DI	19.00	19.20	20.90	17.70	21.10	20.50	20.20	21.60	21.20	17.70
HY	18.60	13.60	18.50	14.40	16.80	19.10	19.00	11.60	16.70	19.80
OL	0.50	4.00	-	2.30	1.50	-	-	5.80	-	0.10
MT	4.60	4.70	4.70	4.40	4.70	4.90	4.80	3.10	4.80	4.70
IL	4.30	4.50	5.60	4.40	4.50	4.80	4.80	4.50	4.90	4.40
AP	0.60	0.60	0.50	0.60	0.60	0.50	0.50	0.50	0.60	0.60
PY	-	-	-	-	-	-	-	-	-	-
D.I.	21.7	21.7	21.1	22.7	20.6	19.5	20.1	22.8	21.9	20.3

TABLE A-2 CIPW NORMS AND DIFFERENTIATION-INDEX VALUES OF THE STUDIED THOLEIITES

	143865	143866	143868	143869	143870	143871	143872	143873	143876	143877
QZ	0.90	0.10	-	1.30	-	-	-	0.30	0.10	2.50
OR	1.70	1.40	2.10	1.10	1.70	0.50	2.30	2.00	0.50	1.20
AB	23.00	22.50	24.00	21.10	16.40	21.10	15.40	23.10	15.50	23.50
AN	27.80	28.90	29.90	30.00	30.60	30.60	31.00	28.30	29.70	28.80
DI	19.90	20.80	19.90	16.90	16.50	20.70	18.20	20.90	20.10	16.80
HY	16.20	17.00	10.40	17.70	22.90	14.40	19.50	14.20	24.10	15.30
OL	-	-	3.80	-	0.10	2.80	3.20	-	-	-
MT	4.90	4.50	4.60	4.90	5.00	4.70	4.70	5.10	4.70	4.80
IL	4.90	4.10	4.60	6.40	6.10	4.80	5.10	5.50	4.80	6.50
AP	0.60	0.60	0.60	0.70	0.70	0.60	0.60	0.60	0.50	0.70
PY	-	-	-	-	-	0.10	-	-	-	-
D.I.	25.7	24.0	26.1	23.5	18.1	21.5	17.7	25.3	16.1	27.2

TABLE A-2 CIPW NORMS AND DIFFERENTIATION-INDEX VALUES OF THE STUDIED THOLEIITES

	143878	143879	143880	143881	143882	143885	143886	143887	143888	143889
QZ	1.10	0.90	2.20	0.70	0.30	-	0.40	-	-	1.00
OR	1.00	1.00	0.70	0.70	0.60	0.70	1.00	1.00	0.70	2.00
AB	14.90	17.60	18.40	16.70	19.70	20.10	20.50	20.60	17.50	23.80
AN	29.70	29.70	30.10	29.70	32.20	30.70	29.30	31.60	32.70	26.40
CI	26.00	22.10	24.20	17.20	19.00	20.30	22.20	20.80	17.80	18.10
HY	14.90	18.90	14.70	23.10	18.50	15.80	16.80	13.20	18.40	16.20
OL	-	-	-	-	-	2.10	-	4.20	3.60	-
MT	5.10	4.40	4.50	5.10	4.50	4.90	4.60	4.50	4.70	5.30
IL	6.70	4.60	4.50	6.00	4.80	4.80	4.80	3.60	4.00	6.40
AP	0.60	0.60	0.60	0.70	0.60	0.60	0.50	0.50	0.60	0.90
FY	-	-	-	-	-	-	-	-	-	-
D.I.	17.0	19.6	21.3	18.2	20.6	20.8	21.8	21.6	18.3	26.8

TABLE A-2 CIPW NORMS AND DIFFERENTIATION-INDEX VALUES OF THE STUDIED THOLEIITES

	143890	143891	143892	143893	143894	143895	143896	143897	143898	143899
QZ	-	-	-	-	-	0.50	0.50	0.50	1.80	0.30
CR	0.80	0.80	0.60	0.70	1.30	2.00	1.40	2.00	1.10	1.70
AB	21.00	19.40	19.80	20.00	20.50	24.20	23.60	24.10	19.00	22.00
AN	31.30	30.20	31.20	29.90	30.80	26.70	29.40	26.40	29.00	30.60
DI	20.60	23.00	19.70	23.30	20.20	19.80	19.00	20.70	18.20	18.00
HY	13.40	14.60	17.80	15.30	14.10	17.00	15.50	16.40	18.80	16.60
OL	3.30	2.60	1.40	1.50	4.40	-	-	-	-	-
MT	4.80	4.60	4.70	4.60	4.50	4.80	4.80	4.70	5.20	4.50
IL	4.30	4.40	4.30	4.30	3.80	4.10	5.30	4.70	6.00	5.70
AP	0.50	0.50	0.60	0.50	0.50	0.60	0.60	0.60	0.80	0.60
FY	-	-	-	-	-	-	-	-	-	-
D.I.	21.8	20.2	20.4	20.7	21.7	27.0	25.5	26.6	21.9	23.9

TABLE A-2 CIPW NORMS AND DIFFERENTIATION-INDEX VALUES OF THE STUDIED THOLEIITES

	143902	143903	143908	143909	143940	143941	143951	143953	143955	143956
CZ	-	-	-	0.70	-	-	-	-	-	1.10
OR	1.70	1.80	2.40	0.90	1.60	1.40	0.70	0.80	1.40	1.10
AB	25.20	16.00	17.40	21.50	21.90	20.80	19.10	18.70	21.50	21.90
AN	22.30	30.20	30.60	29.90	29.10	32.10	31.30	30.20	30.80	28.80
DI	25.60	22.50	16.10	20.20	23.20	18.80	21.50	21.40	20.70	18.60
HY	4.50	12.30	18.10	17.20	8.90	16.20	15.80	18.70	13.40	17.50
OL	9.00	6.10	4.00	-	5.20	1.00	2.50	0.40	2.80	-
MT	4.90	4.80	4.90	4.50	4.80	4.50	4.60	4.60	4.50	5.00
IL	6.00	5.70	5.80	4.50	4.70	4.60	4.00	4.70	4.30	5.20
AP	0.80	0.50	0.70	0.60	0.50	0.60	0.50	0.50	0.60	0.70
PY	0.10	0.10	-	-	-	-	-	-	-	-
D.I.	26.9	17.8	19.8	23.1	23.5	22.2	19.7	19.5	22.9	24.1

TABLE A-2 CIPW NORMS AND DIFFERENTIATION-INDEX VALUES OF THE STUDIED THOLEIITES

	143957	144004	144006	144007	144008	144009
QZ	-	0.40	0.60	-	-	-
CR	0.70	1.10	0.90	3.20	1.10	1.50
AB	19.50	22.90	20.20	19.00	22.10	21.70
AN	30.50	29.30	31.00	26.00	25.70	29.90
DI	22.30	19.60	18.30	24.60	20.00	20.50
HY	14.80	16.30	19.40	12.10	17.40	14.10
OL	2.80	-	-	3.80	0.30	2.60
MT	4.60	4.80	4.60	5.20	4.60	4.70
IL	4.10	5.10	4.40	5.60	4.20	4.40
AP	0.50	0.60	0.60	0.50	0.60	0.60
FY	-	-	-	-	-	-
D.I.	20.2	24.4	21.7	22.2	23.2	23.2

TABLE A-3 FACTOR SCORES FOR 86 THOLEIITES(PROMAX OBLIQUE FACTOR MATRIX KMIN=6)

FACTOR	143804	143805	143806	143807	143808	143809	143810	143814	143820	143824
1	-1.41	-0.32	-1.41	-0.28	-1.64	1.03	0.44	-0.30	-1.38	-1.80
2	-1.01	-1.79	-0.95	-1.29	-0.50	-0.67	-0.46	2.01	1.60	1.18
3	0.36	0.03	0.44	-0.30	1.40	-0.25	0.07	1.46	0.22	1.71
4	-0.96	-1.50	-0.87	-1.34	-0.40	-0.33	-0.75	0.46	1.18	1.68
5	1.78	-1.25	-2.06	-1.78	-2.23	0.90	1.28	0.71	0.06	1.10
6	-2.23	-2.14	-0.99	-0.24	-1.12	0.42	0.81	-0.03	-0.29	3.25
7	0.34	-0.75	-0.07	-0.47	1.42	-0.42	-0.03	1.70	0.63	1.43

TABLE A-3 FACTOR SCORES FOR 86 THOLEIITES(PROMAX OBLIQUE FACTOR MATRIX KMIN=6)

FACTOR	143825	143827	143828	143829	143830	143831	143832	143837	143839	143840
1	0.38	-0.46	-1.35	0.01	1.20	0.50	0.56	-0.39	-0.33	-0.55
2	1.91	3.20	1.40	0.66	-0.39	0.17	0.10	-0.55	-0.02	-0.20
3	2.20	2.38	1.72	0.07	-0.38	0.27	-0.11	-0.28	0.45	-0.52
4	2.00	2.35	1.24	0.02	-0.92	-0.66	-0.64	0.78	1.04	1.02
5	1.57	1.90	0.83	-1.19	0.55	0.73	0.37	-0.01	-1.54	1.27
6	1.08	-0.07	1.96	-0.38	0.71	-0.28	-0.12	-0.73	-0.40	0.32
7	2.43	2.73	1.83	0.31	-0.47	-0.16	-0.15	-0.46	-0.09	-0.33

TABLE A-3 FACTOR SCORES FOR 86 THOLEIITES(PROMAX OBLIQUE FACTOR MATRIX KMIN=6)

FACTOR	143841	143842	143843	143844	143845	143846	143850	143851	143852	143853
1	-2.40	-0.42	-1.18	-2.03	0.21	-0.17	-0.66	-0.38	-0.24	-1.41
2	0.17	-0.67	-0.13	-0.27	-0.54	-2.48	2.63	3.04	1.26	1.92
3	0.72	-1.38	0.12	-0.31	0.18	-1.72	0.42	0.66	0.23	1.81
4	0.74	-0.16	0.61	0.32	0.50	-0.87	0.19	0.44	0.36	1.62
5	-0.41	0.91	-0.58	-0.35	-0.90	-1.97	0.58	1.50	0.56	0.37
6	-0.82	0.35	-1.46	-0.57	-0.38	-0.97	-0.12	0.58	-0.39	-0.63
7	0.03	-1.60	-0.20	-1.07	0.49	-1.45	0.74	0.36	0.83	2.40

TABLE A-3 FACTOR SCORES FOR 86 THOLEIITES(PROMAX OBLIQUE FACTOR MATRIX KMIN=6)

FACTOR	143854	143855	143856	143857	143858	143859	143860	143862	143863	143864
1	-0.21	0.38	0.40	0.57	0.93	0.78	0.17	0.22	-0.12	0.66
2	-0.36	0.16	0.53	-1.83	-0.23	0.86	0.63	-0.50	0.66	-0.57
3	-0.91	-0.99	-0.07	-1.45	-0.37	-0.21	-0.87	-0.68	-0.15	-0.80
4	-0.12	-0.34	0.01	-1.03	-0.17	-0.16	-0.11	0.09	0.04	-0.79
5	-0.33	0.06	-0.51	-2.35	0.15	1.67	-0.06	-0.58	1.12	0.02
6	-0.15	-0.35	0.78	-1.35	0.44	0.46	0.46	0.01	-0.06	-0.17
7	-0.74	-0.95	0.02	-1.36	-0.66	-0.32	1.02	-1.01	-0.59	-0.44

TABLE A-3 FACTOR SCORES FOR 86 THOLEIITES (PROMAX OBLIQUE FACTOR MATRIX KMIN=6)

FACTOR	143865	143866	143868	143869	143870	143871	143872	143873	143876	143877
1	-1.08	-1.12	-0.33	0.30	0.98	0.95	1.32	1.05	0.77	-0.60
2	0.32	-0.92	-0.31	-0.93	-0.40	-0.63	0.08	1.47	-0.81	-0.11
3	0.53	-0.58	-0.40	0.90	1.12	-0.41	0.27	1.16	-0.01	0.92
4	0.66	0.10	0.23	0.69	0.62	0.21	-0.09	0.18	-2.77	-1.56
5	-0.39	-0.94	-0.86	-0.62	-0.81	1.52	-1.80	0.39	1.55	-0.80
6	-0.52	-0.67	-1.68	0.03	2.30	-0.31	2.07	-1.57	2.89	-0.58
7	0.20	-0.39	-0.74	1.63	1.34	-0.23	-0.92	0.24	-0.85	1.60

TABLE A-3 FACTOR SCORES FOR 86 THOLEIITES(PROMAX OBLIQUE FACTOR MATRIX KMIN=6)

FACTOR	143878	143879	143880	143881	143882	143885	143886	143887	143888	143889
1	3.49	0.14	0.57	0.80	0.78	0.28	0.12	-0.06	0.47	-1.14
2	0.14	-1.04	-1.00	0.17	-0.61	0.91	0.26	-0.81	-0.43	1.13
3	0.37	-0.76	-0.75	1.08	-0.75	-0.09	-0.69	-3.68	-1.13	2.56
4	-2.75	-3.27	-2.86	-1.54	-2.03	0.18	-0.54	-0.22	-0.43	2.48
5	0.54	-1.07	1.80	1.33	0.93	0.66	0.37	-0.68	-0.63	1.11
6	1.67	1.26	-0.48	2.51	-0.70	0.20	0.03	-0.22	1.30	-0.27
7	1.08	-0.76	-0.45	0.97	-0.88	-0.29	-0.93	-1.03	-0.90	1.49

TABLE A-3 FACTOR SCORES FOR 86 THOLEIITES(PROMAX OBLIQUE FACTOR MATRIX KMIN=6)

FACTOR	143890	143891	143892	143893	143894	143895	143896	143896	143898	143899
1	0.65	0.44	-0.01	0.27	-0.41	-2.86	-0.36	-1.96	0.19	0.53
2	0.10	-0.64	-0.13	-0.11	-0.72	1.24	-0.19	0.30	1.18	-1.42
3	-0.44	-1.19	-0.60	-1.17	-1.04	-0.10	-0.03	0.23	1.49	-0.10
4	0.32	0.06	0.08	-0.07	0.57	1.62	0.63	1.04	1.00	-0.38
5	2.02	0.55	1.44	0.98	-0.27	0.18	-0.79	-0.25	1.24	-2.22
6	-0.52	0.31	-0.13	0.09	-0.04	-0.85	-0.96	-0.65	0.81	-0.74
7	-0.93	-1.04	-0.91	-1.26	-1.31	0.28	0.08	-0.06	2.17	0.29

TABLE A-3 FACTOR SCORES FOR 86 THOLEIITES(PROMAX OBLIQUE FACTOR MATRIX KMIN=6)

FACTOR	143902	143903	143908	143909	143940	143941	143951	143953	143955	143956
1	1.17	2.13	2.56	-0.90	1.53	0.28	0.31	0.16	0.10	-0.35
2	-1.13	-1.00	-1.39	-0.75	0.72	-1.12	-0.24	-0.08	-1.13	0.58
3	2.04	0.19	1.59	-0.66	-0.54	-0.98	-1.70	-0.68	-1.26	0.73
4	1.43	0.18	-0.04	-0.02	-0.41	-0.66	-0.54	-0.19	-0.22	0.43
5	1.35	0.15	-1.06	0.02	-0.73	-1.36	-0.02	0.19	-1.25	0.93
6	0.93	1.65	1.59	-0.34	-0.07	-0.71	0.73	0.83	-0.59	-0.39
7	1.62	0.59	0.75	-0.69	-0.89	-0.64	-1.34	-1.06	-0.68	0.92

TABLE A-3 FACTOR SCORES FOR 86 THOLEIITES(PROMAX OBLIQUE FACTCR MATRIX KMIN=6)

FACTOR	143957	144004	144006	144007	144008	144009
1	0.18	-0.08	-0.70	2.03	-0.66	-0.39
2	0.41	0.17	-1.14	1.62	-0.68	-0.55
3	-1.56	0.30	-0.40	1.23	-0.63	-0.28
4	-0.30	0.59	0.79	1.21	0.10	0.78
5	0.44	-0.32	-0.06	0.11	-0.71	-0.01
6	0.42	-0.88	-0.05	1.01	-0.37	-0.73
7	-1.16	0.33	-0.44	1.19	-0.94	-0.46

TABLE A-4 ANALYSES OF PLAGIOCLASES IN THE STUDIED THOLEIITES.
PHENOCRYST AND MICROPHENOCRYST COMPOSITIONS ARE INDICATED BY *.(SEE ALSO TABLE A-5)

	143805*	143805*	143805	143805	143805	143806*	143806	143806	143814	143814
WT. %										
SIO2	51.24	51.67	53.19	54.10	58.57	50.76	52.65	53.54	54.90	54.31
TIO2	0.04	0.05	0.11	0.26	-	0.07	0.07	0.14	0.11	0.15
AL2O3	30.00	29.34	28.14	25.23	24.48	30.82	28.39	28.16	27.49	28.01
CR2O3	0.02	-	0.03	0.01	-	-	-	-	-	-
FEO	0.33	0.57	1.07	1.73	1.29	0.61	1.52	1.07	1.13	0.88
MNO	-	0.01	0.03	0.02	-	-	0.01	0.01	0.02	0.02
MGO	0.11	0.10	0.11	0.33	0.02	0.10	0.26	0.20	0.11	0.19
CAO	14.16	13.84	12.98	12.20	9.03	15.23	12.63	12.52	11.40	11.55
NA2O	3.36	3.49	4.27	4.44	6.28	2.55	3.40	4.24	4.25	4.59
K2O	0.11	0.11	0.17	0.22	0.33	0.11	0.16	0.17	0.29	0.23
TOTAL	99.37	99.20	100.09	99.56	100.00	100.65	99.29	100.05	99.70	99.92
ATOMIC PROPORTIONS ON THE BASIS OF 32 OXYGENS										
SI	9.392	9.488	9.692	9.921	10.557	9.225	9.684	9.737	9.968	9.852
TI	0.006	0.007	0.015	0.036	0.000	0.010	0.010	0.020	0.015	0.021
AL	6.485	6.355	6.048	5.673	5.203	6.607	6.135	6.041	5.887	5.992
CR	0.003	0.000	0.004	0.002	0.000	0.000	0.000	0.000	0.000	0.000
FE2+	0.051	0.088	0.163	0.266	0.195	0.093	0.233	0.162	0.172	0.133
MN	0.000	0.002	0.004	0.002	0.000	0.000	0.002	0.002	0.003	0.003
MG	0.031	0.028	0.030	0.091	0.005	0.026	0.072	0.054	0.030	0.051
CA	2.781	2.723	2.534	2.398	1.744	2.966	2.479	2.439	2.218	2.245
NA	1.193	1.244	1.510	1.580	2.197	1.038	1.209	1.494	1.495	1.163
K	0.026	0.027	0.041	0.052	0.075	0.025	0.027	0.040	0.068	0.052
END MEMBER COMPOSITIONS(MOL.%)										
AB	29.83	31.15	36.97	39.20	54.69	25.76	32.45	37.59	39.54	41.25
OR	0.64	0.67	1.00	1.30	1.87	0.61	1.00	1.02	1.79	1.36
AN	69.53	68.18	62.03	59.50	43.43	73.62	66.55	61.39	58.67	57.39

TABLE A-4 ANALYSES OF PLAGIOCLASES IN THE STUDIED THOLEIITES.
PHENOCRYST AND MICROPHENOCRYST COMPOSITIONS ARE INDICATED BY *.(SEE ALSO TABLE A-5)

	143814	143830	143830	143831*	143831*	143831	143831	143831	143844*	143844*
WT. %										
SIO2	56.15	50.83	52.44	48.74	50.34	54.51	56.70	57.88	46.90	47.61
TIO2	0.14	0.13	0.17	0.06	0.06	0.17	0.20	0.24	0.07	0.08
AL2O3	26.62	29.67	29.26	31.41	30.10	26.99	25.92	26.04	32.97	31.96
CR2O3	-	-	-	-	-	-	-	-	-	-
FEO	0.82	0.88	2.07	0.74	0.67	1.04	1.70	1.30	0.65	0.69
MNO	0.04	0.03	0.01	0.01	0.03	-	0.01	0.02	0.01	0.01
MGO	0.12	0.21	0.22	0.23	0.19	0.12	0.12	0.09	0.10	0.09
CAO	10.46	14.19	11.76	15.67	15.14	11.54	10.08	9.41	17.03	16.63
NA2O	5.26	3.58	3.46	2.37	2.88	5.19	5.51	5.52	1.84	2.01
K2O	0.32	0.10	0.20	0.05	0.10	0.18	0.24	0.09	0.05	0.07
TOTAL	99.92	99.60	99.58	99.29	99.49	99.73	100.88	100.87	99.62	99.15
ATOMIC PROPORTIONS ON THE BASIS OF 32 OXYGENS										
SI	10.151	9.340	9.587	9.003	9.260	9.934	10.202	10.345	8.675	8.827
TI	0.019	0.017	0.024	0.009	0.008	0.023	0.027	0.032	0.010	0.011
AL	5.675	6.430	6.308	6.843	6.530	5.802	5.501	5.489	7.193	6.996
CR	0.000	0.000	0.000	0.001	0.000	0.000	0.000	0.000	0.000	0.000
FE2+	0.124	0.134	0.316	0.115	0.103	0.159	0.256	0.194	0.100	0.107
MN	0.006	0.004	0.001	0.001	0.004	0.000	0.001	0.002	0.001	0.001
MG	0.033	0.057	0.059	0.063	0.053	0.033	0.032	0.023	0.029	0.025
CA	2.025	2.794	2.304	3.102	2.985	2.253	1.943	1.803	3.375	3.308
NA	1.844	1.276	1.225	0.848	1.026	1.833	2.060	1.911	0.659	0.723
K	0.073	0.023	0.047	0.012	0.023	0.042	0.054	0.065	0.011	0.017
END MEMBER COMPOSITIONS(MOL.%)										
AB	46.77	31.18	34.27	21.40	25.43	44.40	50.77	50.58	16.28	17.86
OR	1.85	0.55	1.30	0.30	0.58	1.01	1.34	1.72	0.28	0.42
AN	51.38	68.27	64.43	78.30	73.99	54.59	47.88	47.70	83.44	81.72

TABLE A-4 ANALYSES OF PLAGIOCLASES IN THE STUDIED THOLEIITES.
PHENOCRYST AND MICROPHENOCRYST COMPOSITIONS ARE INDICATED BY *.(SEE ALSO TABLE A-5)

	143844*	143844	143844	143846*	143846*	143846	143846	143859*	143859*	143859*
WT. %										
SIO2	49.60	54.06	54.85	49.31	52.02	51.65	52.42	47.39	50.04	50.49
TIO2	0.05	0.12	0.09	0.06	0.14	0.14	0.18	0.08	0.11	0.08
AL2O3	31.37	28.09	27.68	31.33	29.02	28.28	27.85	32.74	31.10	30.81
CR2O3	-	-	-	-	-	-	-	-	-	-
FEO	0.61	1.03	1.31	0.54	0.86	5.14	1.38	0.59	0.69	0.56
MNO	0.01	0.02	0.01	0.02	0.08	0.02	0.02	-	-	0.01
MGO	0.09	0.11	0.13	0.21	0.11	0.25	0.14	0.12	0.18	0.17
CAO	15.13	12.00	10.76	15.89	13.68	11.11	12.43	16.81	14.59	14.70
NA2O	3.16	4.44	5.19	2.68	4.13	3.67	4.37	1.84	2.94	3.08
K2O	0.07	0.26	0.25	0.07	0.20	0.25	0.28	0.04	0.07	0.06
TOTAL	100.09	100.14	100.27	100.11	100.24	100.51	99.07	99.61	99.73	99.95
ATOMIC PROPORTIONS ON THE BASIS OF 32 OXYGENS										
SI	9.083	9.808	9.927	9.038	9.494	9.507	9.699	8.750	9.168	9.227
TI	0.007	0.017	0.013	0.008	0.019	0.019	0.025	0.011	0.015	0.010
AL	6.774	6.011	5.907	6.773	6.247	6.140	6.058	7.130	6.721	6.641
CR	0.000	0.000	0.000	0.000	0.000	0.000	0.000	0.000	0.000	0.000
FE2+	0.094	0.156	0.199	0.083	0.131	0.791	0.213	0.090	0.106	0.085
MN	0.002	0.003	0.001	0.003	0.012	0.003	0.005	0.000	0.000	0.001
MG	0.025	0.031	0.034	0.057	0.030	0.068	0.038	0.033	0.050	0.046
CA	2.968	2.333	2.086	3.120	2.676	2.192	2.456	3.326	2.865	2.879
NA	1.123	1.562	1.823	0.951	1.463	1.310	1.562	0.658	1.043	1.091
K	0.016	0.059	0.058	0.017	0.046	0.058	0.065	0.008	0.015	0.014
END MEMBER COMPOSITIONS(MOL.%)										
AB	27.33	39.50	45.95	23.26	34.96	36.80	38.25	16.48	26.58	27.38
OR	0.39	1.50	1.45	0.43	1.09	1.62	1.59	0.21	0.39	0.36
AN	72.28	59.00	52.60	76.31	63.95	61.58	60.16	83.30	73.02	72.26

TABLE A-4 ANALYSES OF PLAGIOCLASES IN THE STUDIED THOLEIITES.
PHENOCRYST AND MICROPHENOCRYST COMPOSITIONS ARE INDICATED BY *.(SEE ALSO TABLE A-5)

	143859	143859	143868*	143868*	143870*	143870*	143870*	143870	143870	143870
WT. %										
SIO2	51.87	52.46	51.59	53.61	50.29	51.54	51.07	52.94	53.13	57.44
TIO2	0.12	0.14	0.12	0.25	0.11	0.13	0.13	0.14	0.15	0.13
AL2O3	29.01	29.30	29.68	29.33	31.05	29.92	29.70	29.43	29.00	26.20
CR2O3	-	-	-	-	-	-	-	-	-	-
FEO	0.97	1.03	0.76	1.47	0.70	0.69	0.52	0.90	0.76	0.85
MNO	0.01	-	0.01	0.02	0.01	0.01	0.01	-	0.03	-
MGO	0.17	0.15	0.04	-	0.17	0.16	0.15	0.17	0.14	0.08
CAO	13.22	12.87	13.45	10.91	14.20	13.36	13.18	12.61	12.15	8.42
NA2O	3.79	3.71	3.91	3.99	3.30	4.11	4.31	4.22	4.75	6.29
K2O	0.10	0.13	0.17	0.23	0.10	0.14	0.14	0.18	0.07	0.45
TOTAL	99.26	99.80	99.75	99.91	99.94	100.06	99.20	100.95	100.18	99.86
ATOMIC PROPORTIONS ON THE BASIS OF 32 OXYGENS										
SI	9.527	9.564	9.439	9.720	9.194	9.402	9.396	9.577	9.641	10.346
TI	0.016	0.019	0.017	0.034	0.016	0.017	0.018	0.019	0.021	0.017
AL	6.284	6.300	6.404	6.272	6.697	6.437	6.445	6.280	6.207	5.566
CR	0.000	0.000	0.000	0.000	0.000	0.000	0.000	0.000	0.000	0.000
FE2+	0.150	0.158	0.117	0.223	0.107	0.105	0.080	0.135	0.115	0.128
MN	0.001	0.000	0.002	0.003	0.002	0.001	0.001	0.000	0.004	0.000
MG	0.047	0.041	0.012	0.000	0.046	0.045	0.041	0.046	0.038	0.022
CA	2.601	2.514	2.637	2.119	2.783	2.612	2.598	2.445	2.363	1.624
NA	1.350	1.312	1.389	1.403	1.170	1.454	1.536	1.480	1.671	2.198
K	0.024	0.030	0.039	0.075	0.024	0.033	0.033	0.040	0.016	0.102
END MEMBER COMPOSITIONS(MOL.%)										
AB	33.96	34.01	34.16	38.99	29.42	35.48	36.66	37.31	41.26	56.00
OR	0.60	0.79	0.96	2.10	0.60	0.80	0.80	1.02	0.39	2.61
AN	65.44	65.20	64.88	58.91	69.98	63.72	62.34	61.66	58.35	41.38

TABLE A-4 ANALYSES OF PLAGIOCLASES IN THE STUDIED THOLEIITES. PHENOCRYST AND MICROPHENOCRYST COMPOSITIONS ARE INDICATED BY *.(SEE ALSO TABLE A-5)

	143870	143870	143870	143870	143872*	143872*	143872*	143872*	143872*	143872*
WT. %										
SIO2	59.40	57.23	62.60	61.90	49.54	50.87	49.11	50.06	51.40	51.08
TIO2	0.15	0.11	0.08	0.22	0.07	0.06	0.06	0.09	0.07	0.08
AL2O3	23.90	24.49	22.91	23.20	31.07	29.91	32.09	30.09	29.84	29.87
CR2O3	-	-	-	-	-	-	-	-	-	-
FEO	0.94	1.25	0.97	1.17	0.75	1.25	0.70	0.65	0.66	0.63
MNO	0.01	-	0.01	0.03	0.02	-	0.01	0.01	0.02	0.02
MGO	0.06	0.11	0.02	0.04	-	0.16	0.14	0.18	0.20	0.18
CAO	7.78	8.25	6.75	5.47	15.21	13.85	14.13	14.66	14.19	14.30
NA2O	6.68	7.23	6.87	7.62	2.86	2.92	3.02	3.13	3.22	3.41
K2O	0.42	0.44	0.58	0.66	0.03	0.08	0.09	0.10	0.09	0.10
TOTAL	99.34	99.11	100.79	100.32	99.54	99.11	99.34	98.96	99.70	99.67
ATOMIC PROPORTIONS ON THE BASIS OF 32 OXYGENS										
SI	10.723	10.448	11.069	11.009	9.117	9.368	9.031	9.254	9.402	9.359
TI	0.020	0.015	0.011	0.030	0.009	0.008	0.008	0.013	0.010	0.012
AL	5.089	5.272	4.778	4.867	6.744	6.496	6.960	6.560	6.436	6.455
CR	0.000	0.000	0.000	0.000	0.000	0.000	0.000	0.000	0.000	0.000
FE2+	0.142	0.191	0.144	0.173	0.115	0.192	0.108	0.100	0.101	0.096
MN	0.001	0.000	0.001	0.005	0.004	0.000	0.001	0.002	0.004	0.003
MG	0.016	0.030	0.005	0.012	0.000	0.045	0.040	0.048	0.056	0.050
CA	1.505	1.613	1.279	1.042	2.999	2.733	2.784	2.904	2.781	2.807
NA	2.338	2.561	2.354	2.628	1.020	1.044	1.077	1.122	1.141	1.213
K	0.096	0.102	0.132	0.150	0.006	0.020	0.021	0.024	0.022	0.023
END MEMBER COMPOSITIONS(MOL.%)										
AB	59.35	59.88	62.53	68.79	25.35	27.50	27.14	27.71	28.53	30.00
OR	2.44	2.40	3.50	3.93	0.15	0.52	0.55	0.59	0.56	0.58
AN	38.21	37.72	33.97	27.28	74.50	71.98	71.70	71.70	70.51	69.42

TABLE A-4 ANALYSES OF PLAGIOCLASES IN THE STUDIED THOLEIITES.
PHENOCRYST AND MICROPHENOCRYST COMPOSITIONS ARE INDICATED BY *.(SEE ALSO TABLE A-5)

	143872*	143872	143872	143872	143872	143873*	143873*	143873*	143873*	143873
WT. %										
SIO2	53.22	51.31	55.42	60.88	61.82	48.65	49.10	50.52	50.59	54.64
TIO2	0.10	0.15	0.22	0.10	0.26	0.07	0.05	0.09	0.08	0.12
AL2O3	28.18	30.16	26.76	25.27	22.43	31.64	31.35	30.08	30.44	27.41
CR2O3	-	-	-	-	-	-	-	-	-	-
FEO	0.64	0.65	0.81	0.64	1.11	0.55	0.62	0.59	0.67	0.82
MNO	0.02	-	0.04	0.02	-	0.01	0.02	-	0.01	-
MGO	0.61	0.14	0.07	-	0.07	0.14	0.15	0.19	0.18	0.10
CAO	12.55	14.08	10.69	7.28	5.47	15.43	15.25	14.39	13.98	10.88
NA2O	3.92	3.12	5.82	6.33	7.61	2.40	2.57	3.31	3.41	5.55
K2O	0.07	0.07	0.31	0.46	0.67	0.07	0.06	0.09	0.10	0.23
TOTAL	99.50	99.68	100.13	100.97	99.45	98.97	99.16	99.27	99.46	99.76
ATOMIC PROPORTIONS ON THE BASIS OF 32 OXYGENS										
SI	9.711	9.377	10.041	10.740	11.087	9.001	9.062	9.300	9.286	9.936
TI	0.014	0.020	0.030	0.013	0.035	0.009	0.007	0.012	0.011	0.016
AL	6.065	6.500	5.718	5.258	4.745	6.904	6.825	6.528	6.590	5.879
CR	0.000	0.000	0.000	0.000	0.000	0.000	0.000	0.000	0.000	0.000
FE2+	0.127	0.099	0.123	0.094	0.167	0.085	0.096	0.091	0.103	0.126
MN	0.002	0.000	0.006	0.004	0.000	0.002	0.003	0.000	0.002	0.000
MG	0.167	0.038	0.019	0.000	0.019	0.039	0.042	0.053	0.049	0.026
CA	2.453	2.757	2.075	1.375	1.050	3.058	3.016	2.837	2.749	2.120
NA	1.388	1.106	2.045	2.164	2.645	0.862	0.918	1.183	1.214	1.557
K	0.016	0.017	0.072	0.104	0.154	0.017	0.014	0.021	0.023	0.052
END MEMBER COMPOSITIONS(MOL.%)										
AB	35.98	28.51	48.78	59.29	68.72	21.90	23.26	29.27	30.44	47.39
OR	0.43	0.44	1.73	2.86	4.00	0.43	0.36	0.52	0.59	1.27
AN	63.59	71.05	49.50	37.74	27.29	77.67	76.38	70.21	68.97	51.34

TABLE A-4 ANALYSES OF PLAGIOCLASES IN THE STUDIED THOLEIITES.
PHENOCRYST AND MICROPHENOCRYST COMPOSITIONS ARE INDICATED BY *.(SEE ALSO TABLE A-5)

	143873	143873	143873	143878	143878	143878	143879*	143879*	143879*	143879*
WT. %										
SIO2	56.67	60.20	60.07	52.60	54.80	55.86	50.98	50.95	51.64	51.70
TIO2	0.13	0.13	0.14	0.22	0.13	0.14	0.06	0.10	0.10	0.12
AL2O3	26.51	22.84	22.11	29.10	27.20	26.58	30.60	30.55	30.18	29.98
CR2O3	-	-	-	-	-	-	-	-	-	-
FEO	0.83	1.95	1.98	1.65	1.07	0.91	0.55	0.53	0.56	0.55
MNO	-	0.01	-	-	-		0.02	0.03	0.01	0.01
MGO	0.02	0.05	0.15	0.55	0.15	0.08	0.19	0.02	0.19	0.19
CAO	9.11	6.62	6.50	12.73	11.81	11.39	14.49	14.47	14.00	14.18
NA2O	5.88	7.41	8.63	3.40	4.43	5.36	2.53	2.93	3.18	3.49
K2O	0.30	0.46	0.39	0.14	0.19	0.25	0.09	0.10	0.09	0.09
TOTAL	99.47	99.67	99.97	100.39	99.78	100.57	99.52	99.68	99.94	100.31
ATOMIC PROPORTIONS ON THE BASIS OF 32 OXYGENS										
SI	10.255	10.865	10.864	9.550	9.958	10.076	9.322	9.316	9.404	9.400
TI	0.018	0.017	0.019	0.030	0.017	0.019	0.009	0.014	0.013	0.016
AL	5.658	4.863	4.717	6.232	5.829	5.654	6.600	6.589	6.482	6.429
CR	0.000	0.000	0.000	0.000	0.000	0.000	0.000	0.000	0.000	0.000
FE2+	0.126	0.295	0.299	0.251	0.163	0.137	0.084	0.081	0.085	0.083
MN	0.000	0.001	0.000	0.000	0.000	0.000	0.003	0.005	0.001	0.001
MG	0.006	0.014	0.041	0.148	0.041	0.022	0.053	0.004	0.052	0.053
CA	1.767	1.281	1.259	2.477	2.300	2.201	2.839	2.835	2.732	2.762
NA	2.065	2.592	3.025	1.196	1.561	1.875	0.856	1.038	1.122	1.230
K	0.070	0.105	0.090	0.031	0.043	0.058	0.022	0.023	0.022	0.022
END MEMBER COMPOSITIONS(MOL.%)										
AB	52.92	65.16	69.16	32.28	39.99	45.35	23.64	26.64	28.94	30.65
OR	1.60	2.64	2.06	0.85	1.11	1.41	0.58	0.59	0.56	0.55
AN	45.28	32.20	28.78	66.87	58.90	53.23	75.58	72.77	70.50	68.80

TABLE A-4 ANALYSES OF PLAGIOCLASES IN THE STUDIED THOLEIITES.
PHENOCRYST AND MICROPHENOCRYST COMPOSITIONS ARE INDICATED BY *.(SEE ALSO TABLE A-5)

	143879	143879	143879	143889	143889	143889	143902*	143902*	143902*	144008*
WT. %										
SIO2	51.84	50.60	53.49	56.20	57.84	59.37	51.92	51.02	50.97	48.36
TIO2	0.10	0.76	0.16	0.14	0.10	0.12	0.09	0.12	0.11	0.06
AL2O3	29.30	29.57	28.34	26.80	26.66	24.10	29.50	30.04	30.03	31.66
CR2O3	-	-	-	-	-	-	0.01	0.01	0.03	-
FEO	0.91	1.95	0.55	0.55	0.74	1.48	0.61	0.72	0.71	0.73
MNO	-	0.06	0.02	-	-	-	-	-	-	0.03
MGO	0.22	0.66	0.13	0.18	0.03	0.36	0.19	0.20	0.20	0.11
CAO	13.29	13.12	11.81	10.55	9.95	8.69	14.14	14.42	14.65	15.81
NA2O	3.40	3.76	4.36	4.10	4.33	5.87	2.62	3.06	3.21	2.29
K2O	0.13	0.13	0.19	0.32	0.39	0.51	0.12	0.10	0.11	0.09
TOTAL	99.19	100.02	99.44	99.26	100.05	100.51	99.21	99.69	100.01	99.14
ATOMIC PROPORTIONS ON THE BASIS OF 32 OXYGENS										
SI	9.512	9.293	9.761	10.184	10.352	10.634	9.507	9.343	9.319	8.953
TI	0.014	0.105	0.021	0.019	0.013	0.016	0.013	0.016	0.015	0.008
AL	6.342	6.406	6.100	5.728	5.628	5.091	6.371	6.488	6.475	6.913
CR	0.000	0.000	0.000	0.000	0.000	0.000	0.001	0.002	0.004	0.000
FE2+	0.139	0.300	0.145	0.144	0.111	0.221	0.094	0.111	0.108	0.113
MN	0.000	0.009	0.003	0.000	0.000	0.000	0.000	0.000	0.000	0.005
MG	0.061	0.018	0.035	0.050	0.009	0.057	0.052	0.054	0.054	0.031
CA	2.614	2.582	2.309	2.049	1.909	1.669	2.775	2.830	2.870	2.137
NA	1.209	1.341	1.541	1.442	1.504	2.039	0.931	1.086	1.137	0.821
K	0.031	0.031	0.045	0.074	0.090	0.115	0.027	0.023	0.025	0.021
END MEMBER COMPOSITIONS(MOL.%)										
AB	31.38	33.91	39.57	40.44	42.94	53.34	24.93	27.56	28.19	20.63
OR	0.80	0.77	1.15	2.07	2.56	3.02	0.74	0.59	0.63	0.53
AN	67.82	65.31	59.28	57.48	54.50	43.64	74.33	71.85	71.18	78.84

TABLE A-4 ANALYSES OF PLAGIOCLASES IN THE STUDIED THOLEIITES.
PHENOCRYST AND MICROPHENOCRYST COMPOSITIONS ARE INDICATED BY *.(SEE ALSO TABLE A-5)

	144C08*	144C08*	144C08*	144C8
WT. %				
SIO2	48.59	50.89	52.54	52.33
TIO2	0.12	0.08	0.11	0.15
AL2O3	31.37	28.66	28.57	28.58
CR2O3	-	-	-	-
FEO	0.87	1.66	0.86	1.18
MNO	0.01	0.05	0.01	0.02
MGO	-	0.14	-	0.12
CAO	15.52	14.22	13.26	12.20
NA2O	2.92	4.08	3.93	4.44
K2O	0.08	0.12	0.16	0.15
TOTAL	99.48	99.91	99.45	100.16
ATOMIC PROPORTIONS ON THE BASIS OF 32 OXYGENS				
SI	8.982	9.384	9.627	9.560
TI	0.017	0.011	0.015	0.020
AL	6.840	6.233	6.175	6.158
CR	0.000	0.000	0.000	0.000
FE2+	0.135	0.257	0.131	0.180
MN	0.001	0.008	0.002	0.003
MG	0.000	0.039	0.000	0.032
CA	3.073	2.810	2.603	2.565
NA	1.045	1.459	1.397	1.573
K	0.019	0.029	0.038	0.034
END MEMBER COMPOSITIONS(MOL.%)				
AB	25.27	33.94	34.59	37.52
OR	0.46	0.67	0.95	0.51
AN	74.27	65.38	64.45	61.66

TABLE A-5. ANALYSES OF A BIG PLAGICCLASE CRYSTAL(5 X 18 MM) FRCM CORE(A) TO RIM(N).

	A	B	C	D	E	F	G	H	I	J
WT. %										
SIO2	51.17	53.86	52.48	52.53	52.64	52.42	52.88	50.67	52.62	53.17
TIO2	0.06	0.11	0.08	0.09	0.09	0.09	0.07	0.07	0.07	0.05
AL203	2.98	28.35	28.79	28.57	29.15	29.03	29.02	30.80	28.76	29.51
CR203	0.01	0.02	-	0.01	0.01	-	-	-	-	0.01
FEO	0.54	0.60	0.61	0.65	0.53	0.54	0.56	0.55	1.04	0.58
MNO	-	-	-	0.01	-	-	-	-	-	-
MGO	0.12	0.15	0.18	0.14	0.15	0.16	0.13	0.16	0.29	0.14
CAO	14.37	12.95	12.89	12.88	13.30	13.11	12.78	14.79	13.00	13.24
NA20	3.25	3.24	4.06	4.00	3.12	3.73	4.12	3.13	3.49	4.03
K20	0.11	0.14	0.15	0.14	0.13	0.14	0.11	0.09	0.12	0.12
TOTAL	99.43	99.41	99.23	99.03	99.11	99.23	99.67	100.26	99.40	100.88
ATOMIC PROPORTIONS ON THE BASIS OF 32 OXYGENS										
SI	9.389	9.799	9.617	9.645	9.625	9.598	9.635	9.236	9.626	9.583
TI	0.008	0.015	0.011	0.013	0.012	0.012	0.009	0.009	0.010	0.012
AL	6.449	6.083	6.221	6.187	6.286	6.268	6.236	6.620	6.205	6.272
CR	0.002	0.002	0.000	0.001	0.001	0.000	0.000	0.000	0.000	0.001
FE2+	0.083	0.091	0.093	0.100	0.081	0.083	0.086	0.085	0.159	0.088
MN	0.000	0.000	0.000	0.002	0.000	0.000	0.000	0.000	0.000	0.000
MG	0.032	0.040	0.048	0.038	0.040	0.044	0.037	0.043	0.079	0.038
CA	2.824	2.524	2.531	2.533	2.606	2.571	2.495	2.889	2.548	2.556
NA	1.155	1.143	1.143	1.425	1.106	1.324	1.455	1.107	1.239	1.409
K	0.026	0.032	0.035	0.032	0.030	0.032	0.025	0.020	0.029	0.028
END MEMBER COMPOSITIONS(MOL.%)										
AB	28.83	30.89	35.99	35.71	29.55	33.71	36.60	27.56	32.48	35.28
OR	0.66	0.87	0.89	0.79	0.81	0.83	0.62	0.50	0.75	0.71
AN	70.51	68.24	63.12	63.49	69.64	65.46	62.77	71.94	66.77	64.00

TABLE A-5. ANALYSES OF A BIG PLAGIOCLASE CRYSTAL(5 X 18 MM) FROM CORE(A) TO RIM(N).

	K	L	M	N
WT. %				
SIO2	53.30	53.06	53.27	51.99
TIO2	0.10	0.08	0.11	0.12
AL2O3	29.22	29.30	28.99	28.78
CR2O3	0.02	0.02	0.01	-
FEO	0.56	0.58	0.64	0.58
MNO	-	-	-	-
MGO	0.13	0.14	0.13	0.14
CAO	13.23	13.56	13.15	13.43
NA2O	3.62	3.44	3.33	3.59
K2O	0.11	0.12	0.12	0.09
TOTAL	100.30	100.29	99.75	99.13
ATOMIC PROPORTIONS ON THE BASIS OF 32 OXYGENS				
SI	9.643	9.607	9.678	9.557
TI	0.013	0.011	0.015	0.016
AL	6.234	6.257	6.211	6.239
CR	0.003	0.003	0.002	0.000
FE2+	0.085	0.087	0.097	0.089
MN	0.000	0.000	0.000	0.000
MG	0.035	0.039	0.036	0.039
CA	2.564	2.631	2.560	2.644
NA	1.271	1.207	1.175	1.423
K	0.026	0.027	0.027	0.022
END MEMBER COMPOSITIONS(MOL.%)				
AB	32.92	31.23	31.23	34.80
OR	0.68	0.71	0.72	0.54
AN	66.39	68.06	68.05	64.66

TABLE A-6. ANALYSES OF PYROXENES IN THE STUDIED THOLEIITES. PHENOCRYST AND MICROPHENOCRYST COMPOSITIONS ARE INDICATED BY *

	143805	143805	143805	143806	143806	143806	143814	143814	143814	143830
WT.%										
SIO2	51.75	51.27	50.32	51.57	50.61	50.91	51.88	51.08	50.56	49.20
TIO2	0.99	1.04	0.98	1.12	1.06	1.08	1.25	1.53	1.32	1.84
AL2O3	2.12	2.18	2.00	2.19	2.01	2.02	2.48	3.78	2.51	3.33
CR2O3	0.11	0.11	0.04	0.13	0.12	0.07	0.01	0.11	0.27	0.04
FEO	10.93	10.99	15.28	10.96	11.06	12.57	9.91	9.68	9.53	12.12
MNO	0.19	0.22	0.32	0.20	0.26	0.27	0.03	-	0.25	0.24
MGO	15.18	14.88	13.61	15.05	15.01	14.25	14.88	14.25	15.20	14.26
CAO	18.95	18.82	17.13	18.67	19.17	18.45	18.57	18.76	19.47	18.28
NA2O	0.25	0.22	0.24	0.23	0.21	0.21	0.11	0.30	0.23	0.34
TOTAL	100.46	99.74	99.91	100.12	99.53	99.83	99.11	99.50	99.33	99.66
ATOMIC PROPORTIONS ON THE BASIS OF 6 OXYGENS										
SI	1.924	1.922	1.915	1.924	1.908	1.902	1.939	1.903	1.899	1.861
TI	0.028	0.029	0.028	0.031	0.030	0.031	0.035	0.043	0.037	0.052
AL	0.093	0.096	0.090	0.096	0.089	0.090	0.109	0.166	0.111	0.149
CR	0.003	0.003	0.001	0.004	0.004	0.002	0.000	0.003	0.008	0.001
FE	0.340	0.345	0.486	0.342	0.349	0.397	0.310	0.301	0.299	0.383
MN	0.006	0.007	0.010	0.006	0.008	0.009	0.001	0.000	0.008	0.008
MG	0.841	0.831	0.772	0.836	0.843	0.801	0.829	0.791	0.851	0.804
CA	0.755	0.756	0.699	0.746	0.775	0.746	0.744	0.749	0.783	0.741
NA	0.018	0.016	0.017	0.017	0.015	0.016	0.008	0.021	0.016	0.025
END MEMBER COMPOSITIONS (MOL.%)										
FS	17.56	17.83	24.86	17.76	17.74	20.41	16.45	16.37	15.48	19.88
EN	43.44	43.03	39.45	43.46	42.87	41.22	44.04	42.96	44.00	41.68
WO	39.00	39.13	35.69	38.77	39.39	38.37	39.51	40.67	40.52	38.44

TABLE A-6. ANALYSES OF PYROXENES IN THE STUDIED THOLEIITES. PHENOCRYST AND MICROPHENOCRYST COMPOSITIONS ARE INDICATED BY *

	143830	143831*	143831*	143831	143831	143844	143844	143844	143846	143846
WT.%										
SIO2	49.60	52.00	50.42	51.51	51.80	49.38	50.38	51.61	51.37	51.08
TIO2	1.41	0.77	1.11	0.72	0.96	2.14	0.80	0.87	0.97	1.15
AL2O3	2.30	1.53	3.04	1.88	1.58	3.01	1.78	1.72	2.41	2.73
CR2O3	-	0.38	0.25	0.33	-	-	-	-	0.25	0.27
FEO	14.65	7.44	8.67	8.08	12.24	10.08	13.54	15.21	9.54	11.29
MNO	0.35	0.14	0.19	0.19	0.25	0.30	0.36	0.35	0.18	0.21
MGO	13.69	15.98	15.48	16.07	15.01	13.40	14.81	12.90	14.95	14.45
CAO	16.72	20.61	19.71	20.04	17.97	21.59	17.35	17.07	19.86	18.63
NA2O	0.37	0.23	0.25	0.29	0.30	0.33	0.33	0.31	0.29	0.33
TOTAL	99.29	99.49	99.12	99.52	100.12	100.22	99.36	100.03	99.82	100.11
ATOMIC PROPORTIONS ON THE BASIS OF 6 OXYGENS										
SI	1.898	1.932	1.890	1.931	1.940	1.859	1.916	1.955	1.918	1.910
TI	0.041	0.022	0.031	0.020	0.027	0.060	0.023	0.025	0.027	0.032
AL	0.104	0.085	0.135	0.083	0.070	0.134	0.080	0.077	0.106	0.120
CR	0.000	0.011	0.007	0.010	0.000	0.000	0.000	0.000	0.007	0.008
FE	0.475	0.231	0.272	0.251	0.383	0.317	0.431	0.482	0.298	0.352
MN	0.011	0.004	0.006	0.006	0.008	0.010	0.012	0.011	0.006	0.007
MG	0.781	0.885	0.865	0.891	0.838	0.752	0.840	0.728	0.831	0.805
CA	0.686	0.820	0.792	0.799	0.721	0.871	0.707	0.693	0.794	0.746
NA	0.028	0.016	0.018	0.021	0.022	0.024	0.024	0.022	0.021	0.024
END MEMBER COMPOSITIONS(MOL.%)										
FS	24.47	11.94	14.09	12.55	19.74	16.36	21.78	25.32	15.48	18.48
EN	40.21	45.69	44.85	45.90	43.13	38.76	42.46	38.27	43.23	42.31
WO	35.32	42.36	41.05	41.15	37.13	44.88	35.76	36.41	41.30	39.21

TABLE A-6. ANALYSES OF PYROXENES IN THE STUDIED THOLEIITES. PHENOCRYST AND MICROPHENOCRYST COMPOSITIONS ARE INDICATED BY *

	143846	143859*	143859*	143859	143859	143859	143859	143859	143859	143868*
WT.%										
SIO2	50.36	51.58	51.55	51.52	52.10	51.17	51.05	50.80	50.84	52.83
TIO2	1.21	0.70	0.74	0.82	1.03	1.13	1.19	1.07	0.94	0.56
AL2O3	1.69	2.44	2.91	3.02	2.24	1.84	1.50	1.61	1.89	2.04
CR2O3	0.04	0.21	0.26	0.27	0.11	-	-	0.02	-	0.14
FEO	16.14	7.61	7.54	7.79	9.83	13.04	13.41	13.98	16.84	8.86
MNO	0.37	0.16	0.17	0.17	0.21	0.29	0.31	0.30	0.40	0.20
MGO	12.59	15.75	15.58	15.67	15.07	13.14	13.71	13.29	12.23	16.57
CAO	17.38	20.30	20.16	19.72	19.38	18.13	17.89	18.21	15.64	18.55
NA2O	0.22	0.26	0.27	0.32	0.24	0.22	0.22	0.28	0.26	0.27
TOTAL	100.00	99.01	99.18	99.30	100.20	99.05	99.38	99.56	99.04	100.01
ATOMIC PROPORTIONS ON THE BASIS OF 6 OXYGENS										
SI	1.925	1.925	1.919	1.915	1.933	1.946	1.940	1.934	1.954	1.948
TI	0.035	0.020	0.021	0.023	0.029	0.032	0.034	0.030	0.027	0.015
AL	0.076	0.108	0.128	0.132	0.098	0.082	0.067	0.072	0.086	0.088
CR	0.001	0.006	0.008	0.008	0.003	0.000	0.000	0.001	0.000	0.004
FE	0.516	0.237	0.235	0.242	0.305	0.415	0.426	0.445	0.541	0.273
MN	0.012	0.005	0.005	0.005	0.006	0.009	0.010	0.010	0.013	0.006
MG	0.717	0.876	0.864	0.868	0.833	0.745	0.776	0.754	0.701	0.911
CA	0.712	0.812	0.804	0.786	0.771	0.739	0.728	0.742	0.644	0.733
NA	0.016	0.019	0.019	0.023	0.017	0.023	0.024	0.021	0.019	0.019
END MEMBER COMPOSITIONS(MOL.%)										
FS	26.53	12.33	12.33	12.78	15.98	21.85	22.06	22.92	28.70	14.26
EN	36.87	45.50	45.41	45.79	43.65	39.22	40.21	38.83	37.14	47.50
WO	36.60	42.17	42.26	41.43	40.37	38.93	37.72	38.25	34.16	38.24

TABLE A-6. ANALYSES OF PYROXENES IN THE STUDIED THOLEIITES. PHENOCRYST AND MICROPHENOCRYST COMPOSITIONS ARE INDICATED BY *

	143868*	143868	143868	143868	143868	143868	143868	143868	143870*	143870*
WT.%										
SIO2	52.22	51.19	51.73	50.20	50.99	51.05	52.00	50.42	51.47	50.90
TIO2	0.74	1.10	1.04	1.69	0.93	1.21	0.87	0.90	0.99	1.21
AL2O3	3.30	2.43	1.73	2.96	1.89	2.11	1.24	1.88	1.96	1.83
CR2O3	0.21	0.06	0.11	0.11	-	-	0.01	0.01	0.32	0.04
FEO	8.62	9.56	10.57	10.65	13.66	13.96	15.26	14.93	8.96	11.26
MNO	0.21	0.21	0.25	0.21	0.32	0.28	0.39	0.35	0.17	0.25
MGO	15.46	15.41	15.33	13.68	14.38	13.58	14.48	13.53	15.39	14.74
CAO	19.54	19.44	19.22	20.24	16.74	17.43	15.63	16.71	20.24	19.05
NA2O	0.27	0.26	0.25	0.36	0.34	0.35	0.22	0.42	0.28	0.27
TOTAL	100.58	99.66	100.25	100.19	99.26	99.96	100.11	99.15	99.78	99.54
ATOMIC PROPORTIONS ON THE BASIS OF 6 OXYGENS										
SI	1.919	1.912	1.928	1.884	1.935	1.929	1.960	1.929	1.920	1.919
TI	0.020	0.031	0.029	0.048	0.027	0.034	0.025	0.026	0.028	0.034
AL	0.143	0.107	0.076	0.131	0.085	0.094	0.055	0.085	0.086	0.081
CR	0.006	0.002	0.003	0.003	0.000	0.000	0.000	0.000	0.010	0.001
FE	0.265	0.299	0.330	0.334	0.434	0.441	0.481	0.478	0.280	0.355
MN	0.006	0.007	0.008	0.007	0.010	0.009	0.013	0.011	0.005	0.008
MG	0.846	0.858	0.852	0.765	0.813	0.764	0.814	0.772	0.856	0.828
CA	0.769	0.778	0.768	0.818	0.681	0.705	0.681	0.685	0.809	0.770
NA	0.019	0.019	0.018	0.026	0.025	0.025	0.016	0.031	0.020	0.020
END MEMBER COMPOSITIONS(MOL.%)										
FS	14.09	15.44	16.91	17.44	22.50	23.08	24.97	24.70	14.38	18.19
EN	45.00	44.35	43.69	39.90	42.18	40.00	42.24	39.89	44.01	42.40
WO	40.91	40.22	39.40	42.66	35.32	36.92	32.78	35.41	41.61	39.42

TABLE A-6. ANALYSES OF PYROXENES IN THE STUDIED THOLEIITES.
PHENOCRYST AND MICROPHENOCRYST COMPOSITIONS ARE INDICATED BY *

	143870*	143870	143870	143872*	143872*	143872	143872*	143872*	143872	143872
WT.%										
SIO2	49.57	50.15	50.51	51.42	50.58	49.98	50.48	49.16	51.01	51.10
TIO2	2.05	1.45	0.83	1.02	1.10	0.97	1.07	1.23	1.05	1.05
AL2O3	3.68	2.28	1.36	2.44	2.94	1.99	1.81	2.00	2.40	2.81
CR2O3	0.16	0.02	-	0.17	0.26	0.12	0.01	-	0.20	0.20
FEO	10.52	14.08	17.38	8.13	8.22	9.78	12.47	15.72	8.11	8.12
MNO	0.23	0.31	0.42	0.10	0.16	0.22	0.29	0.33	0.15	-
MGO	13.70	13.14	12.61	15.75	15.82	16.30	13.64	12.23	15.79	15.62
CAO	20.08	18.75	16.41	20.33	19.81	19.95	19.08	18.26	20.05	20.46
NA2O	0.29	0.35	0.27	0.27	0.30	0.24	0.11	0.23	0.29	0.33
TOTAL	100.68	100.52	100.18	99.63	99.59	99.55	99.17	99.18	99.05	99.69
ATOMIC PROPORTIONS ON THE BASIS OF 6 OXYGENS										
SI	1.854	1.897	1.946	1.913	1.897	1.882	1.921	1.901	1.909	1.901
TI	0.057	0.041	0.024	0.029	0.031	0.027	0.031	0.036	0.030	0.029
AL	0.162	0.101	0.061	0.107	0.129	0.088	0.081	0.091	0.106	0.123
CR	0.005	0.001	0.000	0.005	0.007	0.004	0.000	0.000	0.006	0.006
FE	0.342	0.445	0.555	0.253	0.256	0.308	0.397	0.508	0.254	0.253
MN	0.007	0.010	0.013	0.003	0.005	0.007	0.009	0.011	0.005	0.000
MG	0.763	0.741	0.718	0.873	0.877	0.914	0.785	0.705	0.881	0.866
CA	0.804	0.760	0.672	0.810	0.790	0.805	0.778	0.757	0.804	0.815
NA	0.021	0.026	0.020	0.020	0.022	0.018	0.008	0.017	0.021	0.024
END MEMBER COMPOSITIONS(MOL.%)										
FS	17.89	22.89	28.55	13.06	13.31	15.19	20.25	25.81	13.09	13.06
EN	39.57	38.06	36.91	45.09	45.62	45.11	40.05	35.78	45.42	44.78
WO	42.13	39.05	34.53	41.85	41.07	39.70	39.70	38.41	41.49	42.16

TABLE A-6. ANALYSES OF PYROXENES IN THE STUDIED THOLEIITES. PHENOCRYST AND MICROPHENOCRYST COMPOSITIONS ARE INDICATED BY *

	143873*	143873	143873	143873	143878	143878	143878	143879	143879	143879
WT.%										
SIO2	50.67	50.88	49.80	50.87	49.25	50.97	49.38	52.00	51.25	50.48
TIO2	1.12	1.19	1.13	0.72	2.06	1.26	1.68	0.96	0.89	1.12
AL2O3	3.23	1.53	1.58	1.11	3.57	1.78	2.95	2.35	2.00	1.63
CR2O3	0.18	-	-	0.01	0.23	0.06	0.18	0.40	0.38	-
FEO	9.07	12.92	16.83	22.20	11.19	12.83	15.05	8.19	8.45	15.85
MNO	0.24	-	0.46	0.64	0.24	0.26	0.34	0.16	0.18	0.34
MGO	14.81	13.60	11.92	11.30	14.22	15.59	11.74	16.23	16.43	14.21
CAO	19.44	18.76	17.04	13.14	18.35	16.34	18.14	19.03	19.49	15.30
NA2O	0.39	0.22	0.25	0.29	0.25	0.15	0.26	0.12	0.27	0.36
TOTAL	99.17	99.09	99.01	100.69	99.36	99.24	99.71	99.44	99.33	99.30
ATOMIC PROPORTIONS ON THE BASIS OF 6 OXYGENS										
SI	1.900	1.937	1.930	1.960	1.860	1.925	1.890	1.929	1.914	1.929
TI	0.032	0.034	0.033	0.021	0.059	0.036	0.048	0.027	0.025	0.032
AL	0.143	0.069	0.072	0.050	0.159	0.079	0.133	0.103	0.088	0.073
CR	0.005	0.000	0.000	0.000	0.007	0.002	0.005	0.012	0.011	0.000
FE	0.284	0.411	0.545	0.715	0.353	0.405	0.482	0.254	0.264	0.506
MN	0.008	0.000	0.015	0.209	0.008	0.008	0.011	0.005	0.006	0.011
MG	0.828	0.771	0.688	0.649	0.800	0.877	0.670	0.897	0.914	0.809
CA	0.781	0.765	0.707	0.567	0.743	0.661	0.744	0.756	0.780	0.626
NA	0.029	0.016	0.019	0.021	0.018	0.011	0.019	0.009	0.019	0.027
END MEMBER COMPOSITIONS(MOL.%)										
FS	15.03	21.12	28.10	37.04	18.64	20.85	25.42	13.31	13.47	26.08
EN	43.71	39.60	35.46	33.59	42.20	45.13	35.33	47.04	46.70	41.67
WO	41.26	39.28	36.44	29.37	39.16	34.02	39.25	39.65	39.82	32.25

TABLE A-6. ANALYSES OF PYROXENES IN THE STUDIED THOLEIITES. PHENOCRYST AND MICROPHENOCRYST COMPOSITIONS ARE INDICATED BY *

	143885	143895	143855	143855	144CC8	144008	144008
WT.%							
SIO2	49.71	51.19	5C.45	5C.39	51.20	50.44	50.18
TIO2	1.47	1.31	1.04	0.96	1.00	0.93	1.11
AL2O3	2.79	2.20	1.87	1.29	2.16	2.29	1.50
CR2O3	0.05	0.07	0.03	0.06	C.15	0.16	-
FEO	12.13	12.43	13.36	17.25	10.39	10.60	13.54
MNO	0.25	0.26	0.28	0.41	0.20	0.23	0.28
MGO	13.62	13.91	13.43	11.99	15.24	14.54	14.38
CAO	19.01	18.69	18.57	17.27	18.91	20.06	17.49
NA2O	0.35	0.27	0.21	0.20	C.35	C.22	0.28
TOTAL	99.39	100.35	99.29	99.84	99.64	99.57	98.76
ATOMIC PROPORTIONS ON THE BASIS OF 6 OXYGENS							
SI	1.868	1.920	1.924	1.939	1.919	1.903	1.921
TI	0.042	0.037	0.030	0.028	C.028	0.026	0.032
AL	0.125	0.097	0.084	0.058	C.095	0.102	0.068
CR	0.001	0.002	0.001	0.002	0.005	0.005	0.000
FE	0.385	0.390	0.426	0.555	C.326	0.334	0.423
MN	0.008	0.008	0.009	0.013	0.006	0.007	0.009
MG	0.771	0.777	0.763	0.687	0.851	0.817	0.821
CA	0.774	0.751	0.758	0.712	C.759	C.811	C.717
NA	0.026	0.020	0.016	0.015	0.026	0.023	0.021
END MEMBER COMPOSITIONS(MOL.%)							
FS	19.96	20.32	21.88	28.40	16.83	17.04	21.99
EN	39.94	40.52	39.18	35.17	43.96	41.64	41.62
WO	40.09	39.16	38.94	36.43	39.21	41.32	36.39

TABLE A-7. ANALYSES OF CLIVINE IN THE STUDIED THOLEIITES. MICROPHENOCRYSTS ARE INDICATED BY *.

	143902*	143902*	143902*	143902*	143902*	143902*	143831	143831
WT.%								
SIO2	38.86	38.87	38.93	38.82	38.88	38.38	35.82	36.96
TIO2	0.04	0.04	0.04	0.01	0.08	0.09	0.08	0.02
AL2O3	0.08	0.08	0.15	0.08	0.08	-	0.09	0.06
CR2O3	0.01	0.03	0.04	0.04	0.03	0.03	-	0.01
FEO	21.38	21.91	21.77	22.52	22.62	22.94	36.29	29.51
MNO	0.31	0.31	0.32	0.32	0.33	0.30	0.48	0.40
MGO	38.69	38.28	37.70	37.57	37.25	37.41	26.45	33.03
CAO	0.40	0.34	0.42	0.37	0.40	0.42	0.46	0.34
NIO	0.22	0.16	0.21	0.21	0.17	0.18	0.15	0.11
TOTAL	100.19	100.02	99.57	99.94	99.83	99.78	99.82	100.43
ATOMIC PROPORTIONS ON THE BASIS OF 4 OXYGENS								
SI	1.0	1.0	1.0	1.0	1.0	1.0	1.0	1.0
TI	0.0	0.0	0.0	0.0	0.0	0.0	0.0	0.0
AL	0.0	0.0	0.0	0.0	0.0	0.0	0.0	0.0
CR	0.0	0.0	0.0	0.0	0.0	0.0	0.0	0.0
FE2+	0.5	0.5	0.5	0.5	0.5	0.5	0.9	0.7
MN	0.0	0.0	0.0	0.0	0.0	0.0	0.0	0.0
MG	1.5	1.5	1.5	1.5	1.4	1.5	1.1	1.3
CA	0.0	0.0	0.0	0.0	0.0	0.0	0.0	0.0
NI	0.0	0.0	0.0	0.0	0.0	0.0	0.0	0.0
END MEMBER COMPOSITIONS (MOL.%)								
FA	23.57	24.31	24.47	25.18	25.41	25.60	43.50	33.39
FO	76.43	75.69	75.53	74.82	74.59	74.40	56.50	66.61

TABLE A-8. ANALYSES OF TITANIFEROUS MAGNETITES IN THE STUDIED THOLEIITES

	143806	143806	143814	143814	143814	143830	143830	143844	143873	143873
WT.%										
SIO2	0.37	0.20	0.15	0.22	0.67	0.37	0.46	0.50	0.13	0.31
TIO2	24.41	22.79	25.51	24.88	25.54	27.20	26.51	21.42	24.90	25.10
AL2O3	1.83	2.43	1.76	1.55	1.50	2.02	2.14	2.12	1.66	2.08
CR2O3	0.04	0.51	0.05	0.06	0.06	0.13	0.16	0.11	0.04	0.08
FEO	69.15	69.50	68.83	69.55	69.10	67.00	65.79	70.80	69.28	67.84
MNO	0.41	0.38	0.49	0.86	0.54	0.56	1.16	1.01	0.50	0.44
MGO	1.28	1.04	0.61	0.31	0.45	1.37	1.32	0.54	0.85	1.41
CAO	0.06	0.01	0.10	0.10	0.22	0.20	0.16	0.13	0.03	0.02
TOTAL	97.55	96.86	97.30	97.53	97.88	99.25	97.70	97.70	97.40	97.28
RECALCULATED ANALYSES										
SIO2	0.37	0.20	0.15	0.22	0.67	0.37	0.46	0.50	0.13	0.31
TIO2	24.41	22.79	25.31	24.88	25.54	27.20	26.51	21.42	24.90	25.10
AL2O3	1.83	2.43	1.76	1.55	1.50	2.02	2.14	2.12	1.66	2.08
CR2O3	0.04	0.51	0.05	0.06	0.06	0.13	0.16	0.11	0.04	0.08
FE2O3	19.13	20.99	17.34	18.51	16.63	14.36	14.20	23.48	18.57	17.36
FEO	51.94	50.61	53.23	53.07	54.14	54.08	53.01	49.68	52.57	52.31
MNO	0.41	0.38	0.49	0.86	0.54	0.56	1.16	1.01	0.50	0.44
MGO	1.28	1.04	0.61	0.31	0.45	1.37	1.32	0.54	0.85	1.41
CAO	0.06	0.01	0.10	0.10	0.22	0.20	0.16	0.13	0.03	0.02
TOTAL	99.47	98.96	99.04	99.36	99.54	100.68	99.12	98.98	99.26	99.02
ATOMIC PROPORTIONS ON THE BASIS OF 32 OXYGENS										
SI	0.110	0.060	0.045	0.064	0.200	0.107	0.136	0.150	0.038	0.091
TI	5.435	5.103	5.690	5.595	5.669	5.957	5.894	4.820	5.582	5.599
AL	0.673	0.852	0.619	0.547	0.525	0.694	0.745	0.747	0.584	0.727
CR	0.009	0.119	0.012	0.014	0.014	0.030	0.026	0.025	0.010	0.019
FE3+	4.261	4.702	3.900	4.120	3.723	3.146	3.159	5.287	4.165	3.875
FE2+	12.860	12.602	13.306	13.272	13.467	13.172	13.106	12.432	13.106	12.949
MN	0.104	0.096	0.123	0.218	0.135	0.236	0.291	0.257	0.126	0.110
MG	0.563	0.461	0.272	0.137	0.198	0.593	0.584	0.241	0.380	0.422
CA	0.020	0.004	0.033	0.032	0.068	0.064	0.050	0.041	0.009	0.007

TABLE A-8. ANALYSES OF TITANIFEROUS MAGNETITES IN THE STUDIED THOLEIITES

	144C8	144C8
WT.%		
SIO2	0.47	0.58
TIO2	24.50	25.69
AL2O3	1.96	1.41
CR2O3	0.26	0.19
FEO	68.30	67.34
MNO	0.69	1.08
MGO	1.96	1.51
CAO	0.13	0.17
TOTAL	98.27	97.97
RECALCULATED ANALYSES		
SIO2	0.47	0.58
TIO2	24.50	25.69
AL2O3	1.96	1.41
CR2O3	0.26	0.19
FE2O3	19.22	16.79
FEO	51.00	52.23
MNO	0.69	1.08
MGO	1.96	1.51
CAO	0.13	0.17
TOTAL	100.21	99.64
ATOMIC PROPORTIONS ON THE BASIS OF 32 OXYGENS		
SI	0.137	0.170
TI	5.381	5.699
AL	0.676	0.490
CR	0.061	0.044
FE3+	4.226	3.727
FE2+	12.455	12.884
MN	0.172	0.269
MG	0.852	0.662
CA	0.040	0.054

TABLE A-9. ANALYSES OF ILMENITES IN THE STUDIED THOLEIITES

	143806	143806	143814	143814	143830	143830	143831	143831	143846	143846
WT.%										
SIO2	0.33	0.50	0.31	0.69	0.64	0.23	0.32	0.32	0.52	0.44
TIO2	50.16	49.85	50.10	50.15	49.16	49.98	48.33	48.42	49.71	48.83
AL2O3	0.22	0.25	0.12	0.17	0.39	0.03	0.43	0.35	0.23	0.23
CR2O3	-	-	-	0.01	0.11	0.08	0.14	0.09	0.11	0.11
FEO	46.63	47.14	47.58	46.40	47.12	47.51	46.70	47.04	44.91	45.93
MNO	0.44	0.42	0.69	0.45	0.64	0.68	0.65	0.53	0.54	0.54
MGO	1.40	0.63	0.59	0.56	0.51	-	2.38	1.54	2.21	2.11
CAO	0.08	0.22	0.24	0.23	0.34	0.24	0.23	0.10	0.23	0.16
TOTAL	99.25	99.00	99.43	98.66	98.91	98.75	99.20	98.38	98.46	98.36
RECALCULATED ANALYSES										
SIO2	0.33	0.50	0.31	0.69	0.64	0.23	0.32	0.32	0.52	0.44
TIO2	50.16	49.85	50.10	50.15	49.16	49.98	48.33	48.42	49.71	48.83
AL2O3	0.22	0.25	0.12	0.17	0.39	0.03	0.43	0.35	0.23	0.23
CR2O3	0.00	0.00	0.00	0.01	0.11	0.08	0.14	0.09	0.11	0.11
FE2O3	4.64	3.93	4.69	2.48	4.60	3.65	8.94	7.26	4.85	5.68
FEO	42.45	43.60	43.35	44.17	42.98	44.22	38.66	40.51	40.55	39.92
MNO	0.44	0.42	0.69	0.45	0.64	0.68	0.65	0.53	0.54	0.54
MGO	1.40	0.63	0.59	0.56	0.51	0.00	2.38	1.54	2.21	2.11
CAO	0.08	0.22	0.24	0.23	0.34	0.24	0.23	0.10	0.23	0.16
TOTAL	99.72	99.40	99.43	98.91	99.37	99.11	100.09	99.10	98.94	99.03
ATOMIC FORMULA ON THE BASIS OF 6 OXYGENS										
SI	0.016	0.025	0.015	0.035	0.032	0.012	0.016	0.016	0.026	0.022
TI	1.889	1.893	1.892	1.912	1.867	1.916	1.802	1.835	1.873	1.843
AL	0.013	0.015	0.007	0.010	0.023	0.002	0.025	0.021	0.014	0.014
CR	-	-	-	0.001	0.004	0.003	0.006	0.003	0.004	0.004
FE3+	0.175	0.149	0.178	0.095	0.175	0.140	0.333	0.275	0.183	0.252
FE2+	1.778	1.841	1.821	1.873	1.815	1.885	1.603	1.707	1.700	1.675
MN	0.018	0.018	0.029	0.019	0.027	0.029	0.027	0.022	0.023	0.023
MG	0.105	0.047	0.044	0.042	0.039	-	0.176	0.115	0.165	0.158
CA	0.004	0.012	0.013	0.013	0.018	0.013	0.012	0.005	0.012	0.009

TABLE A-9. ANALYSES OF ILMENITES IN THE STUDIED THOLEIITES

	143870	143870	143870	143872	143879	143879	144008	144008
WT.%								
SIO2	0.33	0.55	0.39	0.25	0.09	0.04	0.60	0.36
TIO2	49.11	49.97	49.17	50.94	49.60	49.90	49.78	50.30
AL2O3	0.22	0.27	0.25	0.05	0.09	0.06	0.29	0.35
CR2O3	0.14	0.09	0.10	-	0.01	0.02	0.12	0.09
FEO	47.11	45.96	47.45	47.07	47.81	47.64	45.44	44.70
MNO	0.86	0.59	0.60	0.60	0.39	0.42	0.50	0.63
MGO	1.79	1.53	1.30	0.73	1.40	0.91	2.11	2.02
CAO	0.15	0.17	0.15	0.06	0.01	0.01	0.20	0.33
TOTAL	99.70	99.17	99.41	99.70	99.40	99.99	99.04	98.78
RECALCULATED ANALYSES								
SIO2	0.33	0.55	0.39	0.25	0.09	0.04	0.60	0.36
TIO2	49.11	49.97	49.17	50.94	49.60	49.90	49.78	50.30
AL2O3	0.22	0.27	0.25	0.05	0.09	0.06	0.29	0.35
CR2O3	0.14	0.09	0.10	0.00	0.01	0.02	0.12	0.09
FE2O3	7.57	4.37	6.53	3.28	6.67	5.30	4.11	4.11
FEO	40.30	42.03	41.58	44.12	41.80	42.87	41.00	41.00
MNO	0.86	0.59	0.60	0.60	0.39	0.42	0.50	0.63
MGO	1.79	1.53	1.30	0.73	1.40	0.91	2.11	2.02
CAO	0.15	0.17	0.15	0.06	0.01	0.01	0.20	0.33
TOTAL	100.46	99.61	100.06	100.03	100.07	99.52	99.20	99.20
ATOMIC FORMULA ON THE BASIS OF 6 OXYGENS								
SI	0.016	0.028	0.019	0.013	0.004	0.002	0.030	0.018
TI	1.833	1.880	1.848	1.924	1.867	1.895	1.866	1.892
AL	0.013	0.016	0.015	0.003	0.005	0.004	0.017	0.021
CR	0.005	0.004	0.004	-	-	0.001	0.005	0.004
FE3+	0.283	0.164	0.245	0.124	0.251	0.201	0.186	0.155
FE2+	1.673	1.758	1.738	1.853	1.750	1.810	1.707	1.715
MN	0.034	0.025	0.026	0.025	0.016	0.018	0.021	0.027
MG	0.133	0.114	0.096	0.055	0.105	0.068	0.157	0.150
CA	0.008	0.011	0.008	0.003	0.001	-	0.011	0.018